**UNIVERSITY OF CALIFORNIA,**
**IRVINE**

# New technologies for a better understanding of the Golgi: FLIM-FRET and click chemistry

**DISSERTATION**

submitted in partial satisfaction of the requirements
for the degree of

**DOCTOR OF PHILOSOPHY**

In Biological Sciences

by

**Kari Anne Herrington**

**Dissertation Committee:**
**Professor Christine Sütterlin, Chair**
**Professor Grant MacGregor**
**Professor Susanne Rafelski**
**Professor Rahul Warrior**
**Professor Michelle Digman**

2016

# Table of Contents

# List of Figures

# List of Tables

# List of Abbreviations

| | |
|---|---|
| Ace-*t*-Bu-DenA | C12-Acetoxy-*t*-Butyl-Dendrillolide A |
| ARF | ADP-ribosylation factor |
| ARL | ARF-like |
| BFA | Brefeldin A |
| CA | Constitutive active |
| CBD | Cdc42 Binding Domain |
| CDG | Cognitive Disorders in Glycosylation |
| CFP | Cyan Fluorescent Protein |
| cu-click | Copper driven click chemistry |
| DH | Dbl Homology |
| DR4 and 5 | Death Receptor-4 and 5 |
| DN | Dominant negative |
| EB1 | End Binding 1 protein |
| EM | Electron Microscopy |
| ER | Endoplasmic Reticulum |
| ERGIC | ER to Golgi Intermediate Compartment |
| FLIM | Flourescence Lifetime Imaging Microscopy |
| FRET | Förster Resonance Energy Transfer |
| GalT | β1,4-galactosyltransferase 1 |
| GAP | GTPase Activaating Protein |
| GEF | Guanine nucleotide Exchange Factor |
| GFP | Green Fluorescent Protein |
| GRASP | Golgi Reassembly and Stacking Proteins |
| IQ | Ilimaquinone |

| | |
|---|---|
| LN2 | Liquid nitrogen |
| ManII | Manosidase II |
| MacE | Macfarlandin E |
| MACF1 | microtubule-actin crosslinking factor |
| MARK4 | Microtubule affinity-regulating kinase 4 |
| MLB | MacE-Like-Binding |
| MTOC | Microtubule Organizing Center |
| Na asc | Sodium Ascorbate |
| NRK | Normal Rat Kidney cells |
| PBD | PAK Binding Domain |
| PCM | Pericentriolar Matrix |
| $PIP_2$ | phosphatidylinositol 4,5- bisphosphate |
| PM | Plasma Membrane |
| RFP | Red Fluorescent Protein |
| RhoGDI | Rho Guanine Disassociation Inhibitor |
| SNARE | Soluble N-ethylmaleimide sensitive factor attachment protein receptor |
| SIM | Structural Illumination Microscopy |
| *t*-Bu-DenA | C12-*t*-Butyl-Dendrillolide A |
| *t*-Bu-MacE | *tert*-butyl-MacE |
| TNF | Tumor Necrosis Factor |
| YFP | Yellow Fluorescent protein |
| YPet | YFP for energy transfer |

# Acknowledgments

My PhD would not have been possible without the help and support of many people. First and foremost I would like to thank my advisor Christine Sütterlin for giving me the opportunity to work with her and complete my PhD. Without her, this thesis truly would not have been possible. She let me step outside the comfort zone for both of us and embark on a challenging new path for my final project. She has provided endless hours of support and feed back, and may she always know if I ever rolled my eyes it was only because she was probably right and I just needed a few more minutes to absorb her inspiration.

I cannot thank the other members of my thesis committee enough for their guidance and support. Dr. Grant MacGregor, Rahul Warrior, Susanne Rafelski, and Michelle Digman. Each one has given thoughtful and constructive feedback on developing my project. They have helped me to broaden my scope of ideas and to become a more creative scientist.

While at UCI, I have had a great deal of support from numerous fellow graduate students. I feel fortunate that I have been able to work with such a large group of people that I could depend on. I would like to thank the Sütterlin lab for their support and feedback, Kati Tormanen, Valerian Dormoy, Breanne Karanikolas, Jennifer Lee, Kirsten Johnson and Abdelhalim Loukil. Each of these people contributed to making the lab a better place. I would especially like to thank Kati who has been an exceptional friend and colleague during some of the toughest times of my graduate school career. I also would like to thank Carolyn Dang, a talented undergraduate who provided tremendous support in the last year.

Much of my work has been interdisciplinary and would not have been possible without collaborations. I have been fortunate to work with a number of collaborators that have been enthusiastic and supportive. I would like to thank Dr. Larry Overman and his lab, particularly Nathan Genung, Martin Schnermann, and Michelle Garnsey for their work on synthesizing MacE analogs. Dr. Jennifer Prescher and her lab, particularly Lidia Nozarova, who aided with click chemistry. Klaus Hahn for entrusting me with his unpublished biosensor and his feedback. Michelle Digman and Enrico Gratton and their lab, The Laboratory of Fluorescence Dynamics, have been invaluable for their guidance with FLIM-FRET and microscopy, especially Jenu Chacko, Sohail Jihad, and Andrew Trinh who have all gone above and beyond helping me with my project. I would also like to thank Thomas A. Jackson for his help with statistics.

Finally, I would like to thank my family and friends for their support and encouragement. They have never given up on me despite my tendency during the last few year to disappear from the world into the lab. I would especially like to thank my friends Christine (Wallace) Pavel and Becca DeAngelis, my parents Jim Linder and Wendy Linder, and my siblings Eric Linder and Emily Linder. Most of all I would like to thank my husband, Jim Herrington, for his love, support, and patience.

# Curriculum Vitae
## Kari Anne Herrington

## Education

**Hampshire College, Amherst MA** 2003-2007
B.A., Micro and Molecular Biology

**University of California Irvine** 2009-2016
Ph.D. Developmental and Cell Biology
New technologies for a better understanding of the Golgi:
FLIM-FRET and click chemistry

## Research Experience

**Graduate Student Researcher** with Dr. Christine Sütterlin 2010-16
Department of Developmental and Cell Biology, University of California, Irvine
Investigating Cdc42 activity at the Golgi

**Laboratory Assistant** with Dr. Ken Bayles Nov. 2008- 2009
Department of Pathology, University of Nebraska Medical Center, Omaha NE
Investigated Membrane localization and topology of *S. aureus* CidA and LrgA

**Laboratory Intern** with Dr. John O'Leary Sept. 2007- Sept. 2008
Department of Histology, Trinity College Dublin, Ireland
HPV detection technologies and treatments

**Intellectual property Intern** Summer 2007
UNeMed, University of Nebraska Medical Center, Omaha NE
Summarized patented technologies for display on UNeMed website

**Laboratory Assistant** with Dr. Larry Burg Summer 2004; Summer 2006
Cytyc Corp., Marlborough MA
Research and development to improve quality and uses of liquid based pap test

**Research Assistant** with Dr. Jose Romero May 2001- Aug. 2001
Department of Pathology, University of Nebraska Medical Center, Omaha NE
Analysis of Neonatal Enteroviral Disease Over an 8-Year Period

## Teaching Experience

| | |
|---|---|
| Teaching Assistant, Gene Cloning NS-101 | January term 2005, |
| Head Teaching Assistant, Gene Cloning NS-101 | January terms 2006, 2007 |
| Teaching Assistant, DNA to Organisms (Bio 93) | Fall 2010 |
| Head Teaching Assistant DNA to Organisms (Bio 93) | Fall 2011 |
| Administrative Teaching assistant DNA to Organisms (Bio 93) | Fall 2015 |
| Administrative Teaching Assistant Cell Biology (D103) | Winter 2016 |

## Awards and Honors

| | |
|---|---|
| Gregory S. and Toni Prince Scholarship Awards | 2006 |
| Hampshire College School of Natural Science Grants | 2006 |
| UCI-HHMI Graduate Fellow | 2010-2011 |
| Mentor-TA Award, HHMI-UCI Teaching Fellows Program | 2011-2012 |

## Paper, Posters, Abstracts

*Also published as Kari Linder*

Herrington, K.A., Trinh, A. L., Dang, C., O'Shaughnessy, E., Hahn, K.M., Gratton, E. Digman, M. A., and Sütterlin, C. (2016). Spatial analysis of Cdc42 activity reveals a role for plasma membrane-associated Cdc42 in centrosome regulation. *In preparation.*

Herrington, K. A.*, Dang, C., Digman, M. A., Gratton, E., and Sütterlin, C. (2015). Examining Cdc42 activity at the Golgi using a phasor approach to FLIM. FASEB Scientific Research Conference: Regulation and Function of Small GTPases. Program and Abstracts. (Poster)

Linder, K.*, Bose, J. L., Ranjit, D., and Bayles, K.W. (2009). Membrane localization and topology of *Staphylococcus aureus* CidA and LrgA. 53rd Annual Wind River Conference on Prokaryotic Biology, Program and Abstracts. (Poster)

Bose, J. L., Linder, K. A., Ranjit, D., and Bayles, K. W.(2009). Membrane localization and topology of *Staphylococcus aureus* CidA and LrgA. Presented at the Gordon Conference on Staphylococcal Diseases (Waterville Valley, NH). (Poster)

Leng, C., Linder, J., Linder, K., Burg, L. (2005). "Aliquot Removal from ThinPrep® Specimens: Effect on Adequacy and Cytological Diagnosis." *Cancer Cytopathology*; *American Society of Cytopathology 53rd Annual Scientific Meeting*. 105 (5); 391.

Newland, J.G., Romero, J.R., Sarica, A., Zach, T.L., and Linder, K. (2002). Spectrum of Neonatal Enteroviral Disease Over an 8-Year Period. 40th Annual Infectious Diseases Society of America Meeting, Program and Abstracts.

# Abstract of dissertation

New technologies for a better understanding of the Golgi:
FLIM-FRET and click chemistry

By
Kari Herrington
Doctor of Philosophy in Biological Sciences
University of California, Irvine 2016
Professor Christine Sütterlin, Chair

The Golgi is the central component of the secretory system and essential to cell homeostasis, but many mechanisms that regulate Golgi structure and function are incompletely understood. In this dissertation I pursued two projects with the overall goal of applying cutting-edge technologies to answer specific questions about Golgi regulation. In the first project, I investigated the regulation of the Rho GTPase Cdc42 at the Golgi. Cdc42 is critical for Golgi transport and is proposed to be regulated by the Golgi protein GM130 to control centrosome organization. It is not known how GM130 or other Cdc42 regulators control Cdc42 activity at the Golgi. I used the phasor approach to FLIM-FRET with a Cdc42 biosensor, Cdc42-FLARE, to detect localized Cdc42 activity. Using this method I investigated Golgi-associated Cdc42 regulators, FGD1, Tuba, and ARHGAP10, and structure proteins, GM130 and Golgin-84. I found Tuba and FGD1 did not regulate Cdc42 equally, as loss of Tuba, but not FGD1, led to a decrease in Cdc42 activity at the Golgi. However, both were required for Cdc42 activity at the plasma membrane (PM). In addition, I found neither GM130 nor Golgin-84 depletion reduced Cdc42 activity at the Golgi, but both led to a decrease in Cdc42 activity at the PM. It is likely this reduction in Cdc42 activity is due to the disruption of Golgi organization or transport. My results suggest a new model in which GM130 controls centrosome organization through regulating Cdc42 activity at the PM. My second project focused on using click chemistry to identify the mechanism through which the small molecule MacE induces extensive Golgi fragmentation. I observed that MacE bound to numerous proteins in cells and in lysates. Surprisingly, I found non-specific lysine binders with similar structures as MacE analogs produced a MacE-like phenotype. MacE is known to bind lysines, and this result suggests that MacE functions through modifying lysines.

# Chapter 1:
# Introduction

## 1.1 The Golgi Apparatus

Since its discovery, nearly every aspect of the Golgi Apparatus (referred to as Golgi) has been heavily debated. Camillo Golgi first described the organelle that would become known as the Golgi in 1898. Using a novel silver staining method that he had developed, which he called the “dark reaction”, he reported the Golgi as an internal reticular apparatus in neurons (Golgi, 1898; Farquhar and Palade, 1998) (Figure 1.1). Almost immediately after his report, it was called into question if the Golgi was a bonafide organelle or an artifact of heavy metal staining in cells. This doubt was mainly due to the inability of several scientists to repeat Golgi's experiments (Farquhar and Palade, 1981). We know now that the conflicting results that they had obtained stemmed from inconsistent fixation and staining protocols that can disrupt Golgi structure and staining (Novikoff and Goldfischer, 1961). It was not until the 1950's and with the use of Electron Microscopy (EM) that a clearer picture of the Golgi's highly ordered membrane structure was obtained, leading to its wide acceptance as a true organelle (Dalton and Felix, 1954; Sjöstrand and Hanzon, 1954). However, the debate over the function of this organelle persisted. A role for the Golgi in secretion was predicted based on morphology as early as 1902, but this idea was disregarded as a possible staining artifact. Other early theories included an intracellular communication system, an internal canal-like ducts, and the Golgi was proposed to form an "acroblast" for the formation of the acrosome in spermatozoa (Droscher, 1998). In the 1960’s,

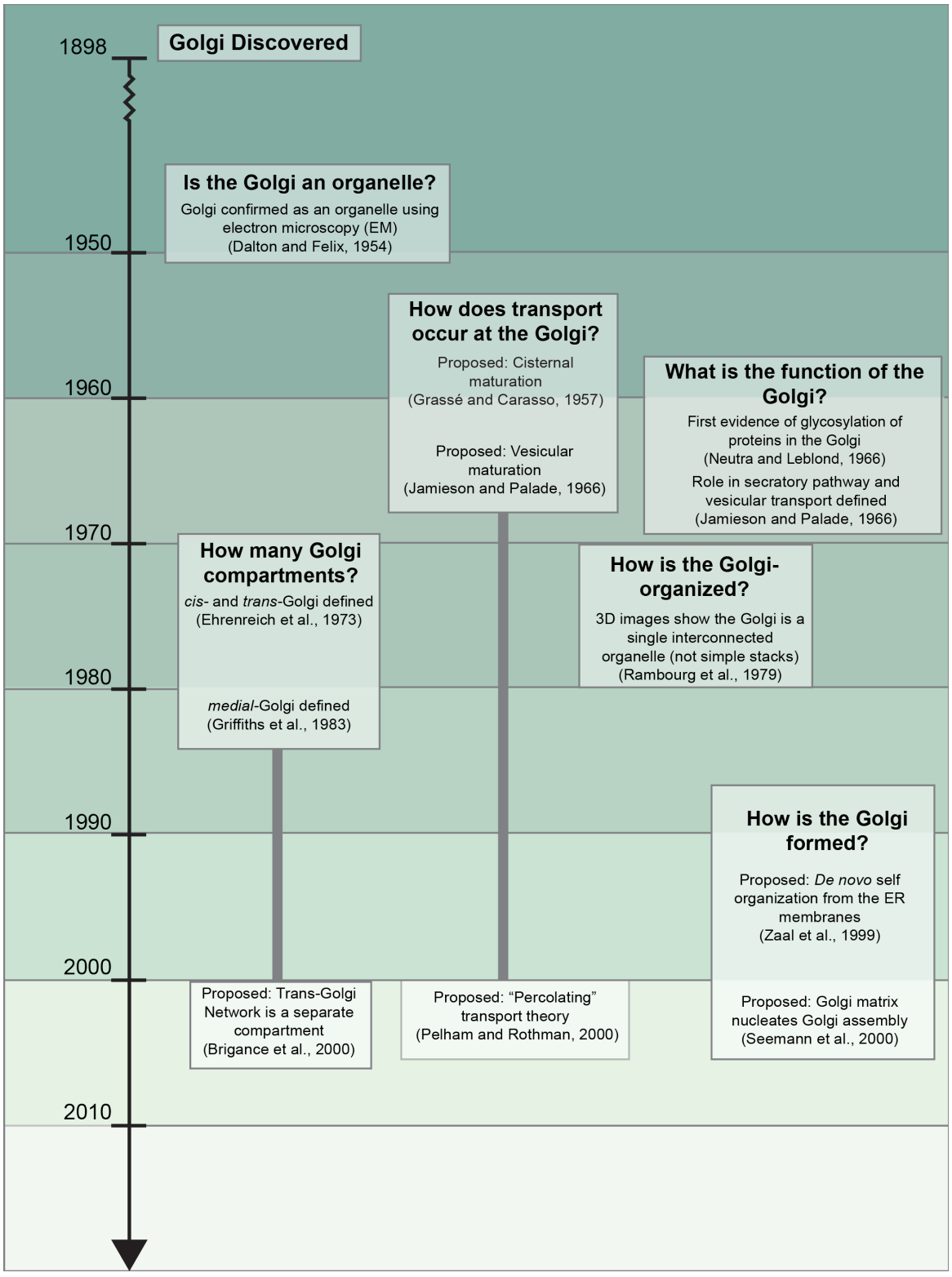


**Figure 1.1 Timeline of major questions and findings about the Golgi since its discovery in 1898 by Camillo Golgi.**

support for the role of the Golgi in secretion and glycosylation emerged from two new methods: EM autoradiography and Golgi fractionation (Neutra and Leblond, 1966a; 1966b; Fleischer *et al.*, 1969; Palade, 1975). These methods allowed for tracking of newly synthesized proteins through the secretory system and isolation of glycosylases from Golgi membranes and resulted in a Nobel Prize to George Palade in 1974. Currently, the Golgi is viewed as a major secretory organelle in the cell, being responsible for the sorting, modification, and secretion of proteins (Gillingham and Munro, 2016). However, the underlying mechanisms that regulate Golgi structure and functions are incompletely understood.

### *1.1.2 Golgi Structure*

The interphase Golgi of mammalian cells is a complex, interconnected membrane system centrally positioned in the cell (Figure 1.2A). The Golgi appears as a series of flattened membrane sacs, called cisternae. Stacks of 2-8 cisternae are laterally linked to form a continuous structure, referred to as the Golgi ribbon, which is adjacent to the nucleus and the centrosome. This positioning and contiguous ribbon structure are required in mammalian cells for normal cell function and polarization (Thyberg and Moskalewski, 1999; Yadav *et al.*, 2009). However, the pericentriolar localization must be lost during mitosis because cells cannot enter mitosis unless the Golgi is converted into small fragments and dispersed throughout the cell (Figure 1.2B; Sütterlin *et al.*, 2005). This perinuclear ribbon structure is not required in other organisms. For example in *Drosophila*, the Golgi forms mini-stacks that are dispersed throughout the cell (Figure 1.2C; Stanley *et al.*, 1997). While in yeast cells the Golgi can form mini-stacks in some species, such as *Pichia pastoris,* or be dispersed as individual cisternae throughout the

cell, such as *Saccharomyces cerevisiae* (Figure 1.2D; Preuss *et al.*, 1992). These differences in Golgi structure present questions as to both how and why the Golgi is structurally different in these organisms. However, for the purposes of this study, only the interphase mammalian Golgi will be discussed.

In mammalian cells the ribbon-like structure of the Golgi is polarized with at least three distinct compartments, the *cis*-, *medial*-, and *trans*-Golgi (Ehrenreich *et al.*, 1973; Farquhar and Palade, 1981; Griffiths *et al.*, 1983). The subcompartments of the Golgi were initially characterized morphologically because the *cis*-Golgi, which contain small vesicles and tubules, and trans-Golgi, which is vesicular and begins to lose the flattened shape of the cisternae, can be recognized as distinctive structures by EM (Ehrenreich *et al.*, 1973). Early staining techniques also revealed the Golgi compartments were biochemically different because osmium selectively stains the *cis*-Golgi where it is preferentially reduced, and thiamine pyrophosphatase (which degrades uridine diphosphatase produced in many glycosylation reactions) is specific for *trans*-Golgi membranes (Friend and Murray, 1965; Dunphy *et al.*, 1985). Differences in protein composition of individual Golgi membranes were detected in fractionation studies. These further demonstrated that specific compartments of the Golgi are enriched in unique sets of glycosylases, and that proteins have to pass through these specific compartments in order to be modified (Griffiths *et al.*, 1982; Deutscher *et al.*, 1983). In parallel to fractionation analysis, the *medial*-Golgi was identified through the use of the small molecule monensin and viral coat proteins that specifically interacted with the central portion of the Golgi (Griffiths *et al.*, 1983). Since these initial discoveries, each

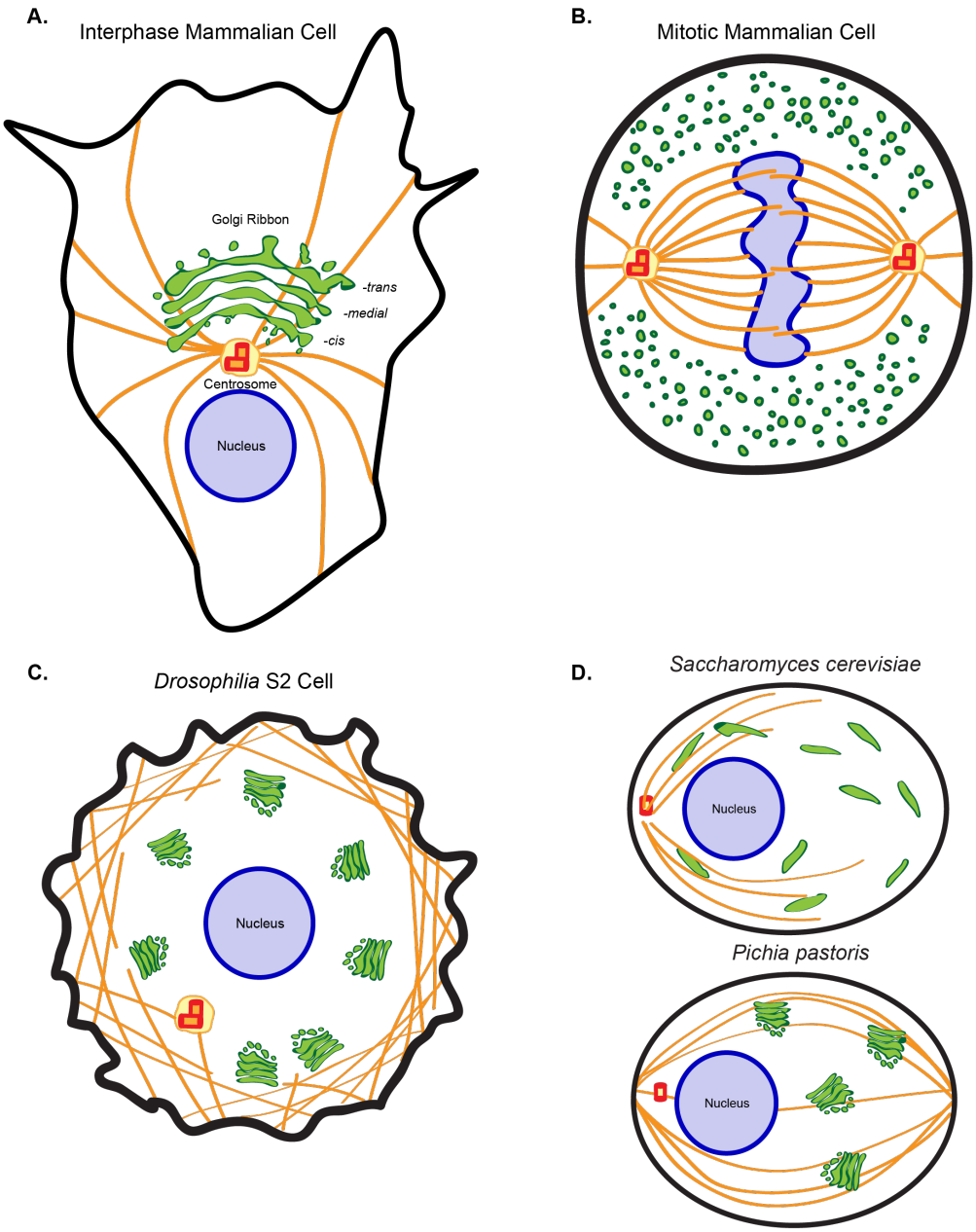


**Figure 1.2 Golgi organization in different eukaryotic cells.**
The organization of the Golgi varies by cell type and cell cycle stage. In these cartoons, the Golgi is depicted in green, the nucleus in blue, the centrosome or spindle pole body (yeast) in red and microtubules in orange. (**A**) The Golgi of an interphase mammalian cell forms a contiguous ribbon that is positioned adjacent to the centrosome and nucleus. (**B**) As cells enter mitosis, the mammalian Golgi is converted into small vesicular/tubular elements that are dispersed throughout the cell. (**C**) Golgi membranes of Drosophila S2 cells are separated into mini-stacks that are dispersed throughout the cell. (**D**) In the budding yeast, *Saccharomyces cerevisiae*, the Golgi is separated into individual cisternae that are dispersed throughout the cell. While in *Pichia pastoris*, the Golgi is arranged as multiple mini-stacks that are spread throughout the cell (Rossanese *et al.*, 1999; Jaspersen and Winey, 2004; Hayles *et al.*, 2013; Scheffler, 2014; Burns *et al.*, 2015; Rabouille, 2009).

Golgi compartment has been found to have a unique set of glycosylases (Kellokumpu *et al.*, 2015). Each of these glycosylases preferentially functions at specific pH, with a higher pH of 6.7 being associated with the *cis*-Golgi to the lower pH of 6.0 in the trans-Golgi (Rivinoja *et al.*, 2012).Reagents to these proteins, such as antibodies or fluorophore-tagged expression constructs, have become essential tools for studying the Golgi, allowing for the distinction between functionally-distinct cisternae (Yilmaz Dejgaard *et al.*, 2007).

The method used to view the Golgi can provide drastically different images of the Golgi. 2 dimension (2D) EM provided detailed information about the stacked membranes that make up the Golgi. However, they can be misleading in regards to the actual structure of the Golgi because they only represent a single cross section through the Golgi. 3 dimension (3D) electron tomography, however, showed that the Golgi is a membrane network with numerous pores in the cisternae though which other cisternae may pass through (cisternae-bypass), and that the same cisternae may appear more than once in a stack that has been observed by 2D methods (Figure 1.3; Mogelsvang *et al.*, 2004). Despite the details provided by 3D or 2D images, both methods still only present snapshots of the Golgi and miss the dynamic behavior of this organelle. Live cell imaging techniques have lower resolution, but they have been used to show that Golgi membranes are in constant flux (Marra *et al.*, 2001). Furthermore, use of live cell imaging with fluorescently tagged proteins has provided information on protein location and movements that may be disrupted by fixation (Michaelson *et al.*, 2001). Thus, 2D imaging has been valuable for fine details, while 3D electron tomography has redefined

our understanding of Golgi structure. Live imaging, in contrast, has provided valuable information on protein and membrane movement.

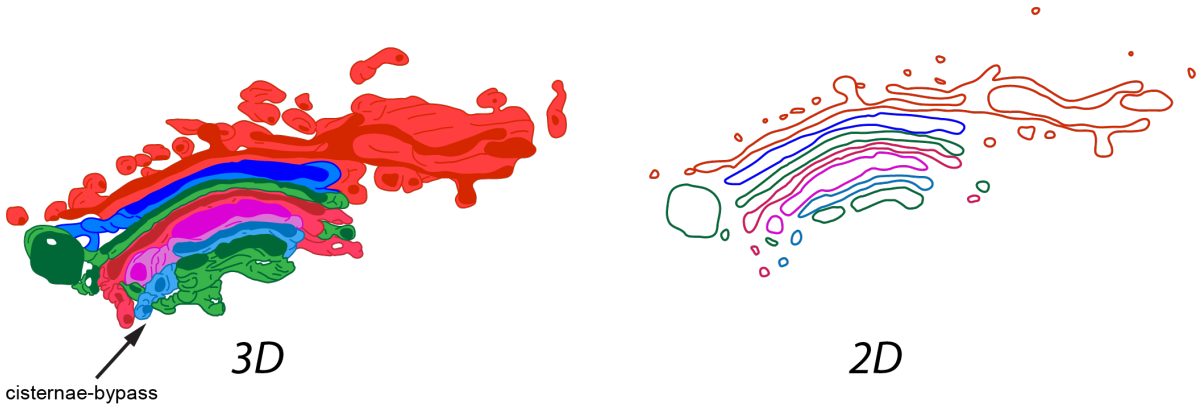


**Figure 1.3 The organization of the Golgi in 3D and 2D**
A comparison of the same Golgi shown as a 3D image, generated by EM tomograph, or a 2D image from the same data set adapted from Marsh *et al.,* 2004. The same colors are used in both images to indicate specific cisternae. This shows cisternae that pass through the other cisternae (cisternae-bypass with green cisternae, indicated by arrow) and fold back into the stack in the 3D image, which appear as two individual cisternae in the corresponding 2D image.

### *1.1.3 Golgi Maintenance*

Several diverse regulatory factors contribute to the maintenance of Golgi structure and position. Two classes of structural proteins, the Golgi Reassembly and Stacking Proteins (GRASP) and golgins, contribute to linking and stacking the Golgi membranes. Both the actin and microtubule cytoskeleton contribute to positioning and shaping the Golgi. In addition, a number of small GTPases of the ADP-ribosylation factor (ARF), ARF-like (ARL), Rab, and Rho families interact with structural Golgi proteins or the cytoskeleton to regulate structure and transport. While each of these

components contribute to regulating Golgi structure and function, the interplay between these proteins is also essential.

Two GRASP proteins, GRASP65 and GRASP55, are critical for the establishment and maintenance of the interconnected perinuclear Golgi ribbon. These proteins are recruited to specific cisternae through golgins and have been proposed to play complementary roles in linking the cisternae together to form stacks (Xiang and Wang, 2010). GRASP65 is recruited to the *cis*-Golgi by the golgin GM130 (Puthenveedu *et al.*, 2006; Kodani and Sütterlin, 2008; Sengupta *et al.*, 2009). Whereas, GRASP55 is recruited to the *trans*-Golgi by Golgin-45 (Ramirez and Lowe, 2009). *In vitro* data has suggested a role for these proteins in Golgi stacking (Nakamura *et al.*, 1995; Griffith *et al.*, 1997). GRASP65 was shown to form homodimers to stack the membranes, which are regulated in a cell cycle dependent manner and must be phosphorylated for the Golgi to fragment and disperse (Sutterlin *et al.*, 2005; Sengupta and Linstedt, 2010). The ability of GRASP65 to stack membranes was further shown in cells through experiments in which GRASP65 was targeted to the mitochondria. This resulted in clustered mitochondria that appeared stacked (Sengupta *et al.*, 2009). Despite these findings, it remains unclear how GRASP proteins contribute to Golgi structure, because their function appears to go beyond just stacking. For example, loss of GRASP65 was reported to prevent the lateral fusion of cisternae of one stack with those from a neighboring stack (Puthenveedu *et al.*, 2006). This function may be related to the golgins, GM130 and Golgin-45, which recruit the GRASP proteins.

The family of golgins forms a second group of proteins that contribute to the organization of the Golgi. There are at least 20 members of this family that share

structural features. Each contains several coiled-coil domains, which facilitate homodimerization and interaction with small GTPases (Barr, 1999; Burd *et al.*, 2004; Gillingham *et al.*, 2004; Short *et al.*, 2005; Rosing *et al.*, 2007). Golgins associate with the cytosolic side of Golgi membranes through either a transmembrane domain, or by binding to small GTPases such as members of the ARF and ARL families (Chan and Fritzler, 1998; Van Valkenburgh *et al.*, 2001; Lu and Hong, 2003; Burd *et al.*, 2004; Ramirez and Lowe, 2009; Munro, 2011; Witkos and Lowe, 2016).

Golgins act as membrane tethers that laterally link cisternae to form the contiguous Golgi ribbon (Barr *et al.*, 1997; 1998; Shorter *et al.*, 1999; Short *et al.*, 2001; Sütterlin *et al.*, 2002). This idea is based on the finding that loss of golgins frequently led to a disrupted Golgi ribbon phenotype. For example, loss of GM130 converted the Golgi ribbon into shortened mini-stacks (Puthenveedu *et al.*, 2006). While the absence of Golgin-84 resulted in mini-stacks that are significantly reduced in size and dispersed throughout the cell (Diao *et al.*, 2003). Golgins also play important roles in vesicle docking, through interactions with vesicle specific tethers, Rab GTPases, and SNARE proteins (Shorter *et al.*, 2002; Puthenveedu and Linstedt, 2004; Diao *et al.*, 2008; Arasaki *et al.*, 2013). Golgins may also contribute to Golgi organization through association with microtubules and molecular motors. For example, Golgin-160 recruits dynein to promote inward trafficking movements of the Golgi membranes (Yadav *et al.*, 2012). GMAP-210, another golgin, was found to bind both the minus end of microtubules and γ-tubulin and has been proposed to aid in positioning the Golgi (Infante *et al.*, 1999; Rios *et al.*, 2004). GM130 is known to interact with AKAP450 to recruit γ-tubulin and nucleate microtubules that are thought to be important for Golgi

organization and structure (Efimov *et al.*, 2007; Hurtado *et al.*, 2011; Rivero *et al.*, 2009). In this study, I have focused on the analysis of the golgin GM130 in its exciting and incompletely understood role in the regulation of Cdc42.

Microtubules play a crucial role in shaping and maintaining Golgi structure. Microtubules that are nucleated at the centrosome and the Golgi were found to be necessary to link Golgi cisternae, transport vesicles to and from the Golgi, and to establish Golgi polarization (Rivero *et al.*, 2009; Vinogradova *et al.*, 2012; Egea *et al.*, 2013; Gurel *et al.*, 2014). In addition, the microtubule-associated motors kinesin and dynein have been shown to be important for maintaining Golgi structure (Manneville *et al.*, 2003; Polishchuk *et al.*, 2003; Bannai *et al.*, 2004). For example, silencing of the kinesin subunit KAP3 led to Golgi fragmentation (Stauber *et al.*, 2006), while dynein was shown to be required for Golgi reassembly after the Golgi had been dispersed through treatment with nocodazole (Miller *et al.*, 2009). Despite an incomplete understanding of many of the underlying mechanisms though which golgins function, golgins are known to bind microtubules, microtubule motor proteins, and microtubule nucleating proteins as discussed above (Infante *et al.*, 1999; Rios *et al.*, 2004; Yadav *et al.*, 2012).

Actin also aids in maintaining Golgi structure and function. Actin is proposed to shape Golgi membranes by providing a physical force that pushes, pulls, and cleaves Golgi membranes (Valderrama *et al.*, 1998; Dippold *et al.*, 2009; Egea *et al.*, 2013; Ng *et al.*, 2013). Two actin regulatory proteins, WHAMM and N-WASP, have been shown to contribute to actin nucleation at the Golgi (Egea *et al.*, 2013). Depletion of WHAMM, which links actin to microtubules, has been shown to disrupt the normal microtubule array and overexpression or depletion of WHAMM disrupts Golgi structure (Campellone

*et al.*, 2008). N-WASP, which recruits the Arp 2/3 complex to nucleate actin, is recruited to the Golgi and is activated by the small Rho GTPase Cdc42 (Luna *et al.*, 2002). In addition, the Golgi resident protein Coronin7, which interacts with both N-WASP and Cdc42, was shown to restrict N-WASP activity to limit actin nucleation. Elevated N-WASP activity through expression of constitutive active Cdc42 or Coronin7 depletion, lead to an increase in filamentous actin and disruption in Golgi structure (Luna *et al.*, 2002; Bhattacharya *et al.*, 2016). In addition, Golgin-245, which interacts with the microtubule-actin crosslinking factor (MACF1) that links microtubules to the actin cytoskeleton is reported to control actin at the Golgi (Kakinuma *et al.*, 2004).

Several families of GTPases contribute to maintaining the Golgi, including ARF, ARL, Rab, and Rho. These proteins all share the common feature that they are regulated in a GTP dependent manner, cycling between a GTP-bound “on state and a GSP-bound “off” state. ARF and ARL contribute to recruiting and localizing Golgins as discussed above. In addition, ARF proteins have been associated with recruitment and regulation of a number of other proteins important for Golgi integrity. For example, ARF1 is important for COPI coat formation and it recruits ARHGAP10, which regulates actin and retrograde transport through Cdc42 (Dubois *et al.*, 2005; Liu *et al.*, 2005; Ménétrey *et al.*, 2007; Hehnly *et al.*, 2009). The Rab GTPases are highly conserved components of the vesicle trafficking pathways that help ensure fusion of a vesicle with a specific membranes and organelles (Barr, 2013). Several Rab GTPases interact with Golgin proteins for targeting to the Golgi. For example Rab1 interacts with *cis*-Golgi golgin GM130, p115, Golgin-84, and Giantin to regulate COPII vesicle tethering to receive vesicles from the ER (Moyer *et al.*, 2001; Ramirez and Lowe, 2009). Finally, the Rho

GTPase Cdc42 regulates N-WASP as discussed previously and has been associated with retrograde transport from the Golgi-to-ER, anterograde from the Golgi-to-PM, and centrosome organization (Dubois *et al.*, 2005; Egorov *et al.*, 2009; Hehnly *et al.*, 2009; Kodani *et al.*, 2009).

### *1.1.4 Protein transport through the Golgi*

The Golgi functions as a central component of the secretory system. The *cis*-Golgi receives proteins in vesicles that are synthesized on ER-bound ribosomes and that have trafficked from specialized domains in the ER (ER exit sites) through the ER to Golgi Intermediate Compartment (ERGIC; Schweizer *et al.*, 1993; Itin *et al.*, 1995). Proteins then progress through the Golgi, from the *cis*-, to the *medial*-, and finally the *trans*-Golgi (Figure 1.4). At each cisternae, these cargo proteins are modified by a unique set of glycosylases that is associated with each cisternae (Kellokumpu *et al.*, 2015). For example, Mannosidase II (ManII), which controls the last step in the N-glycan maturation pathway by conversion of high mannose to complex N-glycans, is at the *medial*-Golgi (Misago *et al.*, 1995). While β1,4-galactosyltransferase 1 (GalT), which is responsible for the N-linked glycosylation of proteins, is localized to the *trans*-Golgi (Bretz *et al.*, 1980; Schaub *et al.*, 2006). Then at the *trans*-Golgi, proteins are sorted and transported to the appropriate destination, such as the plasma membrane or endosome (Guo *et al.*, 2014).

While many aspects of protein transport to, from, and within the Golgi are not well understood, two questions are most commonly raised. 1) How does the Golgi maintain its structure and position in spite of a constant flux of membranes through the

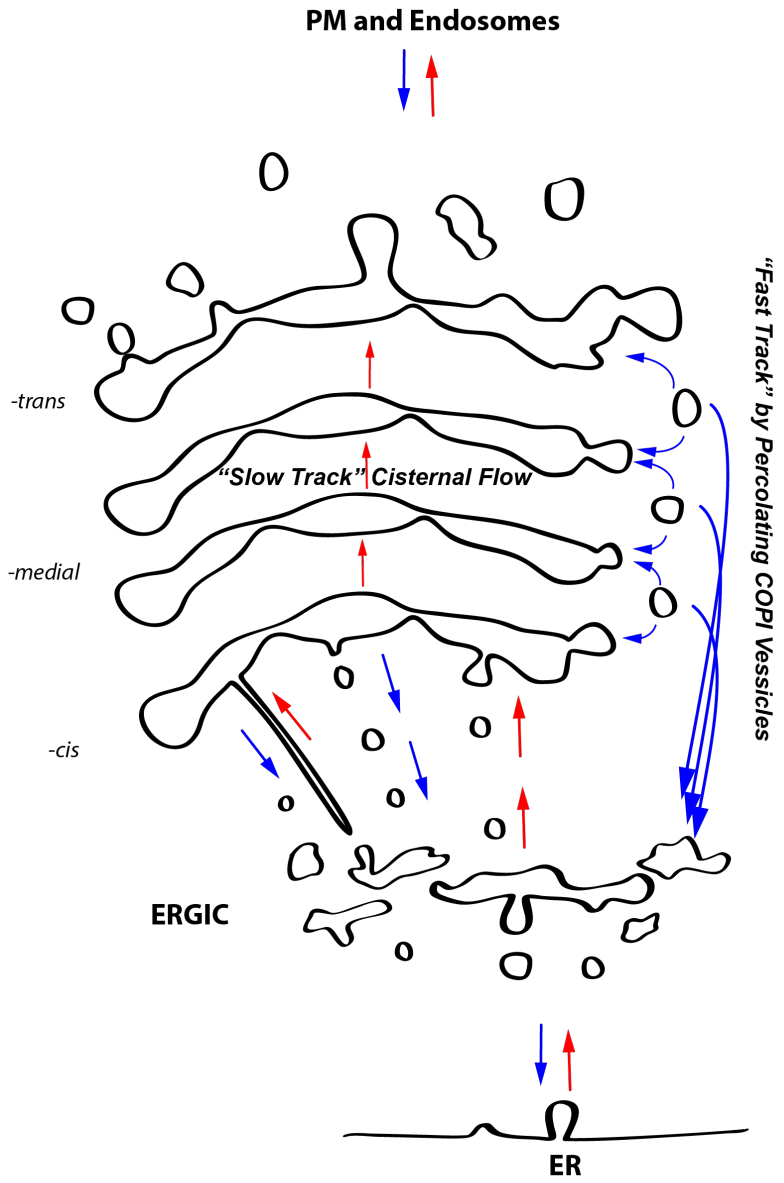


**Figure 1.4 Protein transport through the Golgi**
Cargo leaving the ER from specialized domains, known as ER exit sites, first transverse the ER to Golgi Intermediate Compartment (ERGIC) before entering the *cis*-Golgi. These proteins then progress though the Golgi from the *cis*-, to the *medial*-, and finally the *trans*-Golgi, through either the "slow track" cisternal flow or through the "fast track" by percolating COPI vesicles, which can also return to the ER. At the *trans*-Golgi, proteins are sorted into vesicles for their directional transport to an appropriate destination, such as the PM and endosome. Retrograde vesicles function to retrieve Golgi resident proteins that have been carried forward or, at the *cis*-Golgi, ER-resident proteins (Schweizer *et al.*, 1993; Itin *et al.*, 1995; Guo *et al.*, 2014).

organelle, and 2) How do Golgi cisternae maintain their unique identities while cargo transverses the Golgi membranes (Glick and Nakano, 2009). Two models, cisternal maturation and vesicular transport, have been described for the transport of proteins through the Golgi. The cisternal maturation theory states that proteins progress through the Golgi by remaining within a cisternae that matures, changes its identity from *cis*- to *trans*-cisterane and eventually converts into vesicles at the *trans*-Golgi (Glick and Malhotra, 1998). The vesicular transport model, in contrast, states that cisternae remain constant in regards to protein composition and position while vesicles transport proteins forward from one cisternae to the next (Rothman and Wieland, 1996). Neither model fully explains traffic through the Golgi. The cisternal maturation model indicates that proteins would all progress through the Golgi at the same pace, however, subsets of proteins have been found to traffic through the Golgi much faster than others (Karrenbauer *et al.*, 1990; Patterson *et al.*, 2008). The vesicular transport model fails to explain the transport of molecules, such as pro-collagen, which are too large (300-400 nm) to enter coated vesicles of about 60-80 nm in diameter (Bonfanti *et al.*, 1998; Popoff *et al.*, 2011; Jin *et al.*, 2012). Modifications to each of these models have been made to explain experimental findings, and it is generally accepted that trafficking through the Golgi occurs by the percolating vesicle model, which combines elements of the cisternal maturation and the vesicular transport models (Figure 1.4; Orci *et al.*, 2000; Pelham and Rothman, 2000).

### *1.1.5 Disruption of the Golgi is associated with disease*

Small changes in Golgi structure disrupt cell homeostasis, which can result in a wide range of diseases. Changes in Golgi organization and function have been observed in complex neurological diseases, such as Amyotrophic Lateral Sclerosis (ALS) or Alzheimer's (Reitz, 2014; Climer *et al.*, 2015). Several studies detected a disrupted Golgi ribbon, defective protein transport, increased cleavage of Golgi resident proteins , and incomplete glycosylation in both ALS and Alzheimer's (Aureli *et al.*, 2013; Buschman *et al.*, 2015; Climer *et al.*, 2015; Schreij *et al.*, 2015; Sulistio and Heese, 2015; Sadigh-Eteghad *et al.*, 2016). However, as these diseases are believed to have multiple causes, it is not clear if, and to what extent, Golgi-related defects trigger their onset or contribute to their progression (Sulistio and Heese, 2015; Sundaramoorthy *et al.*, 2015). Glycosylation defects have been reported in several Congenital Disorders in Glycosylation (CDG) that display a disrupted Golgi phenotype (Freeze and Ng, 2011). These disease can be caused by mutations in specific Golgi resident proteins that result in the incorrect modification of proteins at different stages throughout the maturation process (Freeze and Ng, 2011). Such mutations can produce a broad range of symptoms such as abnormal skeletal development, seizures, muscular dystrophy, weak muscles, shortened bones, and arrested development (Freeze and Ng, 2011). The variety in symptoms may be related to the large subset of proteins each glycosyltransferase can act on, and a mutation in a protein that is early in the glycosylation pathway may effect down stream glycosylation steps or chain elongation preventing protein maturation. This could lead to a number of proteins that a unable to preform their functions or miss folded proteins that are retained and accumulate in the

Golgi, which could disrupt Golgi structure and modification or transport of other proteins preventing their ability to interact with other proteins. Changes in the pH within the Golgi can also lead to glycosylation defects. Glycosyltransferases have a pH optimum for their function so that changes in cisternal pH may disrupt their activity. Interestingly, alterations in the pH of Golgi cisternae are often seen in cancer, where a slight increase in pH has been associated with changes in the distribution of proteins within the cell, increased proliferation, invasion, and metastasis (Rivinoja *et al.*, 2012). We have begun to understand diseases associated with the Golgi, but many unanswered questions remain. For example, it is unclear what triggers complex diseases such as ALS and Alzheimer's, can a single mutation in a specific Golgi protein trigger the disease? Or do multiple mutations need to occur before the disease begins to manifest at the Golgi?

## 1.2 The Centrosome

The centrosome functions as the microtubule organizing center (MTOC) that is critical for cell cycle progression. Prior to S-phase, the centrosome is composed of two barrel-shaped centrioles that are surrounded by concentric layers of protein, known as the pericentriolar matrix (PCM; Bettencourt-Dias and Glover, 2007). As a result of template-based duplication in S-phase, a cell in G2 contains two centriole pairs, which can be detected as four small dots by immunofluorescence staining with antibodies to centriolar proteins, such as centrin, or PCM proteins, such as kendrin. These centriole pairs form the poles of the spindle in mitosis (Nigg and Stearns, 2011; Millarte and Farhan, 2012). At all stages of the cell cycle, the centrosome nucleates and anchors microtubules. In interphase, centriolar microtubules are arranged as a radial array and are required for

cell shape and intracellular transport (Bettencourt-Dias and Glover, 2007; Nigg and Stearns, 2011). In mitosis, the centrioles form spindle poles that nucleate spindle microtubules which organize and segregate chromosomes into emerging daughter cells (Khodjakov and Rieder, 1999). In non-cycling cells the centrosome forms the base of the primary cilium, which is necessary for cell signaling (Nigg and Raff, 2009). Because of these diverse functions, dysregulation of the centrosome leads to many diseases (Gao *et al.*, 2011; Anderhub *et al.*, 2012; McIntyre *et al.*, 2012; Sircar *et al.*, 2012). For example, centrosome organization defects have been observed in the majority of human cancers (Nigg, 2002). Defects in many centrosomal proteins, such as centrosomal protein 4.1- associated protein (CPAP) have been demonstrated to cause ciliopathies (Woods *et al.*, 2005).

The Golgi and centrosome are physically linked. The Golgi and the centrosome are positioned in close proximity to each other in interphase. This association in the perinuclear region is required for cell homeostasis and cell polarization (Kupfer *et al.*, 1982; Burakov *et al.*, 2003; Gomes and Gundersen, 2006). Several conditions have been identified in which either the Golgi or the centrosome have been displaced from the perinuclear region. As a result, there were  defects in cilia formation and directional migration, which requires both organelles to orient towards the leading edge (Gonçalves *et al.*, 2010; Hurtado *et al.*, 2011). The physical proximity between the Golgi and the centrosome is lost during mitosis. Prior to mitosis, this close physical proximity is lost as a consequence of extensive Golgi fragmentation and dispersal (Shima *et al.*, 1997). Preventing mitotic Golgi fragmentation blocked normal entry of cells into mitosis,

indicating that the Golgi – centrosome relationship contributes to the control of cell cycle progression (Sütterlin *et al.*, 2002; Preisinger *et al.*, 2005; Liljedahl, et al., 2001).

The Golgi and the centrosome are also functionally linked. Both organelles share a number of functions including the control of polarization, migration, directional exocytosis, and ciliogenesis (Sütterlin and Colanzi, 2010; Hurtado *et al.*, 2011; Rios, 2014). In addition, the centrosome was found to be necessary for the maintenance of Golgi structure and function, and vice versa. For example, centrosome-nucleated microtubules and the microtubule motor proteins, such as dynein, are needed for the transport of newly formed Golgi membranes from the ER to the perinuclear region and for the establishment of a perinuclear Golgi ribbon (Minin, 1997; Manneville *et al.*, 2003; Polishchuk *et al.*, 2003; Miller *et al.*, 2009; Hurtado *et al.*, 2011). In turn, Golgi proteins, including Sac1, Tankyrase-1, and GM130, are reported to regulate centrosome organization and spindle formation during mitosis (Sutterlin *et al.*, 2005). Interestingly, the golgin GM130, which will be discussed in more detail below and is the focus of Chapter 3, is the first Golgi resident protein reported to control the organization of the interphase centrosome (Kodani and Sütterlin, 2008). Currently the mechanism though which this Golgi protein regulates the centrosome is unknown.

## 1.3 GM130, a *cis*-Golgi protein with diverse roles at the Golgi

GM130 is a peripheral Golgi matrix protein that contributes to diverse cell functions through multiple interactor proteins (Nakamura *et al.*, 1995; Barr and Short, 2003). Located to the *cis*-Golgi membrane, GM130 was a founding member of the golgin family of proteins. (Nakamura *et al.*, 1995; 1997; Barr *et al.*, 1998; Barr and

Short, 2003). This protein, which serves as a popular marker for the Golgi, has been believed for the last 20 years to contain 6 coiled-coil domains that facilitate dimer formation (Nakamura *et al.*, 1995; Barr *et al.*, 1998; Yoshimura *et al.*, 2001). However, a recent study by Ishida, *et al.* used biochemical and Nanogold® EM assays to demonstrate that GM130 is composed of 4 coiled-coil domains and that this protein actually forms homotetramers (Ishida *et al.*, 2015). GM130 has been proposed to interact with at least 20 different proteins, including itself (Figure 1.5). These include proteins such as GRASP65, Rab1, syntaxin 5, and AKAP450 (Barr *et al.*, 1997; Moyer *et al.*, 2001; Shorter *et al.*, 2002; Rivero *et al.*, 2009). The NanoGold® EM approach used by Ishida, *et al.,* may help with our understanding of GM130 interactors. For example, four molecules, instead of two, of GRASP65 were found to bind a GM130 tetramer through its C-terminal end (Puthenveedu *et al.*, 2006). Understanding the full three dimensional structure and how the molecules are bound may help our understanding of how GM130 and GRASP65 function to tether and stack the Golgi membranes. GM130 mediates numerous processes at the Golgi through association with other proteins (Figure 1.5). For example, GM130 regulates the Golgi ribbon structure which occurs through interaction with GRASP65 to stack membranes, as discussed above (Puthenveedu *et al.*, 2006). GM130 is also required for nucleation of centrosome-independent microtubules at the Golgi through AKAP450, which recruits γ-Turc (Rivero *et al.*, 2009). Disruption of the GM130 nucleated microtubules lead to a fragmented Golgi that collapsed around the centrosome, indicating their importance for maintenance of Golgi structure and organization (Hurtado *et al.*, 2011). GM130 regulates the mitotic spindle by activating the TPX2-importin complex

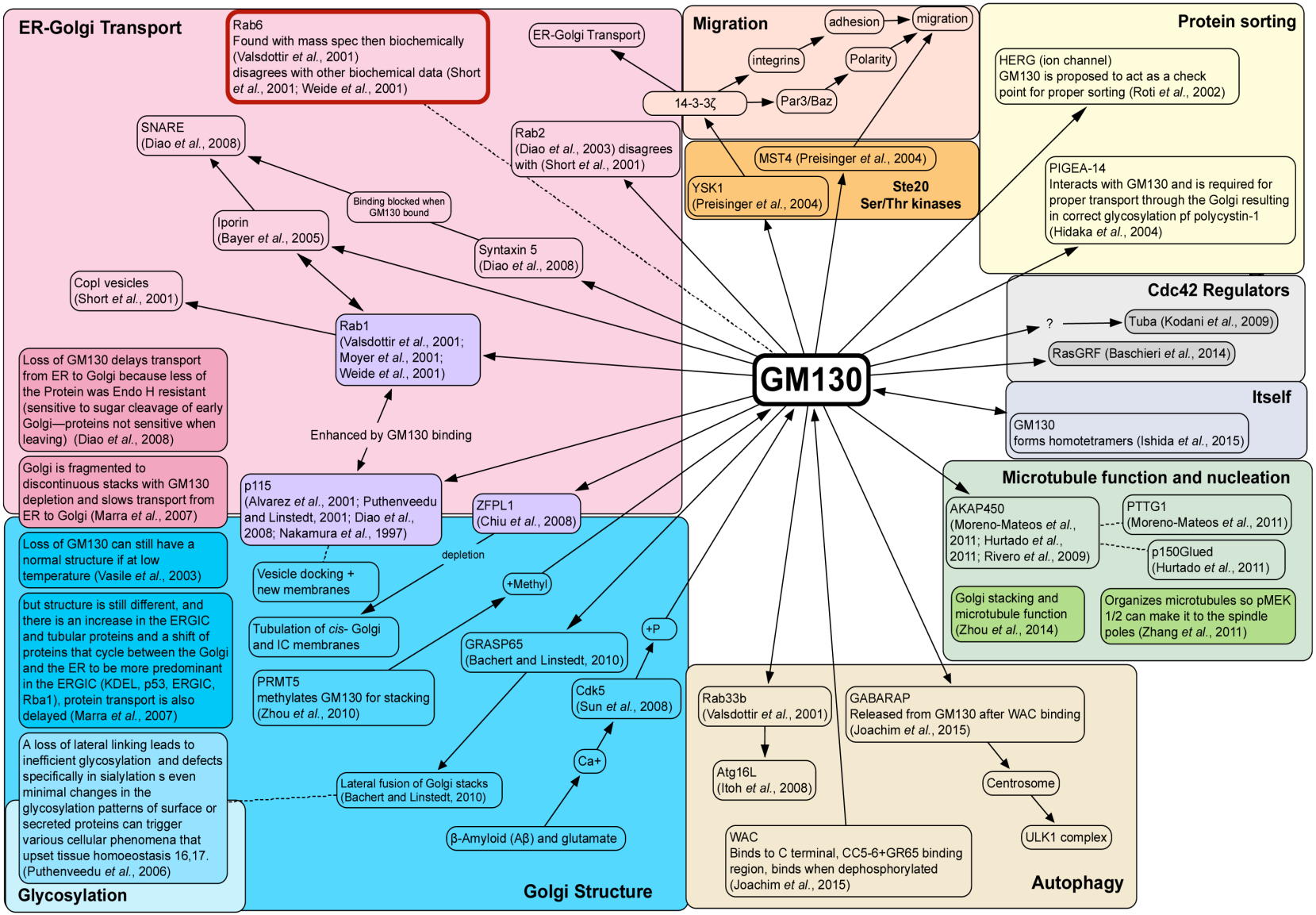


**Figure 1.5 GM130 interacting proteins**
Concept map based on a comprehensive literature search that depicts proteins proposed to interact with GM130 and their associated functions. Each color indicates a function that is associated with GM130.

after its phosphorylation by the mitotic cyclin Cdk1, followed by capturing and stabilizing the microtubules to form the spindle (Wei *et al.*, 2015). GM130 was also found to control the organization of the interphase centrosome (Kodani and Sütterlin, 2008; Kodani *et al.*, 2009). Experiments by our lab showed that GM130 depletion from U2OS or HeLa cells produced a disorganized, non-functional centrosome. Instead of 2 to 4 centrioles that are normally detected by staining with antibodies to centrin or kendrin, there was an increased number of centrosomal foci (>4) that appeared as a cloud-like structure. This centrosome was non-functional because the microtubule array was disrupted and End Binding 1 (EB1) protein staining throughout the cell was decreased. In addition, the centrosome shifted from its normal position adjacent to the nucleus to under the nucleus (Kodani and Sütterlin, 2008). These results indicate that depletion of GM130 disrupts both centrosome function and organization. Additional studies suggested that GM130 may control the centrosome through a Cdc42-dependent pathway (Kodani *et al.*, 2009). Loss of GM130 resulted in a reduction in total cellular Cdc42 activity by about 50%. In addition, a similar defective centrosome phenotype was observed upon depletion of the Cdc42 GEF Tuba or expression of dominant negative (DN)-Cdc42 (Kodani *et al.*, 2009). Furthermore, expression of constitutive active (CA)-Cdc42 was able to rescue the centrosome phenotype caused by GM130 depletion suggesting that these players may all act in the same regulatory pathway (Kodani *et al.*, 2009).

It is not known how GM130 controls Cdc42 activity. Activation of small GTPases is generally controlled by guanine nucleotide exchange factors (GEFs) that contain specific regulatory domains, such as Dbl Homology (DH) or Dock domains (Rossman *et al.*, 2005). As GM130 lacks such specific domains, it is likely that GM130 controls

Cdc42 activity indirectly. Tuba, a Cdc42 activator, whose depletion also affected centrosome organization, was identified in as a potential interactor of GM130 in a GM130-pull down assay followed by with mass-spectrometry analysis (Kodani *et al.*, 2009). While Tuba and GM130 appeared to interact *in vitro* and in detergent extracts of whole cells, it is still not clear if this interaction occurs in intact cells and how it could control Cdc42 activity. From these results we had designed a model in which GM130 was directly or indirectly responsible for activating Tuba, which then led to Cdc42 activation that was necessary for the maintenance of Golgi organization and function (Figure 1.6). In Chapter 3 I discuss a revised model based on my findings with a Cdc42-FRET biosensor to look at the spatial distribution of Cdc42 activity in cells after GM130 depletion.

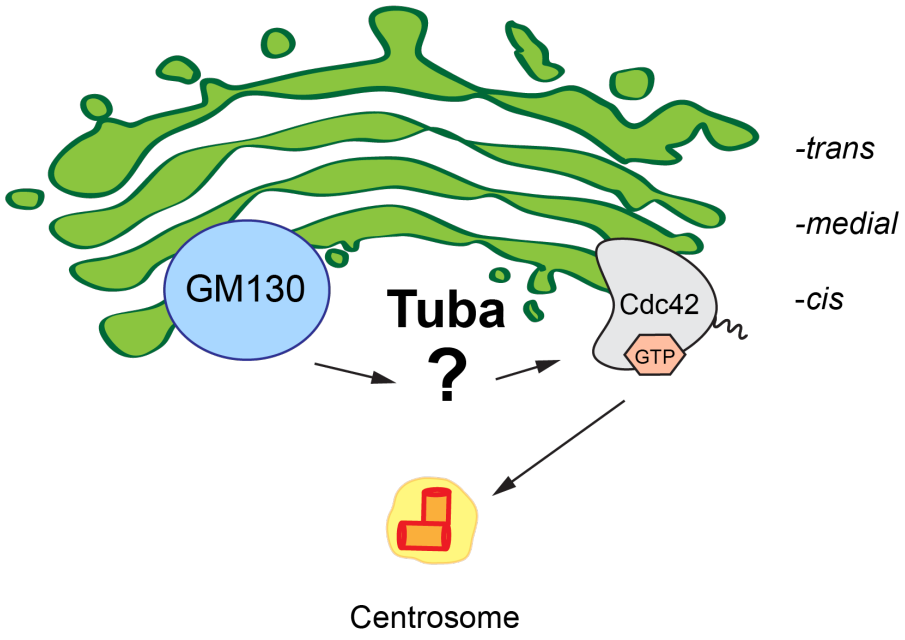


**Figure 1.6 Original model for GM130-mediated centrosome regulation.**
Previous results from the Suetterlin lab led to a model for GM130-mediated centrosome regulation in which GM130 activated Tuba directly or indirectly. This GEF, which had been observed at the Golgi (Salazar, *et al.* 2003), then induced the activation of Cdc42, which then controlled the organization and function of the centrosome (Kodani *et al.*, 2009).

## 1.4 Cdc42 a Rho GTPase required for Golgi function

Cdc42 is a prominent member of the Rho family of small GTPases whose activity is tightly controlled. Rho GTPases are small proteins of ≈21 KDa that switch between an inactive GDP bound state and an active GTP-bound state. In its active conformation, Cdc42 interacts with at least 28 different effector proteins, which each contribute to processes including cytoskeletal organization, polarization, migration, transport, gene transcription and cell cycle progression (Burbelo *et al.*, 1995). To complete these diverse functions, Cdc42 is tightly regulated by three sets of proteins. Guanine Nucleotide Exchange Factors (GEFs) activate Cdc42 at membranes by exchanging GDP for GTP. GTPase Activating Proteins (GAPs) inactivate Cdc42 by enhancing its natural ability to hydrolyse GTP to GDP. Rho GTPase Guanine Dissociation Inhibitors (RhoGDIs) maintain inactive Cdc42 in the cytosol by binding its C-terminal domain that contains the membrane anchor of the protein. Approximately 21 GEFS, 15 GAPs, and 4 RhoGDI proteins can act on Cdc42, however, only one RhoGDI appears to be favored *in vivo,* which may be due to the variable C-terminals or the Rho GTPases. Each of these proteins is tightly regulated itself (Hoffman *et al.*, 2000; Michaelson *et al.*, 2001; Donovan *et al.*, 2002; Schmidt and Hall, 2002; DerMardirossian *et al.*, 2006; Ligeti and Settleman, 2006; Garcia-Mata and Burridge, 2007; Csépányi-Kömi *et al.*, 2012; Goicoechea *et al.*, 2014). Cdc42-mediated control of cellular functions depends on tight spatial control of its activity. Cdc42 is activated at membranes that are rich in phosphatidylinositol 4,5- bisphosphate ($PI(4,5)P_2$; Brown, *et al.,* 2001). Membrane association is mediated by a geranylgeranyl lipid anchor and positively charged amino acids preceding the anchor attachment site (Johnson *et al.*, 2012). Membrane trafficking

is critical for localized activation of Cdc42 at the PM (Osmani *et al.*, 2010). RhoGDI proteins have been shown to direct Cdc42 to specific membranes, although the mechanism is not well understood (Michaelson *et al.*, 2001). In addition, GEFs have been found to contribute to local Cdc42 regulation by recruiting this small GTPase to specific cellular locations. GEFs also facilitate specific interactions with effector proteins. The regulation of the Cdc42 GEF βPIX during cell migration serves as a great example to illustrate the mechanism of Cdc42 regulation at a specific site. During cell migration, βPIX is trafficked together with Cdc42 on ARF6 vesicles from the endosome to the leading edge (Osmani *et al.*, 2010). Upon arrival at the PM, βPIX is activated through phosphorylation in an EGF-dependent manner (Feng *et al.*, 2006). βPIX then associates with the Cdc42 effector PAK1 at the PM to facilitate PAK1-Cdc42 interaction, which is necessary to trigger the formation of microspikes, focal adhesions, and cell migration (Manser *et al.*, 1998; Feng *et al.*, 2006).

Cdc42 activity is required for Golgi functions. While Cdc42 is frequently studied at the PM, it has also been detected at the Golgi (Erickson *et al.*, 1996; Michaelson *et al.*, 2001; Luna *et al.*, 2002). Cdc42 has also been shown to be a BFA sensitive component of the Golgi, (Erickson *et al.*, 1996). Further support for a role of Cdc42 at the Golgi comes from the observation that Cdc42-specific regulators have been detected at the Golgi. These include the two GEFs, FGD1 and Tuba, and the GAP ARHGAP10 (Salazar *et al.*, 2003; Egorov *et al.*, 2009; Kodani *et al.*, 2009; Dubois *et al.*, 2005). In addition, two Golgi resident proteins, GM130 and Coronin 7, have been found to either activate or limit Cdc42 activity, respectively (Kodani *et al.*, 2009; Bhattacharya *et al.*, 2016).Golgi-associated Cdc42 and its regulators have been implicated in Golgi

functions, such as protein transport and centrosome regulation. For example, Golgi-to-PM transport was inhibited in cells depleted of FGD1 (Egorov *et al.*, 2009). In addition, depletion of ARHGAP10 inhibited Golgi-to-ER transport of Shiga toxin (Dubois *et al.*, 2005; Hehnly *et al.*, 2009; Wang *et al.*, 2012). Over expression of constitutive active (CA)-Cdc42 inhibited Shiga toxin and prevented redistribution of Cdc42. As discussed earlier, loss of Tuba or GM130 led to the disruption of centrosome organization and function (Kodani *et al.*, 2009). The interaction of Cdc42 and its effector N-WASP, which is required for actin nucleation, are often linked with Cdc42-associated Golgi functions because actin nucleation contributes to shaping the Golgi membranes (Dubois *et al.*, 2005; Bhattacharya *et al.*, 2016). However, how Cdc42 may control functions, such as centrosome regulation is unclear. A key step in understanding how Cdc42 contributes to its many functions at the Golgi will be tow understand how Cdc42 activity is regulated at the Golgo. For example, is Cdc42 is activated at the Golgi or is an active form delivered to the Golgi from the PM? If active Cdc42 is transported to the Golgi, it would be important to investigate if other proteins are shuttled with it, similar to how Cdc42 and β-PIX are shuttled to the PM together. However, if Cdc42 is activeated at the Golgi, the GEF that activates Cdc42 may recruit effector proteins. I have addressed this question in Chapter 3 of this thesis by taking the first steps in determining is Cdc42 activity is regulated at the Golgi and PM by specific Cdc42 regulators.

## 1.5 Detecting Cdc42 activity using FRET and Biosensors

Genetically-encoded FRET biosensors are powerful tools for deciphering the dynamics of small GTPase activation in single cells. Förster Resonance Energy

Transfer (FRET) is the process in which an excited fluorophore, known as the donor, transfers its energy to a fluorophore with sufficient spectral overlap, known as the acceptor (Clegg, 1995; Förster, 2012). FRET depends on physical proximity between donor and acceptor fluorophore and therefore serves as a measure of molecular interactions between two proteins (Spiering *et al.*, 2013). Donor and acceptor fluorophores are often referred to as a "FRET pair" and are composed of monomeric fluorophores, such as GFP/RFP and CFP/YFP (Rizzo *et al.*, 2004; Nguyen and Daugherty, 2005). CFP/YFP is considered the most versatile FRET pair because the emission spectra of the fluorophores provide sufficient spectral overlap, but can be isolated with minimal crosstalk (Wallrabe and Periasamy, 2005; Shaner *et al.*, 2007). In the study described in Chapter 3, I used the FRET pair of Cerulean/ YPet, which are CFP and YFP derivatives with increased photostability. Genetically-encoded FRET biosensors generally fall within two categories. Intramolecular (single chain) biosensors consist of a single peptide chain with one or more proteins fused to the fluorescent proteins of the FRET pair. In contrast, intermolecular (dual chain) biosensors consist of two unique polypeptide chains to which the fluorophores of the FRET pair are fused (Hodgson *et al.*, 2008; Vilela *et al.*, 2013).

Biosensors facilitate the spatial analysis of small GTPase activity. A variety of single chain and dual chain biosensors have been designed for Cdc42 (Figure 1.7; Itoh *et al.*, 2002; Hodgson *et al.*, 2008; Machacek *et al.*, 2009; Hanna *et al.*, 2014). These biosensors generally detect the interaction between Cdc42 fused to the donor fluorophore and a Cdc42 Binding Domain (CBD), which will only bind active Cdc42, fused to the acceptor fluorophore. In addition to genetically-encoded biosensors, a

solvatochromic dye probe called MeroCBD has been used to detect Cdc42 activity (Nalbant *et al.*, 2004). While MeroCBD may appear ideal because it measures the activity of endogenous Cdc42, generation of the probe and performing microinjection are cumbersome and therefore not suitable for routine lab use. However, the data obtained with this probe has set the standard for what should be seen with the genetically-encoded biosensors. For example, a sensor encoding a GFP bound to a CRIB domain of N-WASP (GFP-CBD) has been used to observe general changes in Cdc42 activity in MCF7 cells (Kim *et al.*, 2000). However, use of MeroCBD, which is also tagged with a GFP to track the probe, has shown that expression of GFP-CBD is dependent on cell thickness and does not always reflect Cdc42 activity (Nalbant *et al.*, 2004).

Single and dual chain biosensors each have unique advantages and disadvantages. Single chain biosensors are often chosen because the presence of donor and acceptor within the same polypeptide chain eliminates the need for channel alignment (Wallrabe and Periasamy, 2005). However, this benefit is a weakness at the same time. Both fluorophores on the same polypeptide chain results in a constant low FRET background, reducing the dynamic range of the biosensor and increasing fluorescent artifacts (Itoh *et al.*, 2002; Seth *et al.*, 2003). Single chain Cdc42 biosensors can also affect proper localization and function because the Cdc42 C-terminus, which mediates binding RhoGDI, is blocked by the fluorophore (Michaelson *et al.*, 2001; 2003; Hanna *et al.*, 2014). Other considerations apply for dual chain biosensor. They have a higher dynamic range because the FRET pair is not constrained to the same peptide chain. In addition, their C-terminal is free and able to interact with GDI. However, the

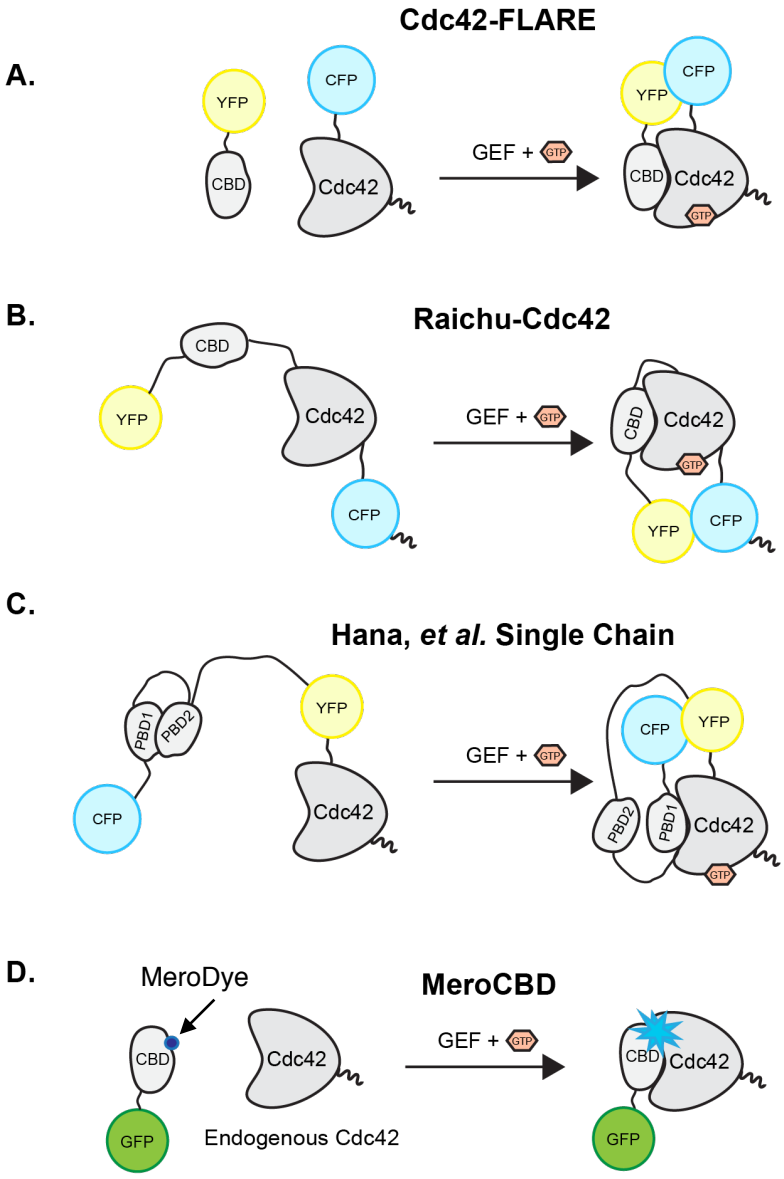


**Figure 1.7 Biosensors available for detecting Cdc42 activity.**
(**A**) The Cdc42-FLARE dual chain biosensor, with YFP-CBD and CFP-Cdc42 expressed as different polypeptide chains. This sensor has been designed by Klaus Hahn's lab (UNC). Both peptides are expressed at a 1:1 ratio from the same promoter as the result of cleavage at the T2A/P2A post translational cleavage site between the two of them (unpublished).B) The Raichu-Cdc42 single chain biosensor, in which donor and acceptor proteins are found on the same polypeptide chain: YFP-CBD-Cdc42-CFP. The CAAX motif, which is necessary for lipid modification and membrane anchoring, has been added to the CFP. Initially the K-Ras CAAX motif was used, but this has now been replaced with a native C-terminal motif (Itoh *et al.*, 2002).(**C**) Single chain biosensor designed by Hana, et al. consisting of CFP-PBD1-PBD2-YFP-Cdc42. This probe contains two tandem PAK binding domains (PBD), a design feature that reduces background FRET when the sensor is inactive (Hanna *et al.*, 2014). PBD1 preferentially binds active Cdc42 , but will interact with PBD2, when not bound to Cdc42. (**D**) MeroCBD, a merocyanine dye, is attached to the CBD, which is bound to GFP for tracking the distribution of the probe inside a cell. The dye is microinjected into cells and increases in fluorescence when bound to active Cdc42 (Nalbant *et al.*, 2004). Thus, this biosensor is capable of detecting the activity of endogenous Cdc42.

separate proteins may not distribute evenly, which could lead to false FRET measurements depending on the analysis method that is used. However, a comparison of a RhoA single chain biosensor and the corresponding dual chain sensor showed that if the ratio of donor to acceptor was kept within a factor of 5, then there was not a significant difference between a dual chain and single chain RhoA biosensor (Machacek *et al.*, 2009).

Measuring the energy transfer between two fluorophores presents many challenges. They often require specialized equipment and complex analysis methods (Wouters and Bastiaens, 2006). In addition, there are possible artifacts, that are based on the physical properties of the fluorophores and which include photobleaching, spectral bleed through, concentration-dependent fluorophore signal, and slight changes in the fluorophore spectra creating new fluorescent species that arise from environment and laser excitation (Chen *et al.*, 2003; Wallrabe and Periasamy, 2005; Colyer *et al.*, 2008; Digman *et al.*, 2008). Three methods are commonly used to detect FRET, but some methods are more prone to fluorescent artifacts and may change the results.

Sensitized emission FRET, often called ratiometric FRET, is what many people think of as traditional FRET (Figure 1.8A). In this intensity-based FRET method the donor is excited and the emission of the acceptor, which is considered the FRET signal, and donor are measured (Wallrabe and Periasamy, 2005; Hodgson *et al.*, 2008). The FRET/donor signal is used as the ratio of FRET to give relative values of changes. This can be done in live or in fixed cells and is potentially the most widely accessible method of FRET because it can be done using a widefield or confocal microscope (Ishikawa-Ankerhold *et al.*, 2012).This method is often considered difficult because it is highly

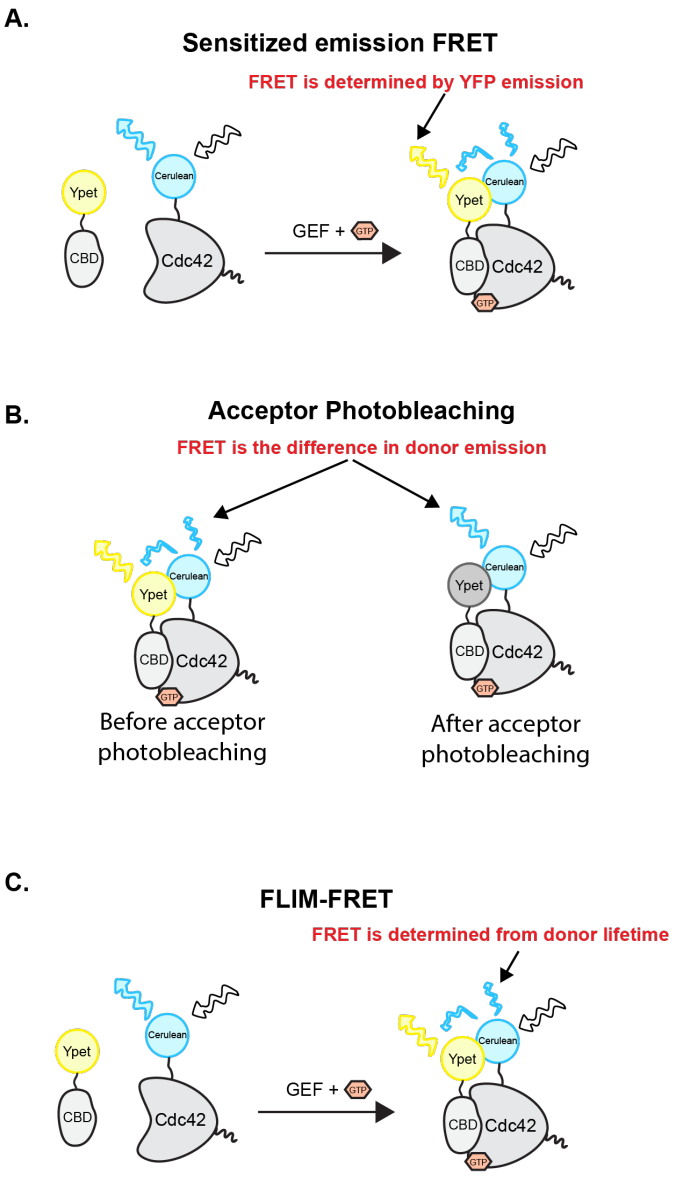


**Figure 1.8 Common methods of measuring FRET**
(**A**) *Sensitized emission FRET* (also called ratiometric FRET): Donor is excited and the emission of the acceptor is measured, which is considered the FRET signal. A ratio of FRET/donor signal is used as the ratio of FRET to give relative changes in values. This method can be performed in live or fixed cells. (**B**) *Acceptor photobleaching*: Method in fixed cells, in which the acceptor is fully bleached. As the presence of an acceptor changes the emission of the donor, donor emission is measured before and after bleaching. If there is FRET, donor emission should increase after bleaching. (**C**) *FLIM-FRET:* Method that utilizes a 2-photon laser and photon counting to excite the donor fluorophore and to measure its lifetime, which is the rate of decay in emission. The donor lifetime alone is set as the baseline and any decrease in lifetime, which will only occur in the presence of the acceptor, is considered a change in FRET.

susceptible to spectral bleed through, as well as photo bleaching, laser toxicity to the cell, sensitivity to fluorophore concentration, and channel alignment. Post imaging processing often results in increased noise that may exceed the FRET level (Hodgson *et al.*, 2008; Ishikawa-Ankerhold *et al.*, 2012). In addition, this method is qualitative as it only provides relative changes and the absolute ratio for these changes is virtually impossible to achieve (Hinde *et al.*, 2012).

Acceptor photobleaching is a second method that has become used to detect FRET (Figure 1.8B; Wallrabe and Periasamy, 2005). With this form of intensity-based FRET, the fluorescence of the donor CFP is measured before and after photobleaching of the acceptor YFP (Wallrabe and Periasamy, 2005). FRET is determined as the ratio of the CFP signal before and after photobleaching in fixed cells. FRET will lead to a smaller signal for CFP before photobleaching when it is donating its energy to YFP, than after photobleaching when YFP is no longer able to absorb the energy of the donor (Wallrabe and Periasamy, 2005). This technique is generally favored because it is a widely accessible FRET technique that only requires a confocal microscope. In addition, because YFP is fully bleached, problems with spectral bleed through are eliminated. However, this approach has several drawbacks. The bleaching event is highly destructive and can only be done once, which limits its use to single measurements (Wallrabe and Periasamy, 2005). Acceptor photobleaching also requires fixation, which has a negative impact on GTPase localization (Michaelson *et al.*, 2001; Wallrabe and Periasamy, 2005). In addition, this method is based on relative ratios of intensity and by nature is a qualitative method. However, post processing of the images to spectrally un-mix the acceptor and donor channels can be done to achieve the quantitative results

(Gu *et al.*, 2004). However, this does not take into account that CFP is susceptible to photobleaching during the YFP bleaching stage and that YFP has the potential of being converted into a CFP-like fluorophore after photobleaching, neither of which will be corrected for by spectral un-mixing (Valentin *et al.*, 2005). Finally, greater manipulations are needed during data analysis to account for unwanted bleaching, channel alignment, and relative changes (Wallrabe and Periasamy, 2005; Hinde *et al.*, 2012).

A third FRET detection method is fluorescence lifetime imaging microscopy (FLIM; Figure 1.8C). This technique measures the specific rate of fluorescence decay, or lifetime, of the donor fluorophore, which is constant unless an acceptor fluorophore is close enough to absorb the emitted energy, i.e. FRET (Elangovan *et al.*, 2002). It is a quantitative assay of FRET because it relies on the change in lifetime of a single fluorophore, which is a rate (Wallrabe *et al.*, 2006). FLIM-FRET measurements only analyze the fluorescent signal of the donor, which eliminates the need to account for two fluorophores and problems associated with spectral bleed through, channel alignment, fluorophore concentration, and photobleaching, all of which plague the other intensity based methods (Chen *et al.*, 2003; Wallrabe *et al.*, 2006; Wallrabe and Periasamy, 2005). In addition, it allows for a more direct data analysis (Wallrabe and Periasamy, 2005). FLIM is performed in live cells because the fluorescence life time is sensitive to changes in the cellular environment (Chen *et al.*, 2003; Wallrabe and Periasamy, 2005).

The phasor approach to FLIM is a powerful program to analyze very large FLIM data sets (Digman *et al.*, 2008). It simplifies data analysis and provides a global view of FLIM data by transforming the numerous complicated exponential curves acquired for each pixel into a 2-dimensional plot called the phasor plot (Digman *et al.*, 2008). The

phasor plot has several advantages. The transformation is almost instantaneous plotting every pixel to a unique position on the phasor plot according to lifetime. It provides a global view of all the lifetimes, accounting for any population changes among the fluorophores. It is directly linked to the image allowing for mapping of the lifetimes back to the image to provide a clear view of the spatial changes in lifetime within the entire image (Digman *et al.*, 2008).

In light of all these considerations, FLIM-FRET and the phasor approach appears to be the most powerful method for FRET detection. It is quantitative without post processing and avoids many of the problems associated with the intensity-based methods. It overcomes potential fluorescence artifacts associated with dual chain biosensors, but maintains the benefits of the dual chain biosensor, which are their great dynamics range and interactions of the small GTPase with regulatory proteins.

## 1.6 Advances in understanding the Golgi with small molecules

Small molecules that disrupt Golgi structure have been central to understanding Golgi organization and function. A wide range of small molecules, such as nocodazole and Brefeldin A (BFA), have contributed to our general understanding of the Golgi (Figure 1.9). These compounds disrupt Golgi membranes to different degrees and have allowed us to study the function of the Golgi as well as pathways that control its maintenance (Table 1.1). Their use is an alternative to genetic overexpression or protein knockdown approaches because they are easy to use, not restricted to cell lines that are easy to transfect, allow for manipulation and study of intramembrane traffic, can identify targets that produce specific phenotypes, and they provide acute does

dependent, often reversible effects. Many of these reagents can be readily obtained commercially and have become routinely used tools to investigate requirements for protein transport and Golgi function. In this section, I will present examples for how the study of three molecules with different effects on the Golgi have been used to increase our understanding of the Golgi.

The first comound, nocodazole has helped us to understand the relationship between Golgi organization and microtubules. This small molecule reversibly binds tubulin subunits and promotes microtubule disassembly (Head *et al.*, 1985; Turner and Tartakoff, 1989). As a result, there is extensive Golgi fragmentation and dispersal of Golgi membranes throughout the cell (Lippincott-Schwartz *et al.*, 1990). This phenotype results from nocodozole inhibiting microtubule-dependent anterograde transport from the ER to the Golgi, while only partially blocking retrograde traffic (Cole *et al.*, 1998). Therefore, Golgi proteins are relocalized to the ER, where they are sorted into vesicles for transport to the Golgi. However, the absence of microtubules leads to protein accumulation at specific locations within the ER known as ER Exit Sites (ERES), creating Golgi mini-stacks. Studies with nococazole have contributed to our understanding of the Golgi in several ways. First, they highlighted the importance of microtubules in placement and formation of the Golgi, which paved the way for later findings on the role of the microtubule motor kinesin in membrane trafficking (Minin, 1997). Second, they demonstrated that Golgi membranes could form *de novo* at specific sites on the ER (Zaal *et al.*, 1999). Lastly, they began to change the view of the Golgi from a static structure to a  highly dynamic organelle.

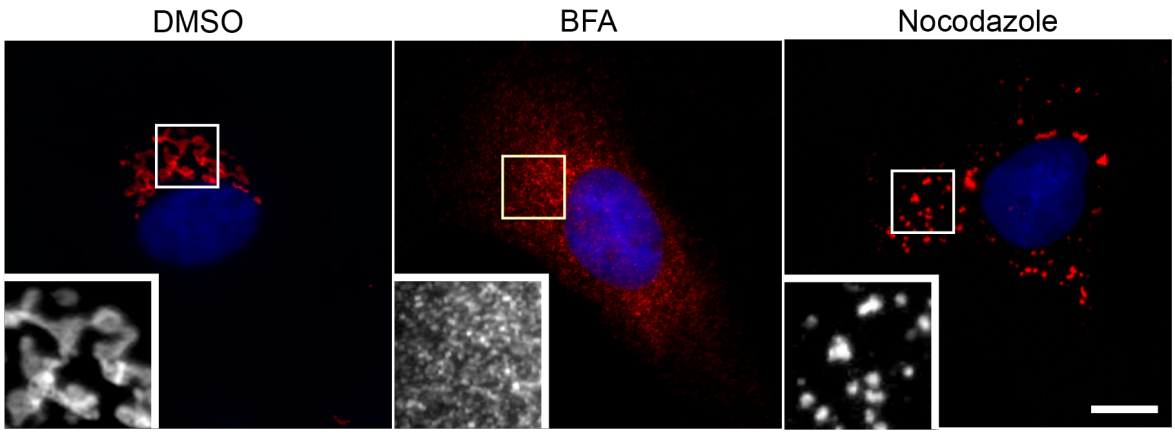


**Figure 1.9 Examples of small molecules that disrupt the organization of the Golgi**
Small molecules with Golgi-disrupting activity have often been used to study the Golgi. NRK cells were treated with DMSO as a control (left), Brefeldin A (BFA) (middle) and nocodazole (right). BFA inhibits the GEFs for Arf1, preventing the recruitment of COPI coat proteins for normal vesicle formation. As a result there is the formation of tubular structures from the Golgi and the relocalization of Golgi proteins to the ER. Nocodazole depolymerizes microtubules preventing the transport of new Golgi membranes to the pericentriolar region, which results in mini-stacks formation at ER exit sites.

**Table 1.1 A selection of small molecules used to study the Golgi**

| Small Molecule | Golgi Phenotype | Targets | Aided with discoveries | Citation |
|---|---|---|---|---|
| **Brefeldin A (BFA)** | Golgi proteins re-localized to the ER | ARF1 GEFs (GBF1, BIG1 and BIG2) | Early secretory pathway/transport and formation of Golgi membranes from the ER | (Donaldson *et al.*, 1992; Klausner *et al.*, 1992; Sciaky *et al.*, 1997; Puri and Linstedt, 2003; Lisauskas *et al.*, 2012) |
| **Nocodazole** | Golgi mini-stacks disperse throughout the cell acumulating at ER exit-sites | α/β tubulin heterodimers | Vesicular transport and Golgi maintenance at the perinuclear space | (Head *et al.*, 1985; Turner and Tartakoff, 1989; Lippincott-Schwartz *et al.*, 1990; Cole *et al.*, 1996) |
| **Ilimaquinone (IQ)** | Golgi membranes break down independent of microtubules leading to dispersal of Golgi membranes through out the cytosol | Affects methylating agents, heterotrimeric G proteins (for ARF GTPases), protein kinase D, direct target is unknown | Post Golgi transport. Methylation and membrane composition at the Golgi | (Takizawa, *et al.*, 1993; Jamora, *et al*;. 1997; Liljedahl, *et al.*, 2001) |
| **Okadaic acid** | Golgi fragments and disperses in vesicle and tubule 'clusters' throughout | Serine/threonine phosphatases types 1, 2a, and 2b | Protein secretion and inositol phospholipid synthes, particularly phosphatidicacid, is essential for the structure and function of the Golgi apparatus | (Lucocq *et al.*, 1991; Siddhanta *et al.*, 2000; Sweeney *et al.*, 2002) |
| **Monensin** | Golgi vesicles swell and disperse throughout the cell, the *trans*-Golgi is more affected then the *cis*-Golgi | Interacts with $Na^+$ and metal ions; disrupts $Ca^{2+}$ gradients and water distribution. | Secretion, retrograde pathway, sorting at the *trans*-Golgi | (Mollenhauer *et al.*, 1990) |
| **Retinoic acid (RA)** | Depending on cell line either an enlargement of the Golgi with the formation of vacuoles (keratinocytes) or an under developed Golgi (leukocytes) | Binds to the retinoic acid receptor (RAR) to induce gene transcription, Specific target for Golgi is unknown, however it is suspected that the protein kinase C cascade for proper membrane curvature is involved | Endocytic cycling, signal transduction, and membrane curvature and its role in transport/signaling | (Brown *et al.*, 1985; Wu *et al.*, 1994; Pineau *et al.*, 2008) |

Brefeldin A (BFA) is another small molecule that has increased our understanding of transport in the early secretory pathway. BFA functions by blocking GEFs for the small GTPase ARF1, preventing the recruitment of COPI vesicle coat leading to the formation of retrograde tubulovesicular structures from the Golgi-to-ER (Donaldson *et al.*, 1992; Dukhovny *et al.*, 2009). Treatment of cells with BFA induces the loss of Golgi structure through these structures, which relocalize Golgi membranes to the ER (Orcl *et al.*, 1991; Klausner *et al.*, 1992). While, BFA does not lead to redistribution of all proteins, such as the peripheral Golgi matrix proteins GM130 and GMAP-210, testing if proteins are BFA sensitive has become a common method for observing resident Golgi proteins and if retrograde transport is affected (Nakamura *et al.*, 1995; Rios *et al.*, 2004).

A third molecule of interest to Golgi researchers is illimaquinone (IQ). Treatment of cells with IQ leads to extensive vesiculation and dispersal of Golgi membranes (Takizawa *et al.*, 1993). IQ differs from nocodazole and BFA, for which molecular targets and pathways have been identified whose manipulations phenocopy the effects of the small compound, as the direct target of IQ is not known. However, IQ has still been used in studies of post Golgi transport and Golgi reassembly (Acharya *et al.,* 1998). This small molecule has been proposed to modify enzymes in the methylation cycle such as, S-adenosylhomocysteinase synthase and S-adenosylmethionine transferase (Takizawa *et al.*, 1993; Radeke *et al.*, 1999). IQ has also proposed to act through signaling of the heterotrimeric G proteins that are upstream of ARF GTPases and coatmers in vesicular transport to induce Golgi vesiculation (Jamora, *et al.,* 1998; de

Figueiredo *et al.*, 1999). The , Gβ/γ subunit of the heterotrimeric G protein is also thought to activate PKD, which is necessary for protein transport to the PM (Liljedahl, *et al*., 2001). IQ vesiculation has also been proposed to occur through phospholipase D (PLD), which generates phosphatidic acid (PA), a multifunctional lipid that has been proposed to alter membrane curvature and be involved in signaling pathways that could lead to the vesiculation phenotype (Sonoda *et al.*, 2007). Furthermore, IQ has been proposed to interact with the Tumor Necrosis Factor (TNF) ligands Death Receptor-4 and 5 (DR4 and 5) (Do *et al.*, 2014) and stabilize p53 (Florian *et al.*, 2007). IQ may interact with multiple targets, but additional work is needed to better understand this compound and its effect on the Golgi.

The study that will be described in Chapter 4 has focused on the small molecule Macfarlandin E (MacE). Incubation of cells with this spongiane deterpene produces a unique Golgi phenotype. Unlike BFA or IQ, MacE is irreversible and induces extensive Golgi fragmentation, but the resulting Golgi fragments remained in the perinuclear region. It also disrupted protein transport from the Golgi to the PM. In Chapter 4, I will discuss the use of click chemistry as an approach to determine the molecular target of MacE.

## 1.7 Conclusion

The development of new experimental procedures has had a profound impact on our understanding of the Golgi. EM paved the way for understanding Golgi morphology. Improved methods with different types of EM lead to 3D imaging, while fluorescence microscopy improvements have allowed for live cell imaging and enhanced our

understanding of protein dynamics. These advancements combined with improved biochemistry and molecular techniques and the application of small molecule studies have aided to understanding Golgi composition, function, and maintenance. We have begun to understand several of the roles played by the Golgi and its proteins play in the cell, but there are still many unknowns, such as how the Golgi regulates centrosome organization.

Understanding how Cdc42 is regulated at the Golgi and the role of GM130 in this process is the next step in clarifying how the Golgi contributes to centrosome organization. GM130 has been reported to have approximately 20 interactors, which contribute to a number of different roles at the Golgi and the cell, many of which are still not fully understood or have conflicting data. It is unclear how any of these interactions could allow GM130, which lacks a Cdc42 activation domain, to mediate Cdc42 activity and centrosome organization. Interactors have been proposed such as Tuba and RasGRF, but there are conflicting reports about localization to the *cis*-Golgi where GM130 is located. Cdc42, which is proposed to be downstream of GM130, is another enigma of the Golgi. Many questions about Cdc42 functions at the Golgi functions, such as actin regulation, have begun to be answered. However, remains unclear how Cdc42 itself is regulated at the Golgi.

To advance our understanding of Golgi functioning, I have used new technologies to produce a better understanding of the Golgi. In Chapter 3, I describe a study on the regulation of Cdc42 at the Golgi using the phasor approach to FLIM-FRET with a dual chain Cdc42 biosensor. I found that the Golgi-associated Cdc42 regulators do not contribute equally to Cdc42 activity at the Golgi. In addition, I observed that loss

of structural Golgi proteins leads to a reduction in Cdc42 activity at the PM, but not the Golgi. To my surprise, loss of Cdc42 activity at the PM correlated with defects in centrosome organization. Suggesting that PM-associated Cdc42 activity may be critical for the regulation of centrosome organization. In Chapter 4, I describe my experiments using click chemistry to identify the molecular targets of the small molecule MacE. I found that MacE appears to modify lysines so that click chemistry is unlikely to reveal a specific target of this compound. However, this finding has lead to important discoveries about how non-specific lysine binding molecules can disrupt Golgi structure. The application of these technologies has provided new information about factors that contribute to the regulation of Golgi morphology and function.

# Chapter 2:
# Materials and Methods

*Molecular biology*

The Cdc42-FLARE biosensor was based on the dual chain biosensors described in Machacek *et al.* (Machacek *et al.*, 2009). Cerulean fluorescent protein (Rizzo *et al.*, 2004) replaced CyPet to improve brightness and FRET efficiency, and residues 201-293 of Wiscott Aldrich Syndrom protein (WASP) were used as the affinity reagent. The two biosensor chains were expressed on one open reading frame with two consecutive 2A viral peptide sequences from porcine teschovirus-1 (P2A) and *Thosea asigna* virus (T2A) inserted between them, leading to the production of two chains during translation (Kim *et al.*, 2011). The biosensor is undergoing further optimization, which will be described in detail in a separate publication. For the establishment of stable Cdc42-FLARE cell lines, we used the PiggyBac (PB) all-in-one cumate expression system, PB-Cuo-MCS-IRES-GFP-EF1-CymR-Puro (PBQM812A-1, Systems Biosciences), and EF1 constitutive active expression system PB-EF1-MCS-IRES-Neo (PB533A-2, Systems Biosciences). The constructs were generated as follows:

- *PB-CuRo-MCS-EF1-CymR-Puro*: digested PB-Cuo-MCS-IRES-GFP-EF1-CymR-Puro with XcmI/AvrII to release IRES-GFP, followed by a Klenow and re-ligation.
- *PB-Cdc42-FLARE*: The Cdc42-FLARE fragment was released from pTriEx-myc-Ypet-CBD-P2A-T2A-Flag-Cer-Cdc42 (provided by Klaus Hahn, UNC) with NheI/BstBI and inserted between NheI/ClaI of PB-Cuo-MCS-EF1-CymR-Puro.

- *PB-ManII-mCherry*: ManII-mCherry cDNA (available in the Suetterlin lab) was inserted between EcoRI/NotI of PB-EF1-MCS-IRES-Neo.
- *PB-GalT-mCherry*: mCherry cDNA was inserted between NheI/NotI in PB-EF1-MCS-IRES-Neo; then GalT cDNA was PCR amplified from pYFP-GalT (generous gift from Dr. John Presley; Yilmaz Dejgaard *et al.*, 2007) and inserted between SacII/NotI 5' of the mCherry cDNA.
- *PB-mApple-p58*: mApple cDNA (generous gift from Michael Davidson; Kremers *et al.*, 2009) was first inserted between NheI/EcoRI of PB-EF1-MCS-IRES-Neo; then p58 cDNA was PCR amplified from pYFP-p58 (generous gift from Dr. John Presley; Yilmaz Dejgaard *et al.*, 2007) and inserted into EcoRI downstream of mApple using the Cold Fusion kit (Systems Biosciences).
- *ARHGAP10-myc*: The fragment encoding for amino acids 885-1346 of ARHGAP10, which contains the PH and GAP domain, was amplified from the KIAA1424 template (Nagase *et al.*, 2000) and cloned into the EcoRI site of PCDNA3.1+.
- *ARHGAP10-PM* (amino acids 1015-1346aa): generated by releasing a fragment encoding for the PH domain of ARHGAP10-PH/GAP from ARHGAP10-myc with restriction digest KpnI/NheI, followed by Klenow treatment and re-ligation mApple-farnesyl (#): Oligos, 5'-CCG GTA AGC TGA ACC CTC CTG ATG AGA GTG GCC CCG GCT GCA TGA GCT GCA AGT GTG TGC TCT CCT GAG TTT-3' and 5'AAA CTC AGG AGA GCA CAC ACT TGC AGC TCA TGC AGC CGG GGC CAC TCT CAT CAG GAG GGT TCA GCT TA-3', containing the farnesyl sequence of mApple-farnesyl-5 (gift from Dr.

Michael Davidson, Addgene plasmid # 54899) were annealed in 1X NEB buffer 2 buffer by heating to 95˚C for 5 min followed by slowly cooling to 21˚C then inserted downstream of myc at sites AgeI/PmeI.

*RNAi*

Protein depletion was carried out by transfecting U2OS cells (HTB96, ATCC) with 200nM (GM130, Golgin-84, and scrambled) or 50nM (Tuba, FGD1, and scrambled) siRNA duplexes using oligofectamine as described by the manufacturer. The following sequences were used to target GM130: 5'-AAGTTAGAGAGATGACGGAACTC-3' (Puthenveedu *et al.*, 2006), Tuba: 5'-GAGCTTGAGGGAACATACAAGATTT-3' (Kodani *et al.*, 2009), Golgin-84: 5'-AAGTAGGATCTCGGACACCAG-3' (Diao *et al.*, 2003), FGD1-*Smartpool*® (M-009612-01-0005, Dharmacon), and a scrambled control sequence 5'-AAACTAAACTGAGGCAATGCC3' (Sütterlin *et al.*, 2005). All siRNA duplexes were obtained from Life Technologies, unless noted.

*Antibodies*

Primary antibodies to the following proteins were used in this study: Calreticulin (C4606, Sigma-Aldrich), Tuba (a gift from Dr. Frank Gertler, MIT and B01P, Abnova,), Centrin2 (a gift from Dr. Jeffery L. Salisbury, Mayo Clinic and Clone 20H5, Milipore), FGD1 (HPA 000911, Sigma), myc (Clone 9E10, Cal Biochem), GM130 (Clone 35, BD Biosciences and G7295, Sigma), Giantin (gift from Dr. Vivek Malhotra, Center for Genomic Regulation, Barcelona, Spain), Kendrin (gift

from Dr. Mikiko Takahashi, Teikyo Heisei University), α-tubulin (T5168, Sigma-Aldrich), γ-tubulin (ab11310, Abcam), Cdc42 (Clone 44, BD Biosciences), and VSVG (BWG85, gift from Dr. Victor Hsu, Harvard Medical School). Secondary antibodies for immunofluorescence were from Theromofisher or Biotium and near infrared antibodies for western blots were from Licor (Lincoln, NE). For immunofluorescence, cells were fixed in either 100% ice-cold methanol (JT Baker) or 4% formaldehyde (Ted-Pella), blocked and permeabilized with 2% blocking buffer (2% FBS, 0.01% TritonX-100, and 1 X PBS), stained with primary antibodies for 1 hour at room temperature followed by staining with secondary antibodies for 1 hour. Coverslips were mounted with ProLong® Gold (Thermofisher) and imaging dishes were filled with Ibidi Mounting Medium (Ibidi).

*Cell culture, establishment of stable cell lines, and protein expression*

Parental U2OS cells (HTB96, ATCC) and all derived clonal cell lines were cultured in Advanced DMEM supplemented with 10 % FBS (Hyclone) and 2 mM GlutaMAX-I (GIBCO, Rockville, MD) at 37˚C with 5% $CO_2$. Stable cell lines were generated using the PiggyBac (PB) transposon system (System Biosciences). In brief, U2OS cells were co-transfected with a PB-transposon construct (PB-mApple-p58, PB-GalT-mCherry, PB-ManII-mCherry, PB-mApple-Farnesyl, or PB-Cdc42-FLARE) and PB-transposase using X-tremeGENE 9 (Roche) as described by the manufacturer. Cells were selected for integration of the transposon using G418 at 500μg/mL or puromycin at 2 μg/mL (Gold Biotechnology). Clonal cell lines were generated through serial dilution in 96 well

plates. Expression Cdc42-FLARE was accomplished by incubating the cells with 300 µg/mL water soluble cumate (Systems Bio Sciences) for 48 hrs. For transient transfections, DNA constructs were introduced into cells using Lipofectamine 3000 (Life Technologies) or X-treme Gene 9 (Roche) according to manufacturers protocol.

*FLIM-FRET experiment and analysis*

Cell preparation: Inducible Cdc42-FLARE cell line was seeded in 6 well dishes 60 hrs before imaging at 50% confluency. At 48 hrs prior to imaging the cells were induced with 300µg/mL cumate (Systems Biosciences) and cumate concentration was maintained constant through out the experiment. For protein depletion assays: 48 hrs before imaging, cells were transfected with RNAi using oligofectamine. For protein expression: ≈18 hrs prior to imaging, cells were transiently transfected with ARHGAP10 constructs using Lipofectamine 3000 (Life Technologies) or the cerulean control using X-treme Gene 9 (Roche). At 24 hrs prior to imaging, cells were transferred to a µDish$^{35mm,\ high}$ with Grid-500 (81166, Ibidi) that was used for live imaging and locating the previously imaged cells after fixation.

Imaging: All FLIM experiments were done in living cells, which were maintained at 37˚C with 5%$CO_2$. After live imaging, cells were fixed and the imaged cells were identified using the grid on the dish and analyzed using immunofluorescence to confirm protein deletion or expression. All data was acquired using a Zeiss LSM780 laser scanning microscope equipped with an

incubation chamber; and coupled to a two-photon Ti:Sapphire laser (Spectra-Physics) and an ISS A320 FastFLIM box to acquire the lifetime data. A LD C-Apchromat 63x/1.15 water immersion objective (Zeiss) was used for all live cell experiments and a Plan-Apochromat 63x/1.40 Oil DIC was used for all fixed experiments. Cerulean was excited at 800nm with 2.5% laser power from the 2-photon laser pulsing at 80fs at a repetition of 80MHz. The laser light was separated from the fluorescence signal using a SP 760 nm dichroic filter. The fluorescence signal was directed through a 509 LP CFP/YFP filter; the signal was then split between two photomultiplier detectors (H7422P-40 of Hamamatsu), equipped with either a CFP 470/22 or YFP 542/27 bandwidth filter. FLIM data was acquired with the SimFCS software developed at the Laboratory of Fluorescence Dynamics (UCI) with a pixel dwell time to 25.61 µs/pixel and the pixel frame size set to 256 x 256, and the electronic zoom used to enhance resolution produced an image size of 24.53 x 24.53 µm (pixel size of ≈ 100 nm). Fifty frames were collected per sample to limit exposure time to the laser to ≈1.5-2 min. For each experiment, a solution of 50µM Coumarin 6 (Sigma) dissolved in 100% ethanol was imaged as a calibration control. Zen Black 2012 (Zeiss) was used to control the microscope and to collect confocal images of the mCherry/mApple cellular markers acquired in parallel with FLIM data and images of fixed cells.

Data analysis: FLIM data was processed to map the FRET efficiency for each cell using the SimFCS software (LFD, UCI) as described previously (Hinde *et al.*, 2012). In brief, files were calibrated against the Coumarin 6 control that has a

known lifetime of 2.6 ns. The fluorescence lifetime of each pixel of the image was then mapped to the phasor plot. The lifetime of the cerulean control cells and the auto fluorescence signal were set on the phasor and the FRET calculator in SimFCS was used to generate the FRET trajectory for mapping activity in cells. To determine percent of FRET at specific locations within the cell, images of mApple/mCherry-Golgi or PM marker taken at the time of live imaging were imported into Fiji using BioFormats and thresholded using the IsoData method or hand traced for the PM with a 20 pixel overlay brush (Ridler and Calvard, 1978; Linkert *et al.*, 2010; Schindelin *et al.*, 2012). Theses images were imported into SimFCS and used to mask the FLIM data for the corresponding cell to calculate the average percent of FRET at the Golgi or plasma membrane. To analyze the data, Analysis of Variance (ANOVA) was used with post-hoc t-tests in the R software.

*Protein Transport*

VSVGts045-myc or VSVG-KDELR (a generous gift from Dr. Jennifer Lippincott-Schwartz, National Institute of Health; Cole *et al.*, 1998) was transiently transfected into wild type U2OS or U2OS-Cdc42-FLARE cells using X-treme Gene 9 (Roche) and incubated at 37˚C at 5% $CO_2$ for 18 hrs. Prior to transport experiments, media was supplemented with 25μM HEPES pH 7.4. Cells were then incubated at 40.5˚C for 4 hrs to accumulate VSVG in the ER, followed by a shift to the permissive temperature of 32˚C to allow the protein to exit the ER. Cells were fixed in 4% formaldehyde (Ted-Pella) at 0, 20, 60, or 120 min after

shift to 32˚C and processed for immunofluorescence analysis using an Axiovert 200M microscope with Axiovision software (Zeiss). Cells with VSVG-KDELR were incubated for 2hr at 32˚C to accumulate protein in the Golgi, followed by a shift to 37˚C for 0, 2, 4, or 6 hrs to permit retrograde transport to the ER. Image analysis was done with image J.

*Click chemistry on coverslips containing cells*

Coverslips with NRK cells were placed in a 24 well dish. 250µL of cell media + 1mM HEPES containing 80µg/mL (unless stated otherwise) MacE-analog was added and samples were incubated for 2 hrs unless stated otherwise. Cells were fixed in 4% FA for 10 min, washed with 1X PBS twice, then added blocking buffer for 45-60 min (1X PBS, 0.1% Triton X, 2% FBS, 0.002% $NaN_3$). 50µL of TEA + Click reagents (150 mM NaCl, 50 mM Triethanolamine, pH 7.4, 1mM CuSO4, 100 µM rhodamine/biotin-N3/alkyne, 100 µM TBTA, 1 mM Na Asc) was carefully pipetted on to parafilm, and the coverslip was placed cell side down on top of the drop. A humid environment was created using wet paper towel and a plastic Tupperware or petridish lid. Incubated at RT for 1hr. Coverslips were transferred back to 24 well dish and washed 5 x 3 min in PBS. If using biotin, all cover slips were stained with anti-biotin (mouse, Invitrogen, dilution 1:1000) at RT for 1hr. If rhodamine-azide was used, coverslips were washed 5 x 3min with PBS prior to staining. The Golgi was stained with rManII (1:5,000, a gift from Dr. Brian Burke, University of Florida, Gainesville, FL). Appropriate Alexaflour secondaries (Invitrogen) and Hoescht 33342 (1:50,000) were diluted in blocking buffer and

used for 1hr at RT. Coverslips were washed 5 x 3 min with PBS then mounted with gelvatol and visualized on Axiovert 210.

*Click chemistry in cell lysate*

Lysate was collected by scraping cells on ice and resuspending in TEA buffer (150 mM NaCl, 50 mM Triethanolamine, pH 7.4) and lysing by 10 freeze-thaw cycles that alternated between liquid nitrogen (LN2) and 37˚C heat block. Reactions containing 25 µg of protein in a total volume 25 uL had 10µg MacE-analog added if they were not treated before. 1.5mL labeling cocktail added (1mM $CuSO_4$, 100 µM biotin-N3/alkyne, 100 µM TBTA, 1 mM Na Asc) and were vortexed briefly. Samples were incubated at RT for 1 hr. Then 1 mL ice-cold methanol was added, reactions were vortexed, then put at -80˚C for 2 hrs for protein precipitation. Precipitated proteins were centrifuged at 13K x g rpm at 4˚C for 10 minutes. Supernatant fluid was aspirated and pellet was air-dried for 30 min - 1 hr. Samples were re-suspended in 15 µL of resuspension buffer (4% SDS, 150 mM NaCl, 50 mM triethanolamine, pH 7.4). Then 15 µL of loading buffer (0.2% bromophenol blue, 20% glycerol, 1.4% beta-mercaptoethanol) was added Samples were heated at 95˚C for 5 min and run on 7.5% SDS-PAGE gel. Western blot analysis was run and proteins were transferred on to nitrocellulose membrane. Biotin-free blocking buffer (7% BSA in PBS supplied with 0.1% Tween-20) was used for 1hr. 690-Streptavidin (1:5000, Licor) was diluted in Biotin-Free blocking buffer and stained for 1 hr. Blot was washed 5 x 5 min with PBST, last wash PBS. Visualized on Odyssey-SA Ponceau staining was used to

confirm if any protein was lost during the cu-click protocol, because protein concentration could not be confirmed by Bradford assay due to high levels of detergent in the sample after the click reaction or DC Bradford due to the residual copper.

# Chapter 3:
# Spatial analysis of Cdc42 activity reveals a role for plasma membrane-associated Cdc42 in centrosome regulation


## Abstract

The ability of the small GTPase Cdc42 to regulate diverse cellular processes depends on tight spatial control of its activity. Cdc42 function is best understood at the plasma membrane (PM), where it regulates cytoskeletal organization and cell polarization. Active Cdc42 has also been detected at the Golgi, but its role and regulation at this organelle is partially understood. Here I describe the spatial analysis of Cdc42 activity with the dual chain biosensor Cdc42-FLARE and the phasor approach to FLIM-FRET. This quantitative approach revealed that Cdc42 is active at each Golgi cisternum, and that this activity is controlled by Tuba and ARHGAP10, two Golgi-associated Cdc42 regulators. To our surprise, FGD1, another Cdc42 GEF at the Golgi, was not required for Cdc42 regulation at the Golgi, although its depletion lowered Cdc42 activity at the PM. Similarly, changes in Golgi morphology did not affect Cdc42 activity at the Golgi, but were associated with a substantial reduction in PM-associated Cdc42 activity. Interestingly, cells with reduced Cdc42 activity at the PM displayed altered centrosome morphology, suggesting that centrosome regulation may be mediated by active Cdc42 at the PM. Our study describes a novel quantitative approach to determine Cdc42 activity at specific subcellular locations and reveals new regulatory principles and functions of this small GTPase.

## Introduction

Tight spatial regulation of the small Rho GTPase Cdc42 is required for many cellular processes, including cell polarity, cell survival, adhesion, migration, cell cycle progression and membrane trafficking (Coso *et al.*, 1995; Nobes and Hall, 1995; Kroschewski *et al.*, 1999; Etienne-Manneville and Hall, 2001). Each of these functions depends on regulated localization and activation of Cdc42, which is achieved through its recruitment to a specific cellular membrane. Membrane association of Cdc42 is necessary for its activation and is primarily determined by the modification of its C-terminal end with a geranylgeranyl anchor (Michaelson *et al.*, 2001). Additional contributing factors are guanine nucleotide exchange factors inhibitors (GEFs) and guanine nucleotide dissociation inhibitors (GDIs) (Michaelson *et al.*, 2001) (Ku *et al.*, 2001; Salazar *et al.*, 2003; Egorov *et al.*, 2009). Membrane trafficking has also been found to be critical for Cdc42 localization and activation (Osmani *et al.*, 2010).

Cdc42 is a functional component of the Golgi. Diverse methods, such as fractionation, immunofluorescence, and electron microscopy, have been used to detect this small GTPase at the Golgi (Erickson *et al.*, 1996; Luna *et al.*, 2002; Matas *et al.*, 2004) (Osmani *et al.*, 2010). This population of Cdc42 is active, as observed directly through biosensor experiments and indirectly through the visualization of the Cdc42 effectors Arp2/3 and N-WASP at the Golgi (Nalbant *et al.*, 2004; Baschieri *et al.*, 2014; Luna *et al.*, 2002; Dubois *et al.*, 2005). Golgi-associated Cdc42 has been implicated in Golgi function because disrupting its activity caused defects in protein transport through the Golgi (Wu *et al.*, 2000;

Luna *et al.*, 2002; Egorov *et al.*, 2009; Hehnly *et al.*, 2009; Park *et al.*, 2015). It addition, it has also been linked to the organization and function of centrosome (Kodani *et al.*, 2009). However, direct support for these models is missing because it has not been possible to disrupt Cdc42 activity only at the Golgi.

The regulation of Cdc42 activity at the Golgi is incompletely understood. Two Cdc42-specific GEFs, Tuba and FGD1, are reported to localize to the Golgi. While Tuba was observed at the Golgi in rat brain cryosections and in the perinuclear region of HeLa cells (Salazar *et al.*, 2003; Kodani *et al.*, 2009), FGD1 localized to the *trans*-Golgi of HeLa, COS-7, and MC3T3 osteoblasts (Estrada *et al.*, 2001; Egorov *et al.*, 2009). Golgi membranes also host a Cdc42-specific GTPase activating protein (GAP), ARHGAP10 (Dubois *et al.*, 2005). In addition, GM130 and Coronin7, two resident Golgi proteins without typical GEF and GAP domains, function in the regulation of Cdc42 activity at the Golgi. Biochemical assays in total cell lysates showed that GM130 controls about 50% of cellular Cdc42 activity (Kodani *et al.*, 2009). This contribution of GM130 is proposed to be through binding and sequestering RasGRF, a Ras GEF that associates with inactive Cdc42 at the plasma membrane (Calvo *et al.*, 2011; Baschieri *et al.*, 2014). Coronin7, in contrast, functions in limiting Cdc42 activity at the Golgi. Its loss resulted in excessive N-WASP-mediated actin polymerization at the Golgi and a disrupted Golgi phenotype (Bhattacharya *et al.*, 2016). In spite of these studies, it remains unclear which of all these regulatory proteins actually contribute to the control of Golgi-associated population of Cdc42.

Several methods have been developed to detect intracellular Cdc42 activity. Biochemical assays, such as the PAK-CRIB binding assay, reveal the level of Cdc42 activity in total cell lysates (Benard and Bokoch, 2002). They use specific effector domains to isolate activated, GTP-bound Cdc42 molecules, but have the disadvantage of not providing any spatial information. Finally, Förster Resonance Energy Transfer (FRET) biosensors provide spatial information on the activity of small GTPase such as Cdc42, inside a cell (Machacek *et al.*, 2009; Kunida *et al.*, 2012), however, as discussed below, the biosensor and the method of FRET detection has to be carefully selected.

Commonly used Cdc42 biosensors have limitations. The MeroCBD probe described by Nalbant *et al*. is an elegant tool to Cdc42 activity measurement in living cells. While it has demonstrated the presence of active Cdc42 at the Golgi, this probe is impractical for routine use because it has to be introduced into cells by microinjection, (Nalbant *et al.*, 2004). Genetically-encoded FRET biosensors are easier to use because they can be expressed transiently or stably. Single chain probes avoid artifacts associated with channel alignment, but their design with the donor fluorophore fused to the C-terminus of the small GTPase, blocks interaction with RhoGDIs, which can affect small GTPase localization and regulation (Michaelson *et al.*, 2001; Itoh *et al.*, 2002; Hanna *et al.*, 2014). Dual chain biosensors have a free C-terminus and display a greater dynamic range of detection than their single chain counterparts, but are prone to fluorescence artifacts due to unequal concentration of fluorophore-tagged proteins inside a cell (Machacek *et al.*, 2009).

FLIM is a powerful method to measure FRET. It detects the specific rate of fluorescence decay, or lifetime, of only the donor fluorophore, which is constant unless an acceptor fluorophore is close enough to absorb the emitted energy, i.e. FRET (Elangovan *et al.*, 2002). Thus, FRET detection by FLIM eliminates the problem of the uneven fluorophore concentration intrinsic to a dual chain biosensor and overcomes a major weakness of this type of biosensor(Wallrabe and Periasamy, 2005). FLIM measurements also avoid issues with spectral bleed-through, channel alignment and photobleaching (Chen *et al.*, 2003; Wallrabe *et al.*, 2006).

FLIM measurements have additional advantages. Because the fluorescence life time is sensitive to changes in the cellular environment, FLIM is performed in living cells, which avoids possible fixation artifacts (Michaelson *et al.*, 2001; Chen *et al.*, 2003; Wallrabe and Periasamy, 2005). In addition, they are able to differentiate between different fluorophore species and generate quantitative maps showing the average fraction of FRET (Hinde *et al.*, 2012). FLIM is superior to traditional intensity-based ratiometric methods because it eliminates fluorescence artifacts inherent to biosensor design, which may lead to false measurements of RhoGTPase activity (Wallrabe and Periasamy, 2005; Hinde *et al.*, 2012).

FLIM data can be readily analyzed with the phasor approach, which describes the transformation of the numerous exponential fluorescence decay curves of each pixel into a 2-dimensional plot called the phasor plot (Digman *et al.*, 2008). This transformation occurs almost instantaneous and plots each pixel

to a unique place on the phasor plot according to lifetime. As the phasor plot is directly linked to the image, it allows the mapping of the lifetimes back to the image to provide a clear view of spatial changes in lifetime within the image. Overall, the phasor approach to FLIM simplifies the analysis of large FLIM data sets and provides a global view of FLIM data inside a cell.

In this study I used the phasor approach to FLIM with the improved dual chain biosensor Cdc42-FLARE (Klaus Hahn, unpublished) to examine Cdc42 activity in response to manipulations of Golgi-associated Cdc42 regulators and Golgi organization. I demonstrate that Cdc42 activity is present throughout the Golgi and that this activity is differentially regulated by ARHGAP10, Tuba, and FGD1. Cdc42 activity at the Golgi was independent of Golgi structure, but I detected a requirement for normal Golgi organization for the activation of PM-associated Cdc42. Interestingly, Cdc42 activity at the PM, not at the Golgi, was necessary for the control of centrosome organization and function.

## Results

### Spatial detection of Cdc42 activity with the Cdc42-FLARE biosensor and the phasor approach to FLIM-FRET

I generated a stable imaging cell line to measure Cdc42 activity in living cells. I used a novel genetically-encoded dual chain biosensor called Cdc42-FLARE (Klaus Hahn, UNC, unpublished), which employs the cerulean/YPet FRET pair. In this FRET pair, which will be described in greater detail in a separate manuscript, the donor fluorophore cerulean is on the N-terminus of Cdc42, while the acceptor fluorophore YPet is fused to the CRIB domain of the Cdc42 effector N-WASP (Figure 3.1A). To avoid excessive expression of the biosensor and to achieve similar expression levels in all cells, I generated a stable clonal U2OS (human osteosarcoma) cell line that expresses Cdc42-FLARE from an inducible promoter. This imaging cell line also constitutively expressed the Golgi protein Mannosidase II (ManII) fused to mCherry to label the *medial*-Golgi cisternae (Figure 3.1B). I routinely induced this imaging cell line for 48 hours, which led to an enrichment of cerulean-Cdc42 at the Golgi as previously reported (Erickson *et al.*, 1996; Michaelson *et al.*, 2001). For this entire study, I focused on cells with a maximum of 1-3 neighboring cells so that most of its plasma membrane (PM) was not in contact with other cells.

Inducible expression of Cdc42-FLARE did not alter cell morphology and behavior. A comparison of WT U2OS, uninduced and induced U2OS-Cdc42-FLARE cells in an immunofluorescence analysis showed no difference in the organization of the endoplasmic reticulum (ER), Golgi and cytoskeleton (Figure 3.2). In addition, Cdc42- dependent functions, such as anterograde and

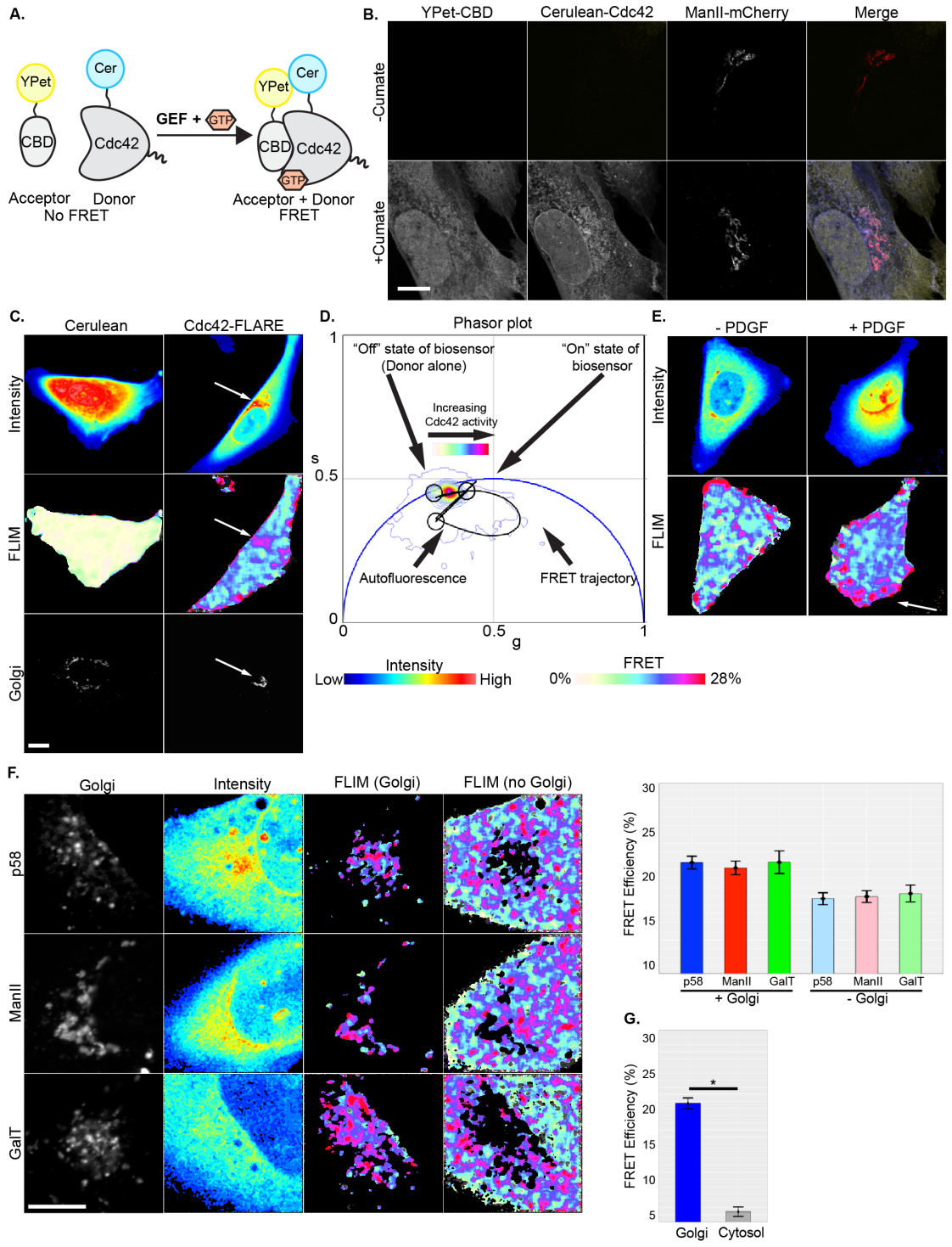


**Figure 3.1 Cdc42 activity inside a cell can be visualized with the phasor approach to FLIM-FRET**

**Figure 3.1: Cdc42 activity inside a cell can be visualized with the phasor approach to FLIM-FRET.** (**A**) Cartoon of the dual chain biosensor Cdc42-FLARE with the FRET pair cerulean-Cdc42 and YPet-CBD in its inactive and active state. (**B**) The stable U2OS-Cdc42-FLARE cell line, which inducibly expresses Cdc42-FLARE while constitutively expressing ManII-mCherry, was left uninduced (top row) or was induced with cumate for 48hours (bottom row). Confocal images of representative cells are shown. (**C**) Intensity and FLIM maps of control cells, which express the cerulean donor alone, or the U2OS-Cdc42-FLARE cell line after induction for 48 hours. The intensity maps (top row) use a blue (low intensity) to red (high intensity) scale to show the distribution of cerulean (left panel) or cerulean-Cdc42 (right panel). The FLIM maps (middle row) use a white to magenta scale to show FRET efficiencies in the range from 0-28%, which are calculated from the lifetimes of cerulean through the phasor plot shown in Fig. 1D. (**D**) Phasor plot of the distribution of cerulean lifetimes for the cells from Fig. 1C with the superimposed theoretical FRET trajectory, calculated with the SIM-FCS software. (**E**) FRET efficiencies of the Cdc42-FLARE biosensor in migrating and non-migrating cells. U2OS-Cdc42-FLARE imaging cells, after cumate induction for 48 hours, were left untreated (left column) or incubated with PDGF to stimulate migration (right column). Intensity maps of cerulean-Cdc42 are shown, as well as FLIM maps, which reflect FRET efficiencies. (**F**) FRET efficiencies at the *cis*-, *medial*-, and *trans*-Golgi cisternae measured in U2OS-Cdc42-FLARE imaging cell lines constitutively expressing either p58-mApple, ManII-mCherry or GalT-mCherry, respectively (left column). The intensity for cerulean-Cdc42 in these cells is shown (second column). FRET efficiencies at specific Golgi cisternae (“Golgi”), or in the area surrounding the Golgi (“no Golgi”), was extracted by overlaying FLIM maps with thresholded images of each Golgi marker. Graph shows the average FRET efficiency at each Golgi cisternae and surrounding area determined form 3 independent experiments with 8 cells per experiment. (**G**) Graph shows a comparison of average FRET efficiencies between randomly selected areas in the cytosol (30 x 30 pixels, half way between the perinuclear region and the PM) and the Golgi, marked by ManII-mCherry. This analysis is based on FLIM maps of whole cells and was performed for 8-12 cells per experiment, and 3 independent experiments. Representative cells are shown for all images. All scale bars: 10μM. * $p < 0.0001$.

---

retrograde protein transport at the Golgi as well as filopodia formation, were unaffected by expression of this biosensor (Figure 3.3A and B). Finally, the organization of the centrosome, which our lab has reported to be altered in cells with reduced Cdc42 activity, was normal (Figure 3.2; Kodani *et al.*, 2009).

I used the phasor approach to FLIM-FRET to detect the activity of this biosensor. I first defined the range of FRET changes. The intensity map (blue to red scale) of cells expressing cerulean in the absence of an acceptor showed greater intensity in the center of the cell (Figure 3.1C, left panel). As FLIM is independent of fluorophore concentration, the fluorescence lifetime of cerulean was uniform (Figure 3.1C, middle panel), corresponding ≈2.8ns on the universal

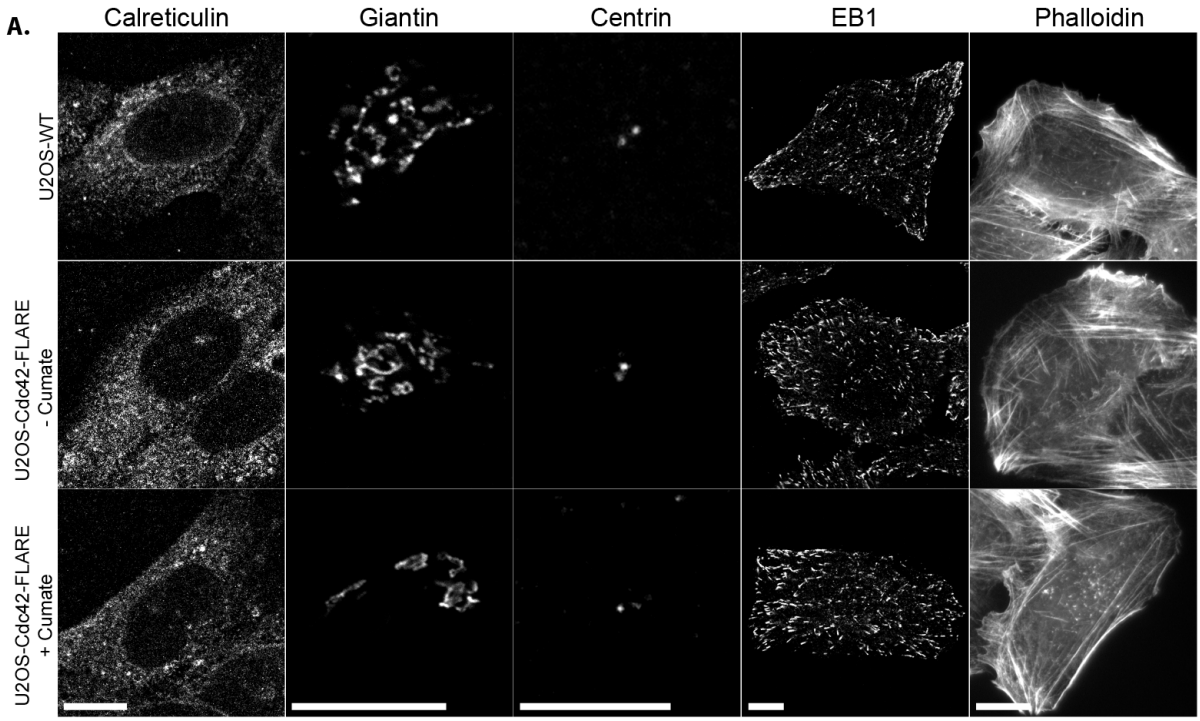


**Figure 3.2 Expression of Cdc42-FLARE does not affect cell morphology**
A comparison of WT U2OS cells, uninduced and induced U2OS-Cdc42-FLARE cells. The ER was detected with antibodies to calreticulin, the Golgi with antibodies to Giantin and the centrosome with antibodies to centrin. I also examined microtubule and F-actin organization, which were visualized with antibodies to the (+) end binding protein EB1 or phalloidin, respectively. Scale bar for all images: 10μm.

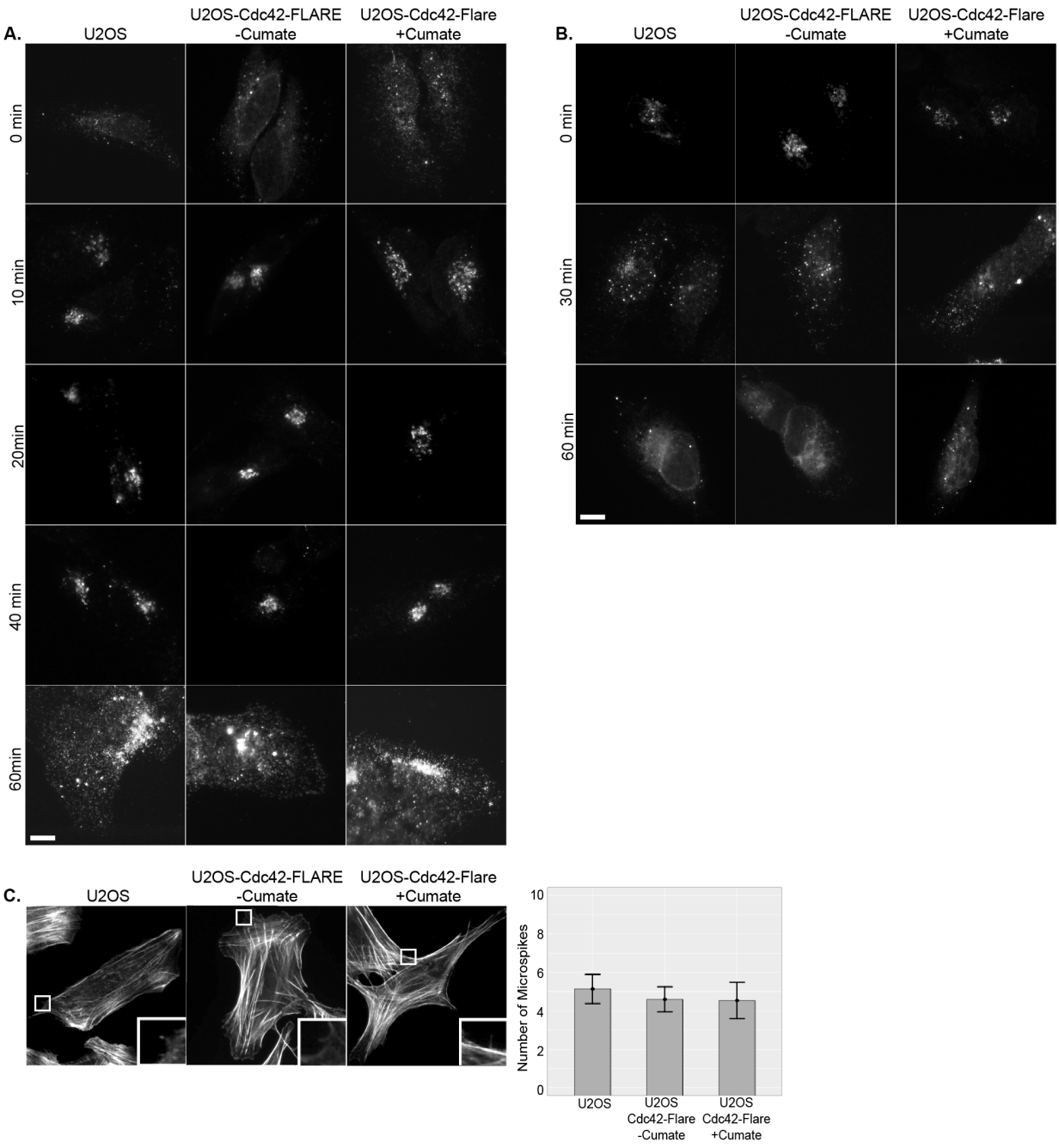


**Figure 3.3 Expression of Cdc42-FLARE does not affect Cdc42-associated functions.**

**Figure 3.3 Expression of Cdc42-FLARE does not affect Cdc42-associated functions.**
(**A**) Anterograde transport of the temperature sensitive mutant *ts*045-VSV-G-myc was observed in WT U2OS, uninduced and induced U2OS-Cdc42-FLARE cells. 48 hrs before the experiment, U2OS-Cdc42-FLARE cells were induced with cumate. 24 hours prior to the experiment, the construct encoding for *ts*045-VSVG-myc was transfected into these cells. *ts*045-VSVG-myc was first accumulated in the ER for 6hrs at 42˚C then allowed to be transported to the Golgi and the PM by shifting cells to 32˚C. Cells were fixed at 0, 10, 20, 10 or 60 min after the temperature shift to 32˚C. Cells were analyzed by immunofluorescence with antibodies to myc to monitor the localization of *ts*-045-VSV-G-myc at the ER, Golgi or PM. (**B**) Retrograde transport was measured in U2OS, uninduced and induced U2OS-Cdc42-FLARE cells using the temperature sensitive mutant KDELR-VSV-G {Cole:1998wq}. 48 hours before the experiment, cumate was added to induce Cdc42-FLARE expression. 24 hours prior to the experiment, the construct encoding for KDEL-VSV-G was transfected into cells. KDEL-VSV-G was first accumulated in the Golgi for 4 hrs at 32˚C and then allowed to be transported to the ER by shifting cells to 37˚C. Cells were fixed at 0, 30 and 60 min and analyzed for the localization of VSV-G with VSV-G specific antibodies. (**C**) I examined the formation of filopodia, a characteristic measure of elevated Cdc42 activity, in U2OS, uninduced and induced U2OS-Cdc42-FLARE cells. Cells were seeded onto glass coverslips and fixed 24 hrs later and staining with phalloidin-rhodamine. > 30 cells were counted per condition (n=3). Scale bar: 10μM.

---

semi-circle of the phasor plot (Digman *et al.*, 2008), and was quenched to a maximum of ≈1.9ns. The elliptical trajectory shown in the phasor plot coordinates indicate that the maximum FRET efficiency detected was 28% for our experiments (Figure 1D). Given that this biosensor is designed to report the on and off FRET states of the optically active biosensor, the line that connects the high FRET (on state) to the no FRET (off state) phasors gives the fractional population of the active biosensor. Thus I report on the fraction of active Cdc42 molecules within the population, with “% of FRET”, with 100% indicating the highest fraction of active Cdc42, while 0 % shows no active small GTPase. Cerulean-Cdc42 was enriched in the perinuclear region of Cdc42-FLARE expressing cells, where it colocalized with the Golgi marker ManII-mCherry. In these cells, the fraction of active Cdc42 molecules was higher at the Golgi and the PM than in adjacent areas, which was detected as a right shift on the phasor

plot (Hinde *et al.*, 2012). This data is consistent with reports by the Hahn lab with the MeroCBD biosensor, which showed activity of endogenous Cdc42 at the Golgi in non-polarized cells (Nalbant *et al.*, 2004).

I validated our assay by monitoring Cdc42 activity at the leading edge of polarized cells, a well-established site for of active Cdc42 (Nalbant *et al.*, 2004; Monypenny *et al.*, 2009; Hanna *et al.*, 2014). I stimulated cell polarization and migration in collagen I-coated chemotaxis chambers using PDGF and performed FLIM-FRET measurements. As expected, there was high FRET at the leading edge of the cell, which was not seen in unstimulated control cells (Figures 1E and 3.4).

I next monitored Cdc42 activity at individual Golgi cisternae. I therefore generated additional U2OS imaging cell lines that expressed Cdc42-FLARE together with specific markers of the *cis*- or *trans*-Golgi (Figure 3.1F). To increase the resolution at the Golgi, I focused on a 25.29 $\mu m^2$ region (≈100nm/pixel), which I found to be the smallest area to contain most Golgi membranes. In each of these cell lines, Cdc42-FLARE was enriched at the Golgi. To isolate Cdc42 activity at each individual Golgi cisternae, I overlaid the FLIM data with a mask of Golgi cisternae-specific markers, which were generated by thresholding images of mApple-p58, ManII-mCherry, or GalT-mCherry recorded in parallel. This approach revealed similar average fractions of active Cdc42 of 76.98%, 74.13%, and 73.8% at the *cis*- (mApple-p58), *medial*- (ManII-mCherry) and *trans*- (GalT-mCherry) Golgi, respectively. Whole cell images also revealed FRET in areas immediately adjacent to each cisternal marker. However, the

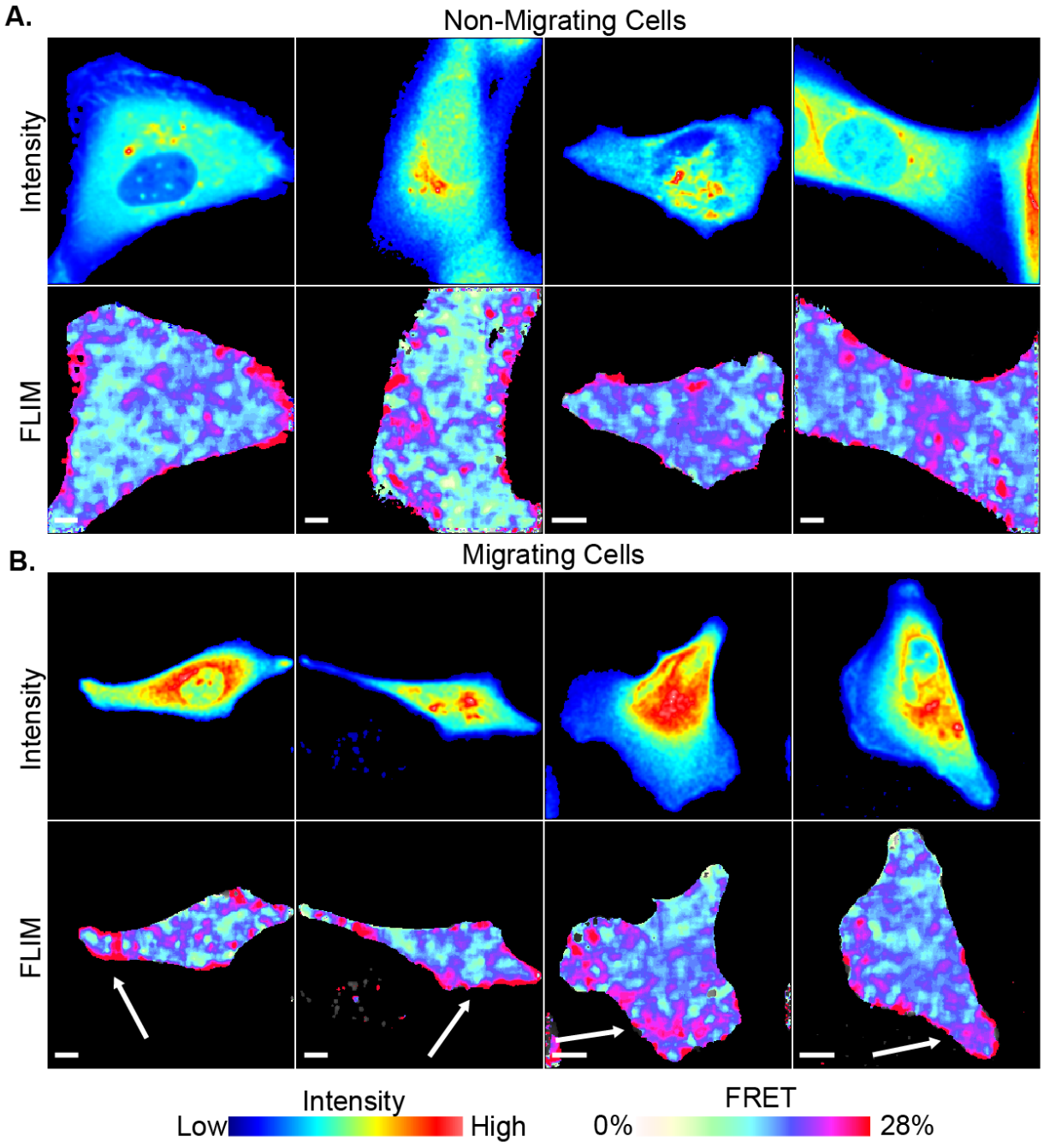


**Figure 3.4 Cdc42 is active at the leading edge in migrating cells**
FRET efficiency of the Cdc42-FLARE biosensor in 4 additional representative non-migrating and migrating U2OS-Cdc42-FLARE cells. U2OS-Cdc42-FLARE cells, induced for 48 hours, were seeded in a 2D chemotaxis slide and (**A**) left untreated as a negative control (left column) or **(B)** incubated with 625 ng/mL PDGF in one chamber to stimulate migration. Intensity and FLIM maps are shown.

percentage of active Cdc42 in these areas was lower than at the Golgi. The

fraction of active Cdc42 was even lower in randomly selected areas in the cytosol at half the distance between the Golgi and the PM (Figure 3.1G). From these experiments, I conclude that the Cdc42-FLARE biosensor with the phasor approach to FLIM-FRET is capable of confirming an enrichment of active Cdc42 at the leading edge and the Golgi. This assay, which provides best spatial resolution at a specific cellular location at a 5.5X fold zoom (25.2 $\mu m^2$, ≈100nm/ pixel) also showed similar levels of Cdc42 activity throughout the Golgi. While I detected a lower level of active Cdc42 also at other membranes in the perinuclear region, randomly selected areas in the cytosol displayed ≈4 fewer active Cdc42 molecules, demonstrating that the signal in the perinuclear region is specific.

**Golgi-associated Cdc42 regulators have differential roles in controlling Cdc42 activity at the Golgi**

I used the U2OS-Cdc42-FLARE cell line to investigate the role of the Golgi-associated GAP ARHGAP10 in the regulation of Cdc42 activity at the Golgi. This protein has been implicated in Cdc42 regulation at the Golgi through indirect measurements of protein transport (Dubois *et al.*, 2005). Consistent with published data, a truncated form that only contains the PH and GAP domains localized to the Golgi in our imaging cell line (Figure 3.4A; Dubois *et al.*, 2005). FLIM-FRET analysis in cells expressing this construct revealed a significant decrease in Cdc42 activity at the Golgi, with a reduction in the percentage of FRET from 71.46 % to 49.2% ($t(52)=18.1771$, $p< 0.0001$; Figure 3.4B). This

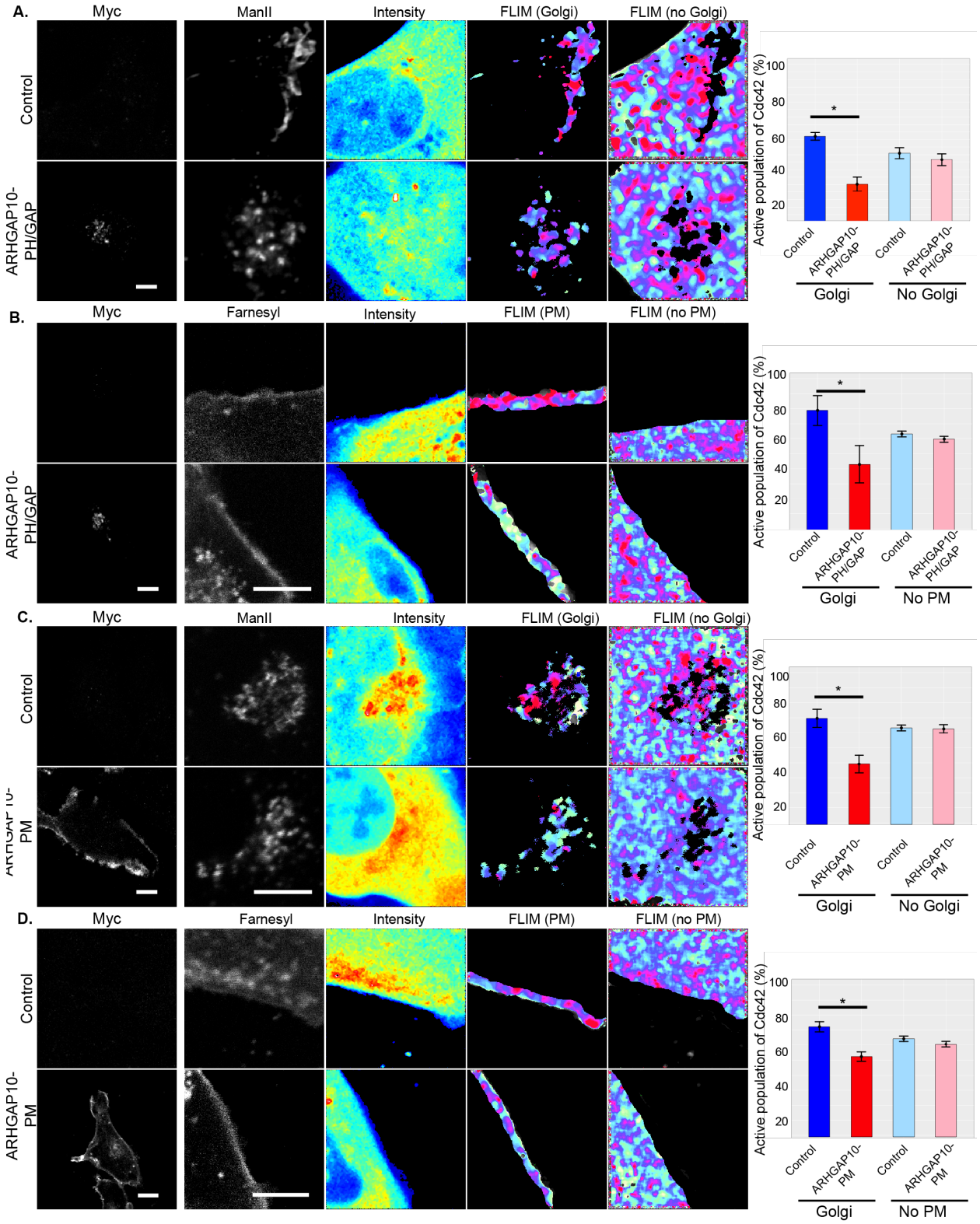


**Figure 3.4 ARHGAP10 controls Cdc42 activity at the Golgi and PM**

**Figure 3.4 ARHGAP10 controls Cdc42 activity at the Golgi and PM**
A myc tagged ARHGAP10 truncation consisting of the PH and GAP domain (ARHGAP10-PH/GAP), which is targeted to the Golgi, and a myc tagged ARHGAP10 truncation consisting of the GAP domain and a farnesylation tag (ARHGAP10-PM), which is targeted to the PM, were transfected into the U2OS-Cdc42-FLARE imaging cell line that constitutively expresses ManII-mCherry or mApple-Farnesyl. FRET efficiencies were determined with the phasor approach to FLIM-FRET for these cells. (**A**) For each cell that was analyzed by FLIM-FRET, expression and localization of the ARHGAP10-PH/GAP truncation to the Golgi, as visualized by ManII-mCherry, was verified through immunofluorescence staining with antibodies to myc. Intensity and FLIM maps of representative cells at the Golgi (marked by ManII-mCherry, "Golgi") and surrounding area ("no Golgi"). The graph shows average FRET efficiencies at the Golgi and surrounding area from 3 independent experiments and at least 8 cells per experiment. (**B**) Same as (A), except ARHGAP10-PH/GAP was transfected into Cdc42-FLARE cells with mApple-Farnesyl. (**C**) Same as (A) except ARHGAP10-PM was transfected into the Cdc42-FLARE line with ManII-mCherry . (**D**) Same as (C) except ARHGAP10-PM was was transfected into Cdc42-FLARE cells with mApple-Farnesyl. *$p < 0.0001$.

---

effect was specific for the Golgi because adjacent areas devoid of Golgi membranes did not show statistically significant changes in the fraction of active Cdc42 molecules, respectively. However, using the ARHGAP10 truncation targeted tot he Golgi I also found the Cdc42 activity was significantly reduced at the PM from 78.83% to 43% ($t(14)=6.0096, p < 0.0001$) of the active population of Cdc42. Similarly at the PM I say that expression of the ARHGAP truncation targeted to the PM (ARHGAP10-PM) was reduced in the fraction of FRET from 72.20% to 52.34% ($t(56)=8.6146, p< 0.0001$) at the PM and from 69.61% to 39.1% ($t(34)=7.6208, p < 0.0001$) at the Golgi. I conclude that expression of ARHGAP10 at either the Golgi or the PM leads to a reduction of Cdc42 activity at both the PM and the Golgi; therefore it functions as a regulator of Cdc42 activity at both location. While this provides the first direct evidence that manipulations of a Cdc42 regulator lead to a decrease in Cdc42 activity at the Golgi and PM, a caveat of this experiment is that it is not know why it is decreasing in both locations regardless of where the GAP domain is targeted.

I next examined the role of the Cdc42-specific GEF Tuba in the regulation of Golgi-associated Cdc42 activity. I transfected U2OS-Cdc42-FLARE imaging cells either with control (scrambled) or Tuba-specific siRNA and collected FLIM data at the Golgi, which was marked by ManII-mCherry. I also collected FLIM data at the PM, which was labeled by expression of the plasma membrane marker mApple-farnesyl. For this experiment, I zoomed in on the PM to the same extent as the Golgi (25.2 $\mu m^2$), focusing on a region of the PM that was not in contact with other cells. After data collection, I verified protein loss in those cells that I had imaged (Figure 3.6A and B). Tuba-depleted cells revealed a much smaller fraction of active Cdc42 at the Golgi and the PM than in control cells, with decreases from 72.7% to 52.1% ($t(52)=9.9833$, $p < 0.0001$, Figure 3.6A) and 70.2% to 49.9% ($t(56)=14.9569$, $p < 0.0001$, Figure 3.6B), respectively. As this drop in the percentage of FRET was not seen in adjacent areas devoid of the Golgi or the PM, I conclude that Tuba is necessary for Cdc42 activation at both sites.

I performed a similar analysis for another known Golgi-associated Cdc42 GEF, FGD1 (Estrada *et al.*, 2001), which is necessary for anterograde transport from the Golgi to the PM (Egorov *et al.*, 2009). To our surprise, the fraction of active Cdc42 at the Golgi was similar in control and FGD1-depleted cells, with 74.28% and 73%, respectively. However, there was a reduction in the percentage of FRET at the PM from 73.9% in control cells to 51.9% in FGD1-depleted cells ($t(36)=5.8322$, $p < 0.0001$). Thus, in spite of its Golgi association, this Cdc42 GEF does not appear to contribute to Cdc42 regulation at the Golgi.

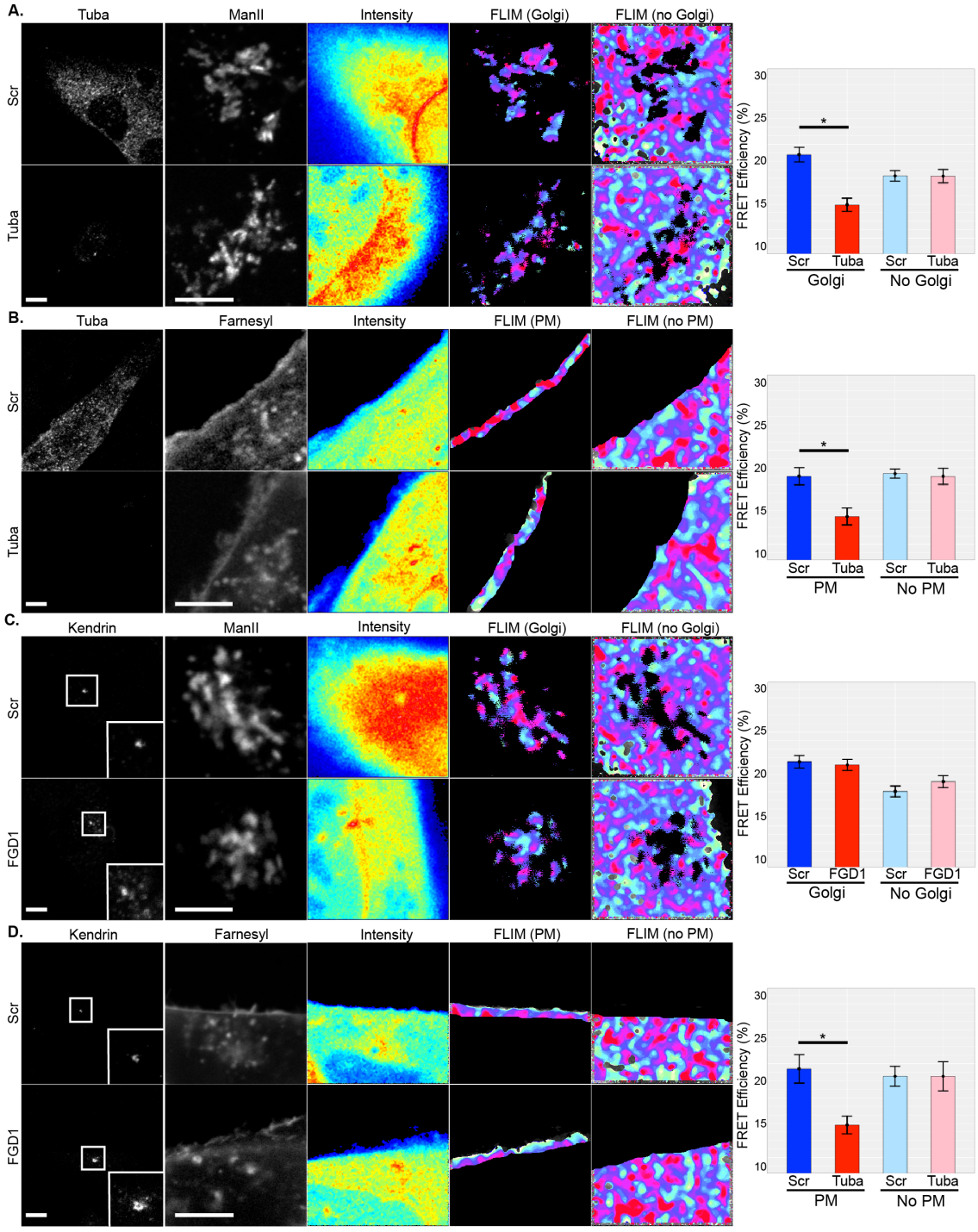


**Figure 3.6 Tuba, but not FGD1, regulates Cdc42 activity at the Golgi.**

**Figure 3.6 Tuba, but not FGD1, regulates Cdc42 activity at the Golgi.**
FLIM-FRET analysis of cells that lacked the Golgi-associated GEFs Tuba or FGD1. The U2OS-Cdc42-FLARE imaging cell line, which also expressed ManII-mCherry or mApple-farnesyl to label the Golgi or PM, respectively, was transfected with scrambled, Tuba, or FGD1-specific siRNA and subjected to FLIM-FRET analysis at the Golgi or PM. For each experimental condition, I show immunofluorescence data to confirm protein depletion (column 1), the marker used to define the site of analysis (column 2), an intensity map of cerulean-Cdc42 (column 3), a FLIM map of the area defined by the specific marker (column 4, “Golgi” or “PM”) and a FLIM map of the surrounding area (column 5, “no Golgi” or “no PM”). FLIM maps show FRET efficiencies ranging from 0% (white) and 28% (magenta). Finally, I show a graph of the average FRET efficiency for the areas of analysis. Each graph is based on the quantification of 8 cells per experimental condition, and 3 independent experiments. (**A**) FLIM-FRET analysis of scrambled (Scr) and Tuba-depleted cells (Tuba) at the Golgi (”Golgi”) and the surrounding area (“no Golgi”). (**B**) FLIM-FRET analysis of scrambled and Tuba-depleted cells at the PM (“PM”) and the area adjacent to the PM (“no PM”). (**C**) FLIM-FRET analysis of scrambled (Scr) and FGD1-depleted cells (FGD1) at the Golgi and the surrounding area. Since FGD1 antibodies do not work by immunofluorescence, FGD1 depletion was verified by staining for the centrosomal protein kendrin, which is disorganized in cells with reduced Cdc42 activity (also see Fig. 5). (**D**) FLIM-FRET analysis of control and FGD1-depleted cells at the PM and the adjacent area. Scale bar: 10μM. *$p < 0.0001$.

---

## Ribbon-like Golgi organization is important for Cdc42 activation at the PM

I next measured Cdc42 activity in cells with altered Golgi organization. I disconnected Golgi stacks in the U2OS-Cdc42-FLARE imaging cell lines through depletion of the structural Golgi protein GM130 and monitored Cdc42 activity with our FLIM-FRET assay. I then fixed the cells and stained them with an antibody to GM130 to confirm protein depletion. To our surprise, the fraction of active Cdc42 at the Golgi were similar in control and GM130-depleted cells, with 70.4 % and 71.8% respectively (Figure 3.7A). However, there was a reduced percentage of FRET, from 69.0% to 50.8% ($t(40)=8.9123$, $p < 0.0001$), at the PM of GM130-depleted cells, when compared to control cells (Figure 3.7B) suggesting that GM130 is important for Cdc42 activation at the PM.

I examined the role of Golgi structure in Cdc42 regulation further by inducing more extensive Golgi fragmentation. I focused on Golgin-84, a structural Golgi protein whose loss leads to Golgi fragmentation, dispersal, and a

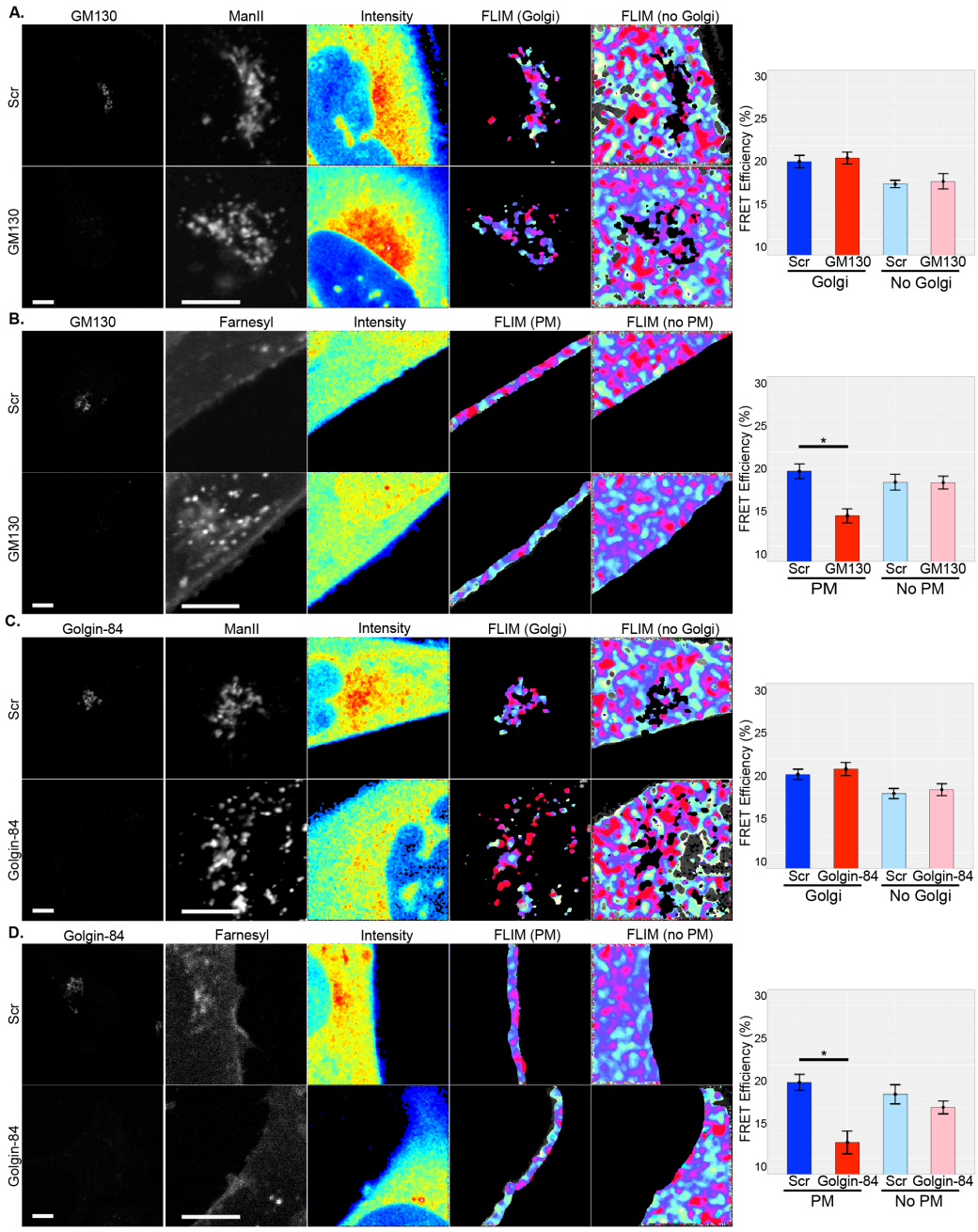


**Figure 3.7 Normal Golgi organization is critical for Cdc42 activity at the PM**

**Figure 3.7 Normal Golgi organization is critical for Cdc42 activity at the PM**
The phasor approach to FLIM-FRET was used to determine Cdc42 activity at the Golgi and PM after disruption of Golgi organization through depletion of GM130 and Golgin-84. Cdc42 activity measurements at the Golgi and PM were performed in induced U2OS-Cdc42-FLARE cells expressing ManII-mCherry or mApple-farnesyl. For each cell that was analyzed by FLIM-FRET, I show immunofluorescence data with specific antibodies to confirm protein depletion (column 1), the marker used to define the area of analysis (column 2), an intensity map of cerulean-Cdc42 (column 3), a FLIM map of the area defined by the specific marker (column 4, "Golgi" or "PM"), and a FLIM map of the surrounding area (column 5, "no Golgi" or "no PM"). FLIM maps show FRET efficiencies ranging from 0% (white) and 28% (magenta). Finally, I show graphs of the average FRET efficiency for the area defined by the specific marker. For each graph, 8 cells were quantified per experimental condition, and 3 independent experiments were carried out. (**A**) FLIM-FRET measurements of cells treated with control (Scr) or GM130-specific siRNA (GM130) at the Golgi ("Golgi") and the surrounding area ("no Golgi"). (**B**) Same as (**A**), but FRET efficiency was determined at the PM ("PM") and the adjacent area ("no PM"). (**C**) FLIM-FRET measurements of cells transfected with scrambled (Scr) or Golgin-84-specific siRNA (Golgin-84) at the Golgi and the surrounding area. (**D**) Same as (**C**), but FRET efficiency was determined at the PM and the adjacent area. All images show representative cells. For each condition, 8 cells were analyzed per experiment, and 3 independent experiments were performed. Scale bar: 10μM. * $p < 0.0001$.

---

reduction in protein transport (Diao *et al.*, 2003). As seen for GM130, the percentages of FRET were similar at the Golgi of control and Golgin-84-depleted cells (Figure 3.7C). However, the absence of Golgin-84 led to a specific decrease in fraction of active Cdc42 at the PM, from 70.6% to 72.8% ($t(38)=11.1093$, $p < 0.0001$, Figure 3.7D). These results suggest that Cdc42 activation at the Golgi is independent of its organization and that disruption of Golgi organization prevents Cdc42 activation at the PM.

### Cdc42 controls centrosome organization from the PM

I tested if Cdc42 activity at the PM is critical for the regulation of the centrosome. I previously observed defects in centrosome organization and function in cells in which GM130 or Tuba was depleted, or dominant negative Cdc42 was expressed (Kodani *et al.*, 2009). As each of these conditions led to reduced Cdc42 activity at the PM (Figures 3.6 and 3.7), I examined a potential

link between PM-associated Cdc42 activity and centrosome organization (Figure 3.8A). I focused on cells depleted of FGD1 and Golgin-84, which affected Cdc42 activation at the PM, but not at the Golgi. Immunofluorescence analysis with antibodies to the centrosomal protein kendrin revealed a cloud of centrosomal foci around the two centrioles, instead of the typical 2-4 centrosomal foci of an interphase cell. Thus, Golgin-84 and FGD1-depleted cells phenocopied the centrosome defects of GM130-depleted cells (Figures 3.8B and 3.8C). These results suggest that Cdc42 activity at the PM, not at the Golgi, is necessary for the maintenance of proper centrosome organization.

GM130 regulates Cdc42 activity as was seen previously, however, this data has provided a new location for the regulation of Cdc42 activity and brings into question the previous finding of GM130-Tuba interaction. There is the potential that both of these proteins interact in lysate, but not in cells. It is known that colocalization using laser scanning microscopy often leads to partial overlap of Golgi proteins on different cisternae and that higher resolution techniques can be used to separate the proteins on different stacks (YilmazDejgaard, *et al., 2007).* Therefore. I used structural illumination microscopy (SIM), which utilizes polarized filters and algorithms to enhance the resolution by 2-3 fold, to determine if GM130 and Tuba would still colocalize. First I determined if SIM could improve on spectral overlap of GM130 proteins using GM130 and ManII, which localize to the *cis*- and *medial*-Golgi, respectively. I found that while ≈30% colocalization of GM130 and ManII was detected by confocal microscopy, this dropped to 5-10% colocalization when SIM was used (Figure 3.9A). This

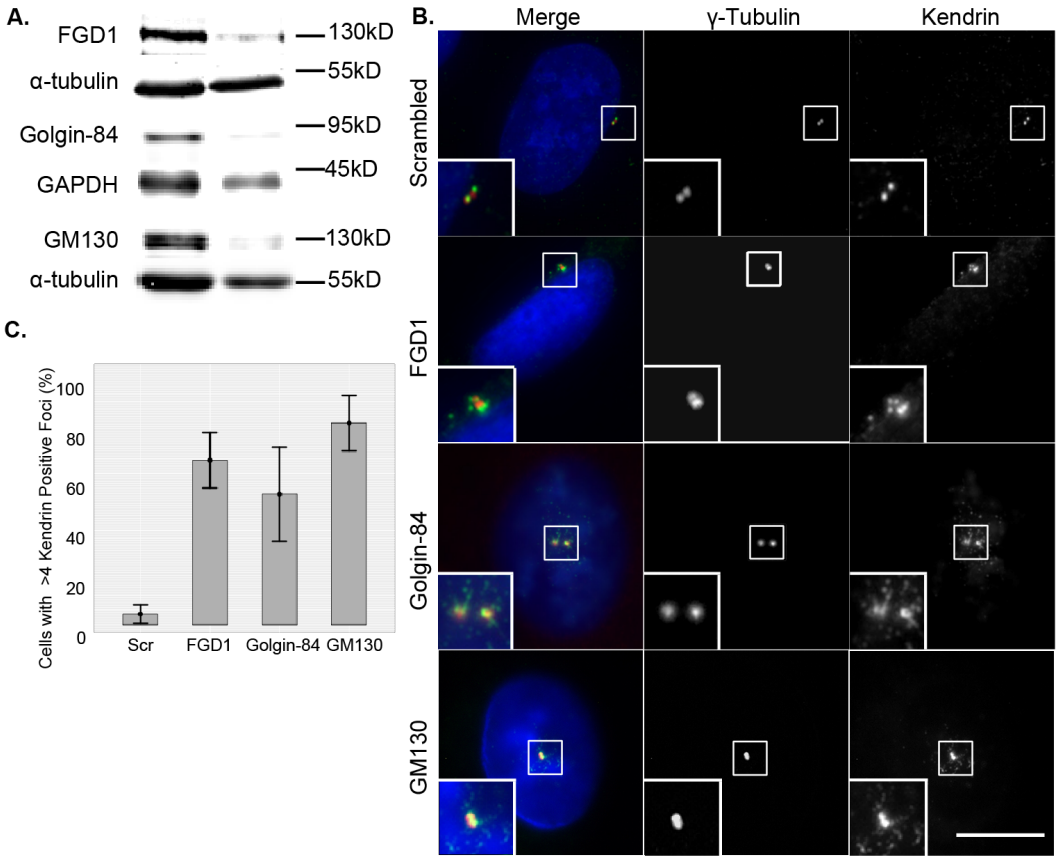


**Figure 3.8 A functional Golgi is critical for the normal organization of the centrosome**
(**A**) Western blot of total cell lysates from U2OS cells transfected with scrambled siRNA as a negative control (first column) or siRNA specific to FGD1, Golgin-84, or GM130 for 48 hours (second column). α-tubulin or GAPDH served as loading controls. (**B**) The cells from (**A**) were analyzed by immunofluorescence with antibodies to the centrosomal proteins γ-tubulin and kendrin. The left column shows a merged imaged, in which γ-tubulin is in red, kendrin in green and DNA, as stained with Hoechst 33342, in blue. Scale bar: 10μM. **(C)** Percentage of control, FGD1-, Golgin-84- and GM130-depleted cells displaying > 4 centrosomal foci (n=3 independent experiments, with >300 cells counted per condition per experiment).

indicated SIM would be a good method to address if GM130 and Tuba colocalized within the cell. I found that confocal microscopy lead to ≈14% colocalization of Tuba and GM130 (Figure 3.9B). However, after application of SIM, this co-localization dropped to ≈0.013%. From this I have concluded that Tuba is on the Golgi, but it does not colocalize with GM130. This is in agreement with previous reports of Tuba at the Golgi in cryosections of rat neurons, which showed that Tuba localized to the Golgi, but did not colocalize with GM130 (Salazar, *et* al., 2003).

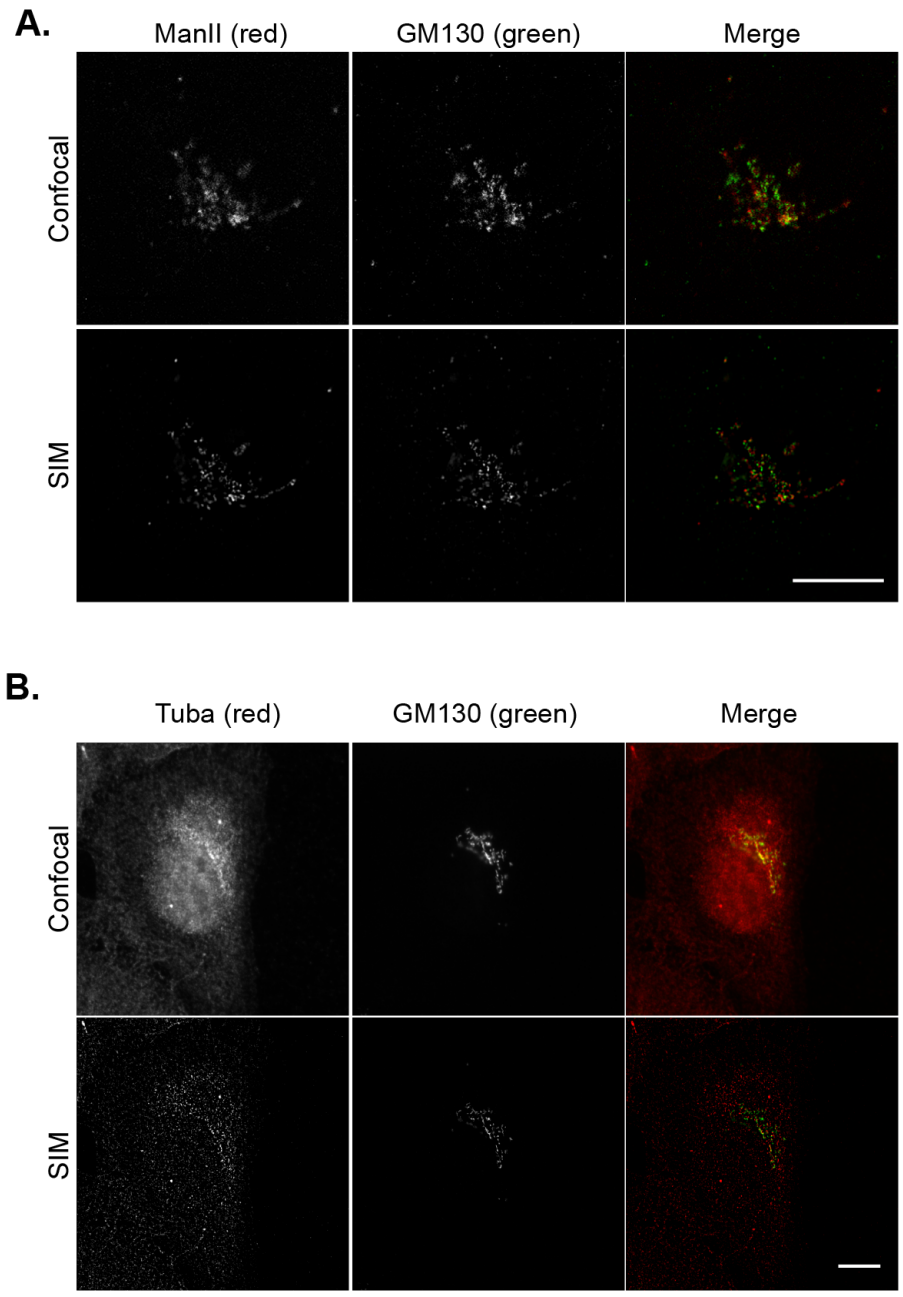


**Figure 3.9 SIM reveals that Tuba and GM130 do not colocalize in cells.**
(**A**) A control to compare the colocalization of ManII and GM130, which localize to the *cis-* and *medial-*Golgi, respectively. Cells were fixed in 4% formaldehyde and stained with antibodies to either ManII or GM130. The cell was first imaged using confocal microscopy (top row), then the cell was image on the same microscope using SIM (bottom row). (**B**) The same procedure was used as in (A), however, cells were stained with antibodies to Tuba or GM130.

## Discussion

This study provides new insights into the control of Cdc42 activity at different cellular locations. I used a dual chain FRET biosensor and the phasor approach to FLIM to compare the factional population of active Cdc42 at the Golgi, adjacent to the Golgi, at the PM, next to the PM and in the cytosol. I report that Cdc42 is active throughout the Golgi, and that this activity is differentially controlled by specific Golgi-associated Cdc42 regulators. In addition, I show that ribbon-like Golgi organization is critical for Cdc42 activation at the PM, but not at the Golgi. Finally, I provide evidence for a possible role of PM-associated Cdc42 in the control of centrosome organization.

I developed and used novel tools to map Cdc42 activity in live cells. First, I established stable U2OS imaging cell lines. These cell lines expressed an improved dual chain Cdc42 biosensor, in which donor and acceptor fluorophores are expressed at equal ratio (Klaus Hahn, unpublished). Inducible expression of this biosensor helped to limit the expression level of cerulean-Cdc42 so that organelle and cytoskeleton morphology as well as cell functions were not disrupted. The imaging cells, which were grown at low confluency with only one to three neighboring cells, also expressed Golgi and PM markers, which facilitated measurements of Cdc42 activity at specific locations at high pixel resolution (25.2 $\mu m^2$, ≈100nm/pixel). Second, I demonstrate that our approach is able to obtain quantitative and specific measures of Cdc42 activity at specific cellular locations. For example, I compared the fractions of active Cdc42 at the Golgi to randomly selected areas in the cytosol in which significantly fewer Cdc42

molecules were active than at the Golgi. The intermediate fraction of active Cdc42 that I detected in areas adjacent to the Golgi, are likely due to the presence of endomembranes and vesicles that are known to contain active Cdc42 (Michaelson *et al.*, 2001). However, manipulations of Cdc42 regulators, such as Tuba and ARHGAP10, did not change the percentage of FRET in these areas. This data leads us to propose that Tuba and ARHGAP10 function as specific regulators of Cdc42 activity at the Golgi. A large fraction of active Cdc42 at the Golgi may be due to higher GEF activity of Tuba at the Golgi, which would then generate more molecules of GTP-bound Cdc42. Similarly, it may reflect lower activity of ARHGAP10 at this specific site so that active Cdc42 remains active longer. Third, I used the phasor approach to FLIM-FRET, a powerful technique to conduct a spatial analysis of small GTPase activity without the fluorescent artifacts inherent to ratiometric FRET measurements. This method allowed for the detection of activity in areas without high biosensor expression levels, which became particularly evident in migration experiments in which the increase in the active population of Cdc42 at the leading edge was not caused by a change in the intensity of cerulean-Cdc42. In addition, the FLIM-FRET approach allowed for analysis in live cells, eliminating possible artifacts as the result of sample fixation.

Our study revealed the differential regulation of Cdc42 at the Golgi and the PM in non-polarized cells. At the Golgi, Cdc42 activity was regulated by ARHGAP10 and Tuba. The effects of targeting ARHGAP10 to the Golgi confirmed that this system responds to a known Golgi-localized regulator of

Cdc42 activity at the Golgi. Our study also establishes Tuba as a specific GEF for Cdc42 at the Golgi. In spite of the controversy about Tuba localization, our functional data suggests that a pool of Golgi-associated pool of Tuba may directly activate this small GTPase at the Golgi.

To our surprise, Cdc42 activity at the Golgi was not dependent on FGD1. FGD1 is reported to contribute to Cdc42 recruitment to the Golgi, but I did not detect any change in the fraction of active Cdc42 at the Golgi in the absence of this GEF. Thus, FGD1 may associate with inactive Cdc42 at the Golgi, or not be active at the Golgi, so its absence would not affect Cdc42 activity at this site. Alternatively, previous studies may not have detected the function of endogenous FGD1 because they were conducted with FGD1 overexpression (Egorov *et al.*, 2009). While additional experiments are needed to better understand the function of FGD1 at the Golgi, our results demonstrate a role for this GEF at the PM, which is consistent with reduced Cdc42 activity in total lysates of FGD1-depleted cells (Egorov *et al.*, 2009).

Interestingly, the fractional population of active Cdc42 activity at the PM was dependent on a functional Golgi. I manipulated Golgi organization in two different ways: I removed GM130, which leads to disconnected Golgi mini-stacks, glycosylation defects, and delayed protein transport (Puthenveedu *et al.*, 2006; Marra *et al.*, 2007). I also depleted Golgin-84, which induces extensive Golgi fragmentation and a general reduction in protein transport (Diao *et al.*, 2003). I do not yet know which Golgi function is linked to Cdc42 activation at the PM because GM130 or Golgin-84 depletion may interfere with protein modification,

sorting, or transport of Cdc42 itself or a specific regulator. However, a mechanism involving post-Golgi transport would be consistent with previous findings on the requirement for membrane trafficking for Cdc42 activation at the leading edge of cells (Osmani *et al.*, 2010).

Our results lead to a revised model of Cdc42-mediated regulation of the centrosome. Our lab had previously proposed that Cdc42 activity at the Golgi was required for normal centrosome organization because GM130-depleted cells displayed reduced Cdc42 activity in biochemical assays and defects in centrosome organization and function (Kodani *et al.*, 2009). However, the spatial analysis of Cdc42 activity establishes a strong correlation between Cdc42 activity at the PM and the regulation of the centrosome. Cells in which PM-associated Cdc42 activity was specifically reduced, for example as a result of FGD1 or Golgin-84 depletion, displayed abnormal centrosome organization, with an increased number of centrosomal foci. These experimental conditions had no effect on Cdc42 activity at the Golgi suggesting that Golgi-associated Cdc42 does not contribute to the regulation of this adjacent organelle. This revisited model is consistent with previous findings on abnormal centrosomes in cells that either lacked Tuba or that expressed dominant negative Cdc42 (Kodani *et al.*, 2009).

The mechanism through which PM-associated Cdc42 controls the centrosome is unclear. Cdc42 at the PM could control centrosome organization through effects on microtubules. The polymerization and dynamics of microtubules, which contribute to the assembly of the centrosome (Young *et al.*,

2000), depend on the association of activated Cdc42 with the PAR complex at the PM (Etienne-Manneville and Hall, 2003). Consistent with this idea, disruption of microtubules with low concentrations of nocodazole caused changes in centrin and kendrin organization that were similar to those seen in the absence of GM130 or Golgin-84 (Dammermann and Merdes, 2002). Microtubule attachment to the PM also promotes tension, which help position the centrosome (Burakov *et al.*, 2003). Alternatively, active Cdc42 may contribute to the activation of the PAR complex, possibly controlling the centrosomal localization of the PAR6 isoforms Par6α and Par6γ, which are necessary for the proper assembly of the centrosome (Dormoy *et al.*, 2013).

A recent study reported a role for GM130 in the control of Cdc42 activity at the Golgi, which is inconsistent with our findings (Baschieri *et al.*, 2014). Baschieri and colleagues found that GM130-depleted HEK393T cells had reduced levels of active Cdc42 at the Golgi, while the levels of Cdc42 activity at the PM were unaffected. Their model suggests that GM130-mediated Cdc42 regulation does not involve a GEF, but the association with RasGRF2, a known negative regulator of the small GTPase Ras (Fernández-Medarde and Santos, 2011). The discrepancy between our study and the findings by Baschieri *et al*. may be due to the choice of biosensor, method of activity measurements, and cell line. Baschieri *et al*. expressed a single chain biosensor, in which the Rho GDI binding site is blocked, in HEK293 cells. In addition, they used the acceptor photobleaching method, which requires sample fixation prior to FRET measurements. In contrast, I detected the fractional population of active Cdc42 at

the Golgi and the PM in live U2OS cells with a dual chain biosensor and the phasor approach to FLIM-FRET. Unfortunately, I was unable to corroborate the results by Baschieri and colleagues because I was unable to specifically detect RasGRF in HeLa cells, which they also used to show RasGRF at the Golgi, or U2OS by immunofluorescence or western blot (data not shown) with the reported antibody (Santa Cruz, sc-863 C18) or two other commercial antibodies (Santa Cruz, sc-224 C-20; ProteinTech, 19717-1-AP) or to deplete RasGRF with the reported siRNA (Qiagen SI04235147).

In conclusion, I used a novel dual chain Cdc42 biosensor and the phasor approach to FLIM-FRET to demonstrate for the first time how manipulations of different cellular factors, including GEFs, GAPs and structural Golgi proteins, affect Cdc42 activity at the Golgi and the PM. Future studies will focus on understanding how Golgi organization and/or function controls Cdc42 activation at the PM and how active Cdc42 at the PM regulates the centrosome. The assay and cell lines that I have developed will help to develop a comprehensive model about Cdc42 regulation at the Golgi, the PM and other cellular locations.

## Contributions

Kari Herrington preformed the majority of experiments and analysis and made the figures. Christine Sütterlin provided guidance and helped with the design of experiments. Michelle A. Digman and Enrico Gratton provided guidance and support for microscopy and analysis. Klaus Hahn provided Cdc42-FLARE and advice. Andrew A. Trinh aiding with migration experiments and Carolyn Dang cloned the ARHGAP10 constructs and data processing for FLIM experiments.

# Chapter 4:
# Visualizing binding of MacE analogs in cells using click chemistry


## Abstract

Small molecules have frequently been used to study the Golgi apparatus. The small molecule Macfarlandin E, has been shown to induce a unique Golgi phenotype that is characterized by extensively fragmented Golgi membranes that remain in the perinuclear region. Work with the molecule has been limited due to scarce amounts of the natural product until recently when an analog of the active domain of MacE has been synthesized. *In vitro* experiments indicated that these analogs interact with lysines, but it was not known where in the cell or what proteins may be affected. In this study, I describe novel MacE derivatives that can be used with click chemistry. I used these compounds in binding experiments in intact cells, which allowed me to visualize the site of protein binding and parallel biochemical binding assays revealed that these MacE analogs interact with a large number of proteins wit in the cell. Furthermore, I present the surprising finding that lysine modifying MacE derivatives produce a similar fragmented Golgi phenotype as MacE. While this study provides support for the idea that lysine are critical for Golgi maintenance, it is not know which protein, or proteins, are responsible.

## Introduction

Small molecules have been useful tools to dissect Golgi structure and function. Much of our knowledge of the early secretory system has come from small molecules. For example, BFA leads to the relocalization of the Golgi membranes into the ER when retrograde transport is increased by the generation of tubulovesicular structures when COPI coats could not form. These experiments showed the role of ARF1 GTPases in COPI coat formation and provided insight into retrograde traffic (Lippincott-Schwartz *et al.*, 1990; Klausner *et al.*, 1992).

The use of Ilimaquinone (IQ) has helped with the elucidation of the later secretory pathway. Treatment of cells with IQ led to complete, but reversible vesiculation of the Golgi (Takizawa *et al.*, 1993). This sponge metabolite has then been found to activate a heterotrimeric G-protein on the Golgi, which in turn activates and recruits Protein Kinase D (Jamora *et al.*, 1997; Añel and Malhotra, 2005). These molecules have provided important mechanistic information about protein transport though the Golgi suggesting that investigation into other small molecules may be beneficial to broadening our understanding of the Golgi.

The small molecule Macfarlandin E (MacE) may lead to valuable insight into the regulation of Golgi structure and positioning. A screen of small molecules with Golgi-disrupting activity led to the isolation of MacE, a spongian diterpene from the marine mollusk *Chromadoris macfarlandi*, (Molinski and Faulkner, 1986). It was later found that incubation of Normal Rat Kidney (NRK) cells for 60 min with 20µg/mL MacE produced an irreversible phenotype of Golgi membranes that were extensively fragmented but remained positioned in the pericentrosomal region of the cell. This phenotype is in

contrast to those of BFA, nocodazole, and IQ, which led to a concomitant loss of Golgi structure and Golgi position (Schnermann *et al.*, 2010). While the effect of MacE appeared to be specific for the Golgi, it was not known if this compound affects protein transport and other Golgi-related functions. In addition, understanding the positioning of the Golgi is not lost with MacE could provide new understanding into Golgi maintenance and positioning.

The use of MacE as a tool to understand Golgi structure and position required the production of synthetic MacE analogs. While MacE generated an exciting and unique phenotype, the natural compound was unsuitable for biochemical studies. It was only available in limited amounts, and its complex structure made it inaccessible to modifications that would facilitate the isolation of its target (Schnermann *et al.*, 2010). MacE, shown in Figure 4.1A, has a complex structure that is difficult to synthesize. Its classical "spongian diterpene skeleton" displays two important portions of the molecule: a subunit that is highly oxygenated and a hydrophobic subunit (Fig. 4.1A, indicated by dashed line). The highly oxygenated ring structure is rare and only found in MacE and 13 other rearranged spongian diterpenes, such as norrisolide, chromodorolide, and dendrolide (Guizzunti *et al.*, 2006; Keyzers *et al.*, 2006; Schnermann *et al.*, 2011). However, a fruitful collaboration with the laboratory of Larry Overman (UCI) has led to the synthesis of *tert*-butyl-MacE (*t*-Bu-MacE), whicgcontains the oxygenated ring of MacE (Schnermann *et al.*, 2010). It mimicked the effects of MacE on the Golgi, producing a highly fragmented Golgi that was retained in the pericentriolar region (Schnermann *et al.*, 2011).

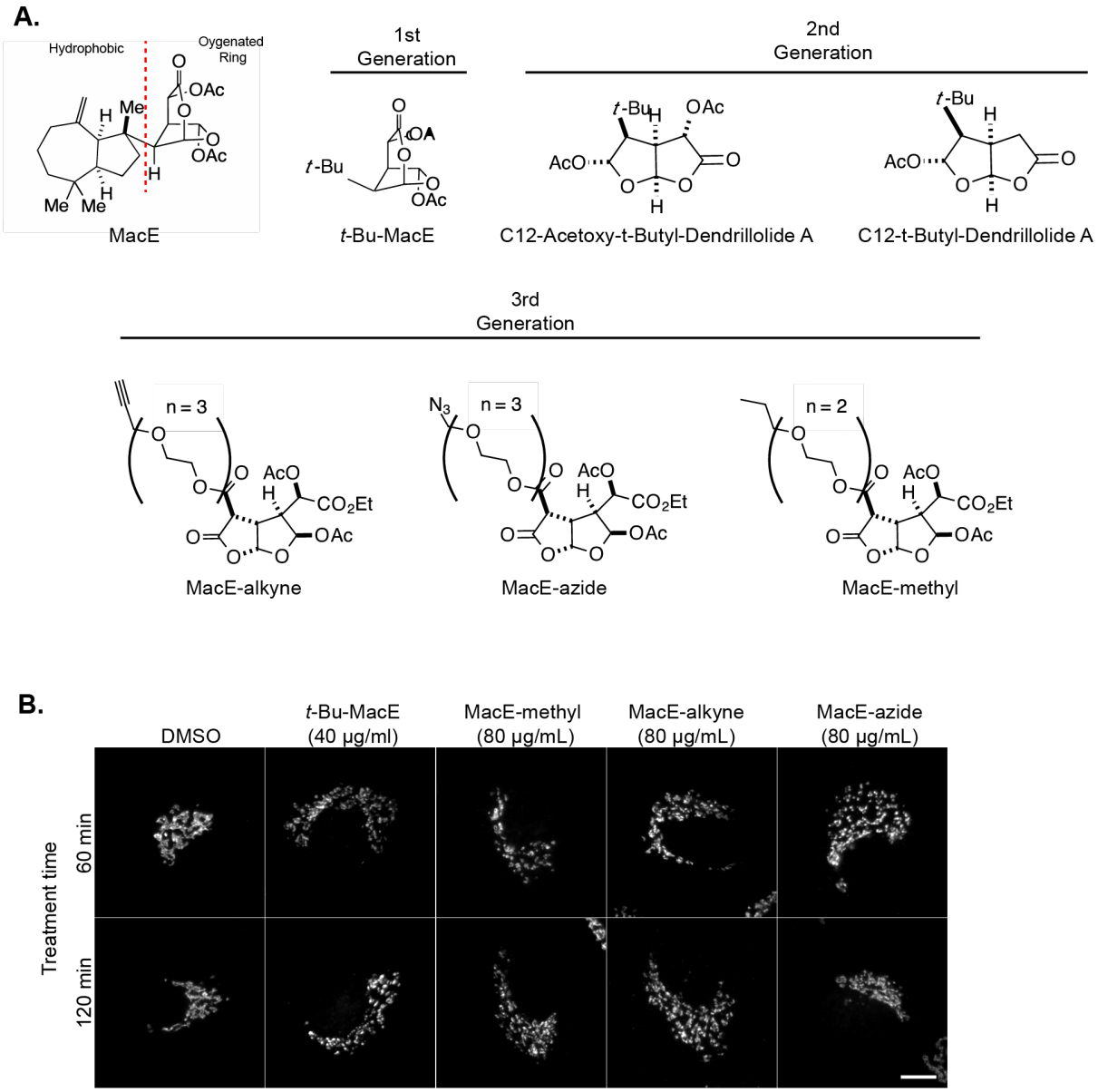


**Figure 4.1 Clickable and non-clickable MacE analogs reproduce the MacE phenotype**
Analogues of the hydrophilic region of MacE that were designed for used with click chemistry reproduce the MacE phenotype. (A) Previously published analogues that correspond to the hydrophilic region of MacE (right of dashed line in MacE molecule) are shown in the top row and newly derived molecules that can be targeted with the click-reaction, MacE-alkyne and MacE-azide, and the non-clickable control, MacE-methyl (bottom row). (B) NRK cells were treated for 60 min(top row) or 120 min (bottom row) with DMSO (control), t-Bu-MacE at 40 µg/mL, MacE-methyl at 80 µg/mL, MacE- alkyne at 80 µg/mL, or MacE-azide at 80 µg/mL. Representative images are shown. Scale bar represents 10 µM.

The use of *t*-Bu MacE induced the fragmentation of the *cis*-, *medial*-, and *trans*-Golgi as well as at the ultra structural level, which revealed shorten Golgi stacks with swollen cisternae (Schnermann *et al.*, 2011). Also, like MacE, *t*-Bu-MacE did not affect the organization of the ER, or the actin and microtubule cytoskeleton (Schnermann *et al.*, 2011). Furthermore, both *t*-Bu-MacE and the natural compound blocked forward transport from the Golgi to the PM without affecting retrograde transport. In addition to being more readily available, *t*-Bu-MacE had the advantage over the natural compound that it showed reduced cytotoxicity. However, the mechanism behind MacE/*t*-Bu MacE-induced Golgi fragmentation remained unknown.

The identification of the MacE target, a first step towards understanding the mechanism of MacE-induced Golgi fragmentation, required the synthesis of additional MacE analogs. Although *t*-Bu-MacE phenocopied the effects of MacE on the Golgi and could by synthetically generated, it could not be easily modified and, therefore, just like the natural compound itself, was unsuitable for biochemical studies. A second generation of simplified analogs of the oxygenated subunits of MacE had to be designed and tested for their Golgi fragmentation activity in intact cells (shown in figure 4.1A; Schnermann *et al.*, 2011). Interestingly there was correlation between Golgi fragmentation and the ability of a compound to modify lysines, which had been predicted from the original MacE structure (Schnermann *et al.*, 2011). A new analog, C12-Acetoxy-*t*-Butyl-Dendrillolide A (Ace-*t*-Bu-DenA), produced a nearly identical Golgi fragmentation phenotype as *t*-Bu-MacE and MacE, and was found to react with lysines similarly to t-Bu-MacE. In contrast, a similar ring structure missing the acetoxy group, C12-t-Butyl-Dendrillolide A (*t*-Bu-DenA), modified lysines at a slower rate and had no

effect on the Golgi (Schnermann *et al.*, 2011). These second generation analogs led to the synthesis of a new set of analogs that was amenable to click chemistry.

Click chemistry is a method for reacting an alkene on one molecule with an azide of another molecule to covalently join the molecules. It can be accomplished through two different methods, a copper-driven click (cu-click) reaction or the Staudinger reaction. The cu-click reaction is fast and uses copper as a catalyst for joining the azide and alkyne. The use of copper requires the cells to be fixed, but can be done with either MacE-alkyne of MacE-azide provided the reporter being added has an azide or alkyne, respectively. The Staudinger reaction utilizes a phosphine group that can make a nucleophilic attack on the azide. This reaction is much slower and can only be accomplished with MacE-azide. However it can be charred out in live or fixed cells.

Both reactions are used to add, or "click", tags to a molecule, such as a MacE-analog, after it has bound to its target in intact cells. For example biotin, which can be recognized by streptavidin or anti-biotin antibodies, can be added to the small moleule. Fluorophores and dyes, such as rhodamine, can also be added, which facilitates the visualization of a compound inside a cell by microscopy. Click chemistry mediated tagging of small molecules is highly beneficial because it allows for the addition of a much larger reporter group, such as biotin or rhodamine, to a small molecule, such as MacE, after it has bound its target. The new MacE analogs can be used with click chemistry because they contain a polyethylene-glycol (PEG) chain with an azide or alkyne attached, (Figure 4.1A, bottom row; unpublished data, Genung, N., Schnermann, M. and Overman, L., Dept. of Chemistry, UCI).

In this chapter, I describe my experiments with a new generation of clickable-MacE analogs. I first confirmed that these analogs induce a similar Golgi fragmentation phenotype as the natural compound or *t*-Bu-MacE. Then used them for click chemistry to demonstrate binding of these molecules to proteins by immunofluorescence microscopy and by western blot analysis. I also present a novel finding on the effects of lysine modification on Golgi organization, which may in the future aid with our understanding of Golgi structure.

## Results

### New clickable MacE analogs reproduce the MacE Golgi fragmentation phenotype

Clickable MacE analogs were tested for their ability to induce alteration to Golgi membranes. Figure 4.1 shows MacE and three generations of analogs: 1) The first MacE analog, *t*-Bu-MacE, has been shown to have similar Golgi fragmentation activity as the natural compound. 2) The simplified analogs Ace-*t*-Bu-DenA and *t*-Bu-DenA, which were reported to show or not show the Golgi phenotype, respectively (Figure 4.1A top row). These molecules mimic the oxygenated MacE ring as it appears in a pH environment similar to the cytosol, but they lack the complex chair structure of *t*-Bu-MacE and the natural compound that prevented modification. 3) The third generation analogs, which can be used for click chemistry (Figure 4.1A bottom row), include 2 clickable and one non-clickable molecule. These 3 molecules only vary with the PEG chain ending in an alkyne, azide, or a methyl group and will be referred to as MacE-azide, MacE-alkyne, and MacE-methyl in this document. The design of each of these clickable analogs was based on the structure of Ace-*t*-Bu-DenA, which induces Golgi

fragmentation, similar to MacE. All these molecules are therefore predicted to be able to induce Golgi fragmentation. While I used the alkyne and azide tags with click chemistry, the related compound with a methyl group, which is not able to be undergo the click reaction and served as a specificity control. I tested these third generation compounds on NRK cells. *t*-Bu-MacE was used for comparison because it has been shown to faithfully reproduce the MacE phenotype, and DMSO served as a solvent control. MacE-alkyne and MacE-azide induced a similar fragmented Golgi phenotype as *t*-Bu-MacE after 60 min of incubation with 80 µg/mL. MacE-methyl, which appeared to have a partial phenotype at 60 min, was able to induce the phenotype after 120 mins (Fig 4.1B). I conclude that MacE-azide, MacE-alkyne, and MacE-methyl are all capable of inducing a similar extensively fragmented Golgi phenotype in the perinuclear region as observed with MacE and *t*-Bu-MacE.

**Biochemical and microscopy-based assays detect binding of MacE-azide and MacE-alkyne to numerous cellular proteins**

Click chemistry revealed MacE binding to proteins throughout the cell. For immunofluorescence analysis, the click reactions were preformed in NRK cells grown on coverslips treated with MacE-azide, MacE-alkyne, or DMSO (control) at 80µg/mL for 2 hours. Cells were then washed to remove excess drug and were fixed. Cells treated with MacE-azide were subjected to the Staudinger reaction in 180 min. Cells treated with MacE-alkyne were treated with a cu-click reaction with azide-biotin for 30 min. All cells were stained with antibodies to Mannosidase II (ManII) as a Golgi marker and the biotin of the click reaction. Both methods revealed a fluorescence signal throughout the

cell with potential enrichment in the pericentriolar region and some filamentous type structures (Figure 4.2A). This signal was specific for these MacE analogs because it was not detected in cell treated with MacE-methyl. I conclude that I could detect binding of both MacE-azide and MacE-alkyne using the Staudinger and cu-click reactions, respectively. This result suggest that MacE-analogs bind a large number of proteins in the cells.

A parallel biochemical assay revealed that MacE binds to cellular proteins in a time dependent manner. There is the potential that the analogs are binding a highly abundant protein through out the cytosol or on the membrane. Therefore I performed a western blot analysis of cell lysate to investigate the quantity of bound proteins. I also used this western blot analysis to determine how long it took for the MacE analogs to bind and saturate the binding site of proteins proteins. NRK cells were treated with MacE-alkyne at 80 µg for 10, 30, 60, or 120 min or with 80 µg/ml MacE-Methyl as a negative control for 30 and 60 min followed by preparation of total cell lysates(Figure 4.2B). 25 µg of each lysate was treated with a cu-click reaction to attach azide-biotin, which can be readily detected with streptavidin or anti-biotin antibodies The clicked lysate was separated on a poly acrylamide gel and analyzed by western blotting with streptavidin, which was directly conjugated to a near infrared fluorophore for use with the Odyssey-imager. I observed the a dependent binding of MacE-alkyne to numerous proteins. At 10 min, at least 20 faint protein bands were labeled. This signal became stronger over time so that at 30 min, it appeared nearly saturated. At 60 and 120 min, there was complete saturation of the signal, which indicated that a large number of proteins were being

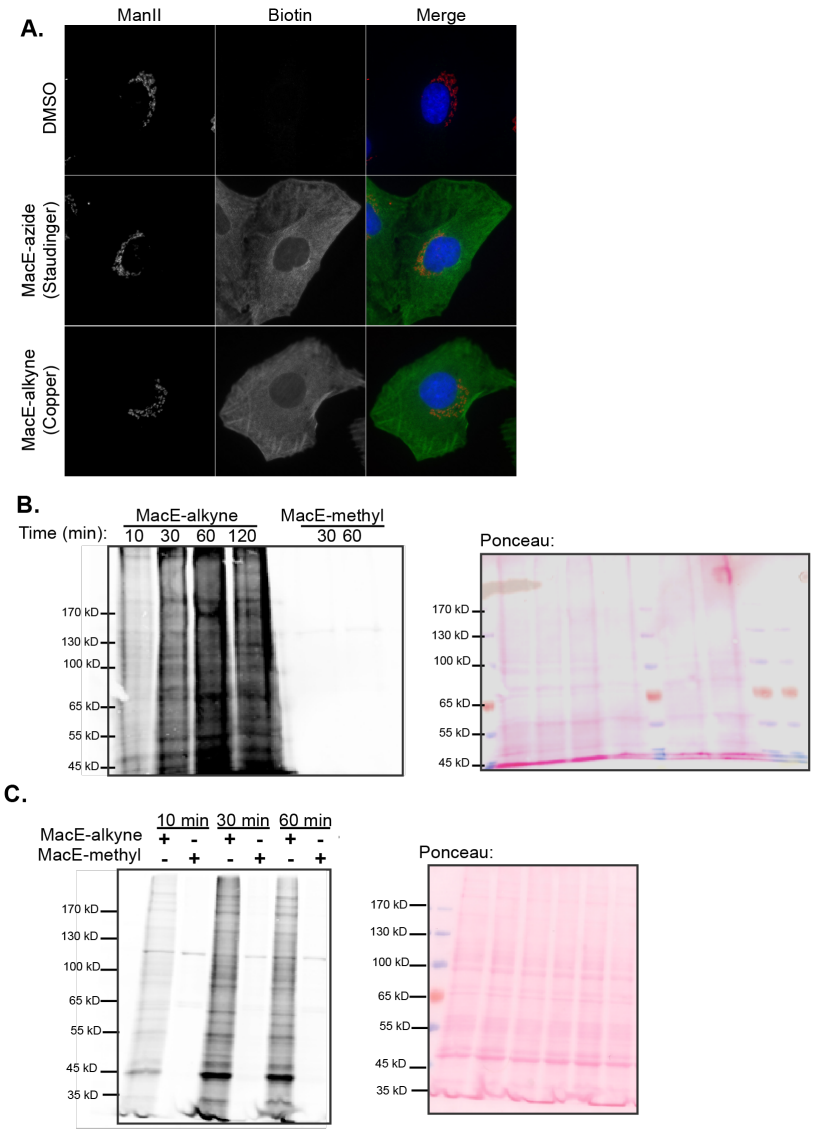


**Figure 4.2 Click chemistry was used to detect MacE binding by immunofluorescence and western blot**

MacE analogs were visualized in cells and cell lysate using click chemistry. (**A**) Cells were treated with DMSO, MacE-azide or MacE-alkyne at 80 µg/mL for 2 hrs. Two different click chemistry methods were performed to covalently attach a biotin group to the MacE analog. The Staudinger reaction was done in live cells treated with MacE-azide and cells were fixed immediately after. Copper driven click reaction was performed in fixed cells that had been treated with MacE-alkyne. Cells were fixed and stained with antibodies to ManII to mark the Golgi (red) and biotin (green).(**B**) NRK cell lysates were diluted in lysis buffer to 25µg/25µL, 5µg/25µl, or 1µg/25µl then treated with 10µg/mL or 5µg/mL MaceE-alkyne or 10µg MacE-methyl. Samples were incubated on ice for 1 hr. Then a cu-click reaction was used to attach biotin to MacE-alkyne. Biotin was detected using streptavidin conjugated to a near infrared probe and analyzed on an Odyssey (Licor). Ponceau shown for loading.(**C**) Cells were treated with 80 µg/mL MacE-Alkyne for 10, 30, 60, or 130 min, or MacE-methyl for 30 and 60 min. Prior to harvesting the small molecule was washed out with fresh media, then cells were collected by scraping cells on ice and lysing in 1%NP-40 buffer. Biotin was attached to MacE-alkyne using the copper click reaction i*n vitro*, MacE-methyl was treated as well for consistency. Approximately 10 µg of lysate was run on the gel. Biotin was detected using a streptavidin conjugated to a near infrared probe and analyzed on an Odyssey (Licor). Ponceau shown to indicate loading.

bound. As expected, MacE-methyl, which cannot be clicked and which I used as a negative control, did not show any signal.

A parallel *in vitro* time course with MacE-alkyne and MacE-methyl produced similar results (Figure 4.2C). In this experiment, lysates from NRK cells were prepared prior to the addition of 10 µg of MacE-alkyne or MacE-azide for 10, 30, or 60 min. Reactions were stopped by precipitating the sample with methanol before performing the cu-click reaction. I obtained a similar result as in intact cells. At least 20 bands between 45 kDa and 300 kDa were labeled. Intensity of the signal increased with time. The binding to these bands appears to be specific because MacE-methyl did not show any significant signal.

**Competition experiments demonstrate the specificity ofMacE analogs binding to proteins.**

I investigated if the binding sites for MacE analogs are saturable in a competition experiment. In a first experiment, I incubated NRK cells with 80 µg/ml MacE-alkyne for 60 min, followed by addition of 80 µg/ml MacE-azide for 30 min. MacE-alkyne was subjected to a cu-click reaction to add azide-rhodamine. MacE-azide was treated with phosphine-biotin for the Staudinger reaction, followed by staining with antibodies to biotin. Both compounds were able to bind proteins inside the cell. Staining for MacE-alkyne was stronger and was detected in the cytosol as well as in the nucleus. However, click reactions performed on MacE-alkyne in other experiments with azide-biotin (see Figure 4.3A) did not show this nuclear staining, therefore this may be an artifact of the azide-rhodamine. MacE-azide still produced a fairly bright signal, which

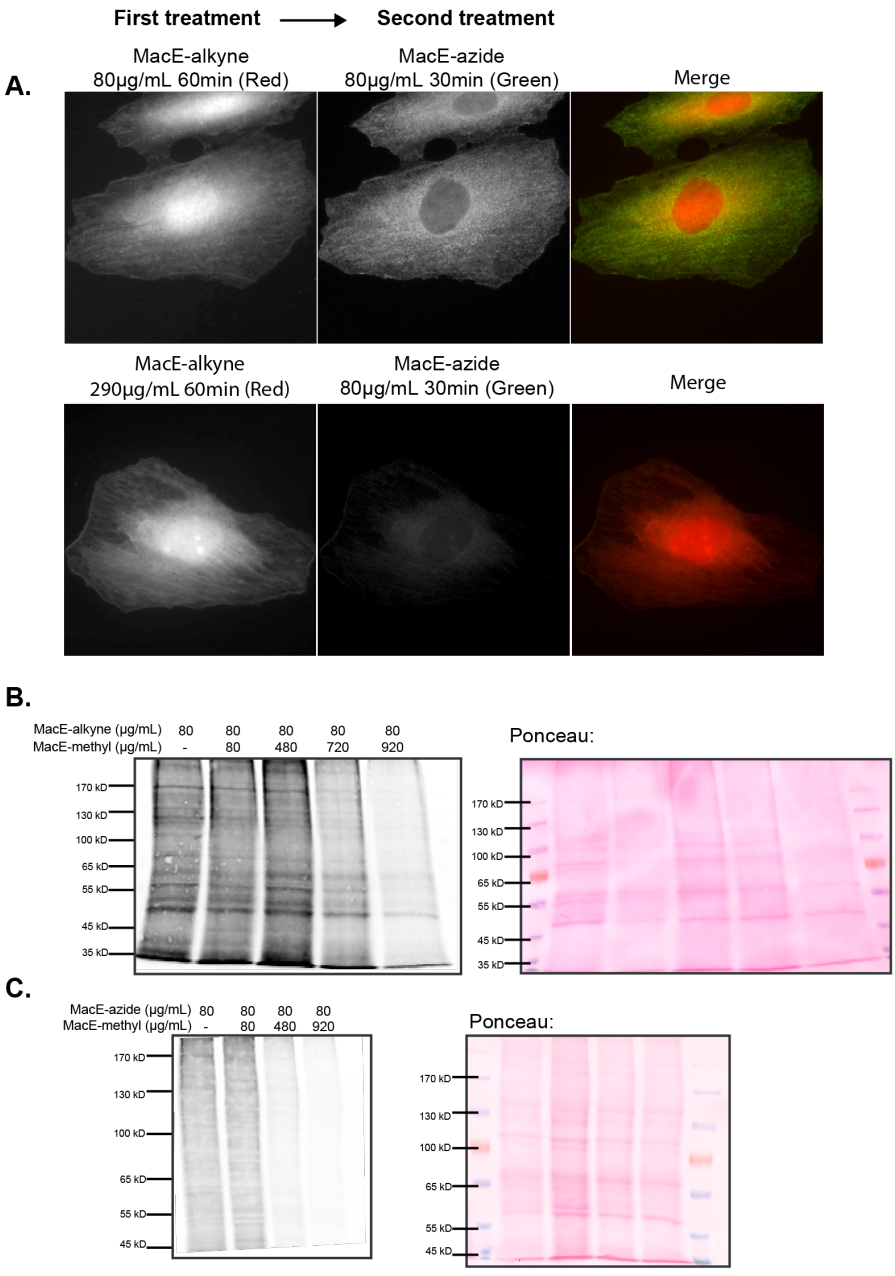


**Figure 4.3 MacE-analogs compete with other MacE-analogues**
Clickable MacE analogs were tested for specificity in binding by competing the MacE-alkyne against MacE-azide, and MacE-azide and MacE-alkyne against MacE-methyl. (**A**) Competition between MacE-alkyne and MacE-methyl visualized in cells. NRK cells were first treated with MacE-alkyne with either 80 µg/mL or 290 µg/mL for 30 min. Then MacE-alkyne was washed out and replaced with 80 µg/mL of MacE-azide for 30 min. Cells were fixed and a Staudinger driven click reaction was used to add a biotin tag to the MacE-azide and a copper-driven click reaction was used to add a rhodamine tag to MacE-Alkyne (red). Biotin was detected with antibodies to biotin (green).(**B**) Competition between MacE-alkyne and MacE-methyl. Cells were treated First with MacE-Methyl at 0 (DMSO), 40, 480, 720, and 920µg/mL 30min. Then drug was washed out and MacE-Alkyne was added at 80µg/mL for 30 min. Cells were lysed and lysate was treated with a cu-click reaction to add biotin then analyzed with poly acrylamide electrophoresis and western blotting and probing with streptavidin conjugated to a near infrared fluorophore. Ponceau is shown for loading. (**C**) Same as B, except MacE-azide was used.

may be reduced, and it did not show any nuclear staining. I next increased the concentration of MacE-alkyne to 290 µg/ml for 60 min, followed by 80 µg/ml for 30 min. These conditions prevented binding of MacE-azide to cellular proteins. I conclude from these results that there is a limited number of binding sites for MacE analogs that, at high concentrations of MacE-alkyne, are occupied by MacE-alkyne.

Similar results were obtained in biochemical competition experiments from lysates of cells treated the MacE analogs (Figure 4.3B). Competition conditions were set up in the following way. Cells were treated for 60 min with MacE-methyl at 0 (DMSO only), 80, 480, 720, or 920 µg/mL, which was the maximum amount possible for these batches of MacE-methyl and alkyne without exceeding 2% DMSO in the medium. The cells were washed and incubated with 80 µg/mL MacE-alkyne for 30 min. Total cell lysate was prepared for each condition and azide-biotin was added for a cu-click reaction. The analysis of the clicked lysates revealed that increasing amounts of MacE-methyl led to a reduction in the signal for MacE-alkyne. A parallel experiment with MacE-azide showed similar results (Figure 4.3C). I conclude from these experiment that the signal we observed with the clickable MacE analogs can be blocked with non-clickable MacE forms, suggesting that both analogs bind to the same site and that there are a limited number of binding sites. Competition was only successful if the non-clickable form was in large excess. Clickable analogs mimic the behavior of non-clickable forms.

**MacE analogs bind quickly to proteins, but the development of the fragmented Golgi phenotype takes more time**

I compared the timing of MacE binding and Golgi fragmentation. Cells were treated with increasing concentrations of MacE-alkyne for 3, 10, and 30 min, followed by fixation and staining(Fig. 4.4A). There was a time and dose dependent labeling of intracellular proteins, but no effect on Golgi organization. Binding of MacE-alkyne was detected after as little as 3 min, and increased with both time and concentration. However, these cells did not display the fragmented Golgi phenotype, suggesting that 30 min was not long enough to induce the phenotype despite a large amount of the molecule binding. In a modification of this experiment, I performed the same drug treatments followed by incubating the cells at 37˚C for a total of 120 mins, which is the normal incubation time that induces the fragmented Golgi phenotype (Figure 4.4B). This experiment was made possible by the irreversibility of MacE binding because washout of unbound compound at the time points left the drug that was already bound. I detected similar staining of proteins throughout the cell as seen with the absence of the additional incubation time. However, cells that had been incubated with the drug for 30 min, showed obvious effects on Golgi organization. Samples treated for 3 or 10 min did not always produce the fragmented Golgi phenotype. Paradoxically, higher concentrations did not always have completely fragmented Golgi phenotypes either. I conclude that at least 30 min of drug treatment and 120 mins of total incubation time is required to generate the Golgi phenotype.

The observed delay in Golgi fragmentation led to the re-evaluation of a previously tested analog MacE analog *t*-Bu-DenA (Schnermann *et al.*, 2011). This

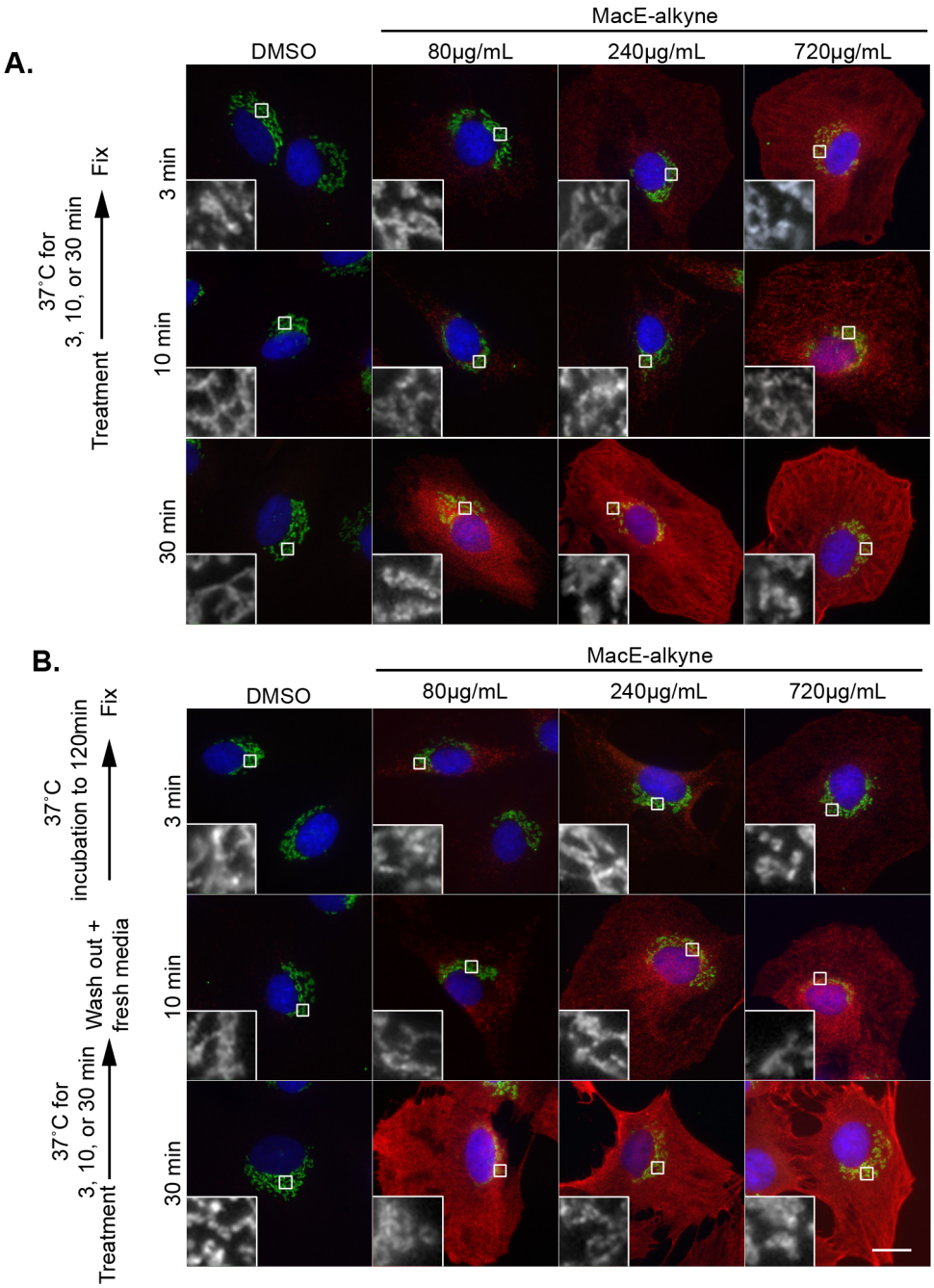


**Figure 4.4 Clickable-MacE-analog binding to proteins and development of the fragmentation phenotype is time and dose dependent.**
The irreversible binding of the clickable MacE analogs were used in cells to determine the minimal amount and time required to form the characteristics Golgi phenotype. (**A**) NRK cells were treated with DMSO, or MacE-Alkyne at 80, 240, or 720µg/mL for 3, 10, or 30 min. After treatment, cells were washed with warm fresh media. Cells were fixed and biotin was attached to any remaining MacE using a copper driven click reaction. Cells were stained with antibodies toward ManII (green) that mark the Golgi, Hoechst 33342 (blue) to mark the DNA, and antibodies to biotin (red) for MacE. (**B**) Same as A, except that at the time of MacE removal, cells were placed in fresh media and incubated for 120 min (this includes drug treatment time) to allow the phenotype to form. Cells shown are representative samples. Scale bar 10µm.

analog did not induce Golgi fragmentation when incubated at 80µg/mL for 60 min, which is the condition at which Ace-*t*-Bu-DenA induced Golgi fragmentation (Schnermann *et al.*, 2011). Interestingly, incubation of NRK cells with *t*-Bu-DenA for 2 hours resulted in a partially fragmented Golgi phenotype that is typical for MacE (Figure 4.5). However, higher concentration concentrations of this analog induced Golgi fragmentation after both 1 and 2 hours incubation. A key difference between *t*-Bu-DenA and Ace-*t*-Bu-DenA, is that *t*-Bu-DenA modifies lysines at approximately half the rate of Ace-*t*-Bu-DenA (Schnermann *et al.*, 2011). This result suggests that the phenotype is dependent on the number of extent of modified lysines.

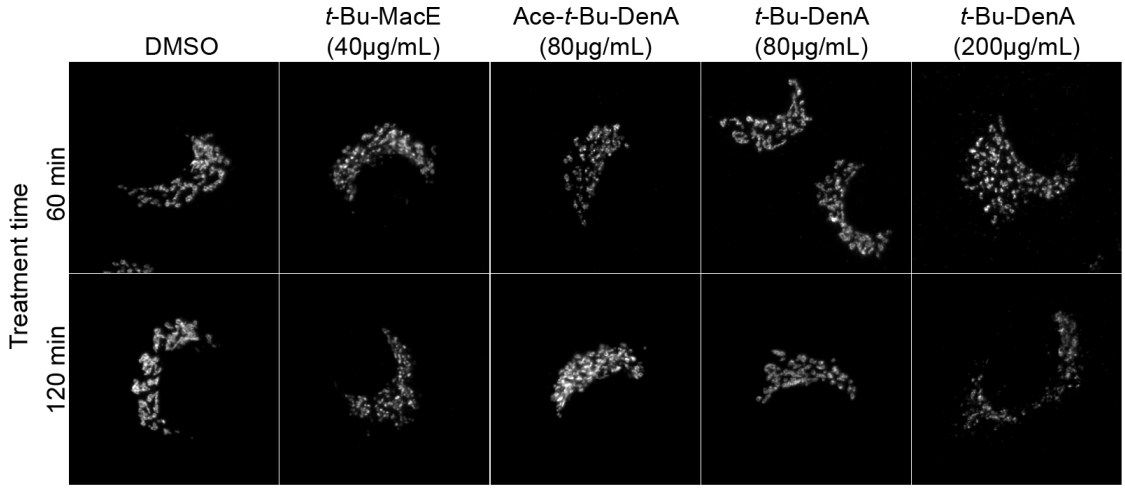


**Figure 4.5 *t*-Bu-DenA induces MacE phenotype**
NRK cells were treated for 60 min (top row) or 12 min (bottom row) with DMSO (control), t-Bu-MacE at 40 µg/mL, Ace-*t*-Bu-DenA at 80 µg/mL, *t*-Bu-DenA at 80 µg/mL, or *t*-Bu-DenA at 200 µg/mL. Representative images are shown. Scale bar represents 10 µM.

## Lysine-modifying compounds produce a similar Golgi phenotype as MacE

Molecules that bind lysines were tested for their ability to induce the Golgi fragmentation phenotype (Figure 4.6A). As NHS-esters are well-known lysine binders, we tested the effects of an azide-modified NHS ester. An uncharged NHS molecule,

**Figure 4.6. General lysine modifiers show fragmented Golgi phenotypes.**

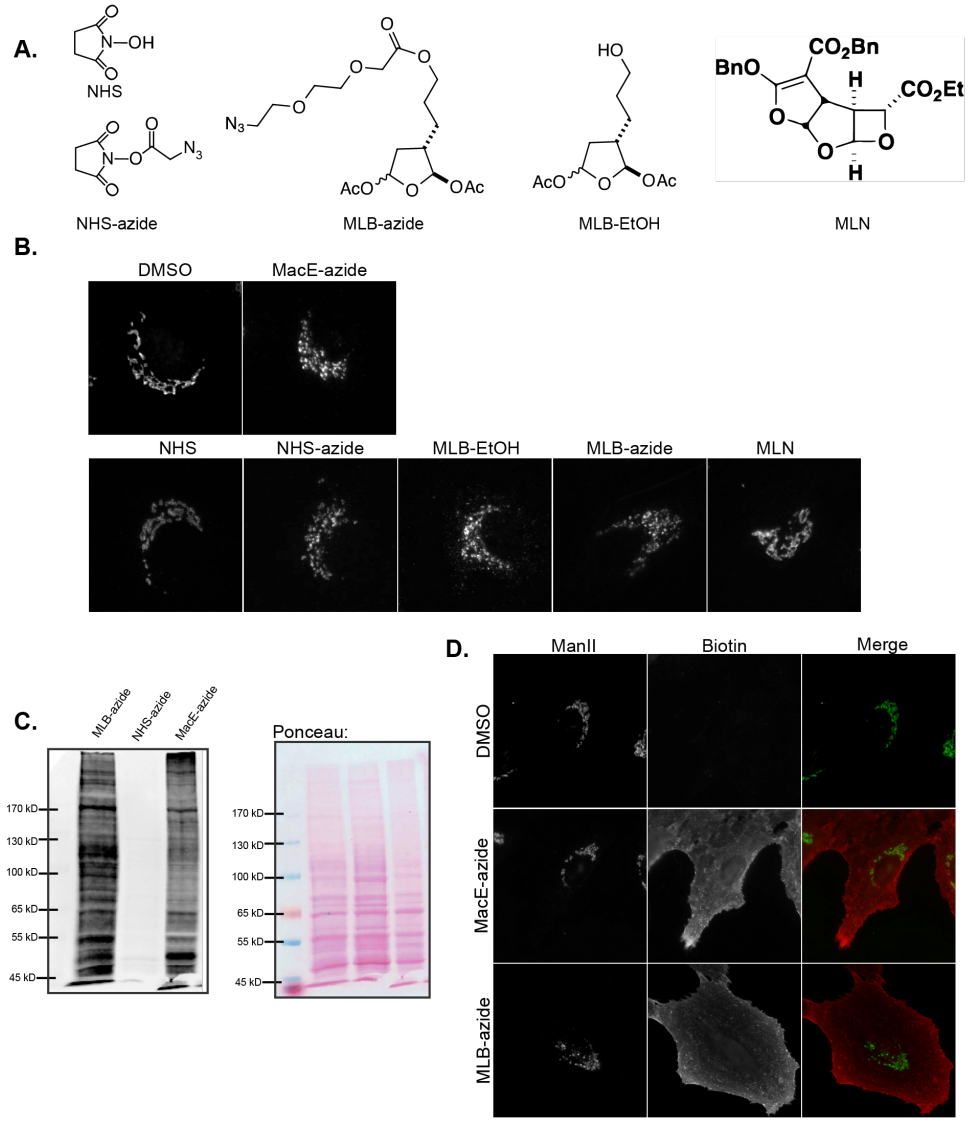


**Figure 4.6 General lysine modifiers induce fragmented Golgi phenotypes.**
The general lysine modifiers NHS ester and a simplified MacE-Like Binding (MLB) molecule were tested for the ability to form the Golgi phenotype. (A) The structure of the new molecules and controls are shown: uncharge NHS, NHS with an ester and azide tag (NHS-azide, note this molecule could modify lysines, but was unable to be clicked), an MLB with an azide group (MLB-azide), the MLB with the non-clickable EtOH group (MLB-EtOH), and a MacE Like Non-binding (MLN) molecule that cannot intact with lysines.(B) Immunofluorescence images of cells treated with DMSO (control) or 80µg/mL MacE-azide, NHS, NHS-azide, MLB-EtOH, MLB-azide, or MLN for 1hr. Cells were fixed and immunostained with antibodies to the Golgi resident protein ManII.(C) Western blot showing NRK cell lysates treated with MLB-azide, NHS-azide, or MacE-azide as a control for 30 min followed by cu-click reaction to add biotin. The western blot was probed with streptavidin conjugated to a near infrared probe and analyzed on an Odyssey-SA (Licor). Ponceau shown for loading.(D) MLB was incubated at 80µg/mL for 30 min with NRK cells, which were then fixed and subjected to a copper driven click reaction to attach a biotin. Cells were stained with antibodies to biotin (red) and ManII (green). MacE-Azide and DMSO were used as controls.

which should not bind lysines, was used as a control. Three molecules were provided by Dr. Larry Overman's lab: Two compounds had an oxygenated ring structure were predicted to behave similar to MacE, (MacE-Like-Binding: MLB). Both should bind lysines, however one has an azide that can be clicked (MLB-azide) while the other has a non-clickable EtOH group (MLB-EtOH). A control with a dual ring structure similar to MacE, but which cannot bind lysines (MacE Like Non-binding: MLN) was used. I found that NHS-azide, MLB-Azide and MLB-EtOH, which are known or predicted to bind lysines, induced a similar fragmented Golgi phenotype as MacE (Figure 4.6B). However, NHS and MLN, which do not modify lysines, had no effect on Golgi organization. These results suggest that wide-spread non-specific lysine binding can produce the fragmented Golgi phenotype.

A parallel biochemical and cell analysis with click chemistry revealed that lysine modifiers bind to similar proteins as MacE-azide. I treated cells with 80 µg/ml MLB, NHS-azide and MacE-azide (control) for 120 min. Lysates from these cells were subjected to the cu-click reaction to add alkyne-biotin, and analyzed by western blotting with streptavidin (Figure 4.6C). While MLB-azide and MacE-azide modified numerous proteins bands in the range from 45 to 300, NHS-azide did not. It is likely that the NHS-azide is not able to be clicked and this is leading to the lack of bands on the western blot because it can produce the fragmented Golgi phenotype. In addition, incubation of 80 µg/ml MLB-azide for 60 min, followed by cu-click reaction to add a alkyne-biotin and analysis with anti-biotin antibodies showed specific staining throughout the cell, similar to MacE-azide. I conclude that MLB-azide reacted with similar proteins to MacE-azide,

or potentially more proteins from the western blot data. Additionally, the azide in the NHS-azide is unable to be clicked.

## Discussion

In this study, I describe the characterization of a new generation of MacE-analogs that are amenable to click chemistry. These molecules, which induced a MacE-like Golgi phenotype, showed binding to multiple proteins as detected in a biochemical and microscopy-based assays. The binding of these MacE analogs to these proteins was time and dose dependent. I also discovered that the development of the Golgi phenotype required time even if enough of the molecule was present and protein bound to produce the phenotype. This led to the finding that one of the molecules previously published not to act on the Golgi, *t*-Bu-DenA, was able modify Golgi membranes and alter its organization, provided it was given enough time and a high enough concentration. My investigations into small molecules that bind lysines demonstrated that these molecules are able to produce a similar fragmented Golgi phenotype as MacE and its analogs. In addition, they appear to bind to similar proteins as MacE analogs.

These findings have led to a model for MacE-induced Golgi fragmentation through irreversible lysine binding. While the exact interactors are unknown it is likely that MacE binds the lysines of a number of proteins and that the modification of at least one or a subset of these lead to the Golgi phenotype. The non-specific lysine binding molecules likely act on the same targets through binding all lysines available. There is the potential that the proteins affected could be involved in forward transport at the

*trans*-Golgi, because H89, a small molecule that blocks transport to the *trans*-Golgi, has a similar phenotype (Puri and Linstedt, 2003). However, H89 also has other effects on the cytoskeleton and Rho kinase, which leads to membrane ruffling, that are not seen with MacE or its analogs (Leemhuis *et al.*, 2002).

This preliminary characterization of MacE analogs has led to a number of questions to be addressed in future studies. How is a specific phenotype produced with the modification of lysines in numerous proteins? Most cellular proteins contain lysines and are therefore likely to be modified by MacE, its analogs and non-specific lysine binders. However, I observed a very specific effect on the Golgi, and not on other organelles or the cytoskeleton. Such a specific effect could be explained by accessibility of the lysines on the protein or the presence of two lysines adjacent to each other that can be modified by the same molecule. This is because the more efficient MacE analogs can bind two lysines, while the much slower *t*-Bu-DenA, which also requires increased drug concentrations, only has the ability to bind one lysine. This idea can be tested in competition experiments between lysine binders and MacE analogs to determine if there are any specific proteins that are bound by one and not the other. Such comparisons would benefit from additional clickable lysine modifiers. For example, NHS-ester with a PEG arm that is similar to the MacE analogs would be useful because it would position the azide group at a large enough distance from the ring structure of the molecule. In addition, lysine modifiers that are structurally bulkier so that they may not gain access to all lysines in a protein may provide useful information. What are the structural components that appear to be bound by MacE? While I observed filament-like staining patterns, I was unable to associate them with a specific organelle or

cytoskeletal filament. Simple staining with actin and microtubules were difficult to evaluate with the wide field microscope because there are large amounts of MacE-analog that flooded the signal throughout the cell with little difference between the structural components and the cytosol. Colocalization experiments in the future would benefit from shorter treatments of 10-15 min with MacE analogs to reduce the signal from MacE, which could allow for the easier identification of specific staining patterns. Additionally a confocal microscope with higher resolution and focus on a narrower z-plane would benefit these experiments. Finally, this study revealed a wide range of proteins bound by MacE analogs. While this was initially surprising, it does raise the question of drug specificity. Drugs and chemicals are frequently used in scientific research, but click chemistry to determine where they bind in cells is not common. What interactions may be missing by not looking at other drugs by click chemistry? This study highlights the need to evaluate the small molecules and drugs that are used more carefully and click chemistry is an excellent method for addressing these interactions.

## Contributions

Kari Herrington preformed the experiments and made the figures. Christine Sütterlin provided guidance and helped with the design of experiments. Larry Overman, Nathan Genung, and Martin Schnermann designed and synthesized MacE analogs. Jennifer Prescher and Lidia Nazarova provided guidance with click chemistry and click chemistry reagents.

# Chapter 5:
# Conclusion and future directions

## Summary of my findings

In this thesis, I describe my contributions to a better understanding of the Golgi apparatus. I carried out two completely independent studies that addressed exciting and important questions about this organelle. Both studies used cutting edge technology to change the way that we look inside cells and see the relationship of the Golgi with proteins and small molecules. In my first study, I used the phasor approach to FLIM-FRET to quantify the spatial activity of the small GTPase Cdc42 using the biosensor Cdc42-FLARE. I extended the normal applications of these biosensors by designing a system that co-expresses the biosensor Cdc42-FLARE inducibly and a cell marker protein for the Golgi or PM constitutively at low levels. Furthermore, I designed my system so it is possible not only to monitor the effects of depleting Cdc42 regulators in live cells, but also verify that these proteins have been depleted in the cells that were measured. Thus my method combines a number of highly beneficial techniques including, low protein expression, resolution of spatial activity at specific locations, and verification of protein knockdown into one powerful system. In my second study, I used click chemistry to look directly at the binding of small molecules to proteins in cells. While the approach is different, this method also provides spatial information that is not usually observed. It allowed me to directly observe where and when the analogs of the small molecule MacE bind to potential targets. Furthermore I was able to use two different forms of click chemistry to simultaneously look at the binding of two different molecules in the cell and determine directly how the molecules affected the binding of

other molecules. While I used fixed cells, these experiments could also be expanded on and done with live cells, which would create further opportunities for exploring the spatial relationships of small molecules and proteins with the Golgi in cells. Each of these experiments has allowed for visualizing interactions with the Golgi in ways that were impossible before and provided new information that has changed the current model of how Cdc42 functions to control the centrosome and how MacE binds.

**Detection of Cdc42 activity at specific locations within the cell using Cdc42-FLARE**

In my Cdc42-FLARE study, described in Chapter 3, I used this advanced imaging method to examine if Golgi-associated Cdc42 regulators contribute to the regulation of Golgi-associated Cdc42. I found that Cdc42 activity is regulated at the Golgi by the GEF Tuba, but not FGD1. I also demonstrated that both FGD1 and Tuba were able to regulate Cdc42 activation at the PM. I also tested for a link between Golgi organization and Cdc42 activity at the Golgi. I found that loss of GM130 or Golgin-84, which disrupt Golgi organization to different degrees, did not alter Cdc42 activity at the Golgi. Their loss, however, led to reduced Cdc42 activity at the PM. Finally, I investigated the requirement for Cdc42 activity in centrosome regulation. I identified a correlation between reduced Cdc42 activity at the PM and centrosome organization defects. These centrosome alterations were similar to those observed with depletion of Tuba or expression of DN-Cdc42, suggesting that the regulation of centrosome organization by Cdc42 occurs at the PM. These results prompted me to modify our previous model for GM130-mediated centrosome regulation (Figure 5.1). This new model predicts that

depletion of GM130 affected a Golgi function that prevents activation of Cdc42 at the Golgi. This could be through a disruption in the transport of Cdc42 or a Cdc42 regulator to the PM leading to reduced Cdc42 activity at the PM. Alternatively, it could prevent the proper modification of a Golgi regulator. It also proposes that Cdc42 activity at the PM is required for centrosome regulation, possibly by controlling the microtubule and actin cytoskeleton. Thus, my results have changed our understanding of how Cdc42 is regulated at the Golgi and the roles that it plays at the Golgi and PM. However, many questions about how Cdc42 is regulated between the Golgi and the PM, at the PM to control the centrosome, and how specific GEFs are controlling Cdc42 activity still remain.

**The phasor approach to FLIM-FRET with Cdc42-FARE to measure Cdc42 activity in cells**

The FRET biosensor Cdc42-FLARE is a powerful tool to measure the spatial distribution of Cdc42 activity in a living cell. This dual chain biosensor is beneficial because it is a genetically encoded biosensor with a high dynamic range and the C-terminal of Cdc42 is undisrupted. It is superior over other Cdc42 biosensors in these regards. For example, the Raichu probe is a single chain biosensor, which has a blocked C-terminus that prevents it from interacting with Rho GDI proteins that are important for Cdc42 regulation. The MeroCBD biosensor is a fantastic tool to detect the activity of endogenous Cdc42, but it is not practical in routine use because the dye has to be synthesized and introduced into cells by single cell microinjection. FLIM-FRET is superior over intensity based FRET because is based off the lifetime, which is the rate

of decay of emission, and it uses a less toxic 2-photon laser for excitation. These two features provide for a quantitative method that is not prone to the fluorescent artifacts associated with intensity based FRET (e.g. photo bleaching, spectral bleed through, and fluorophore concentration) Its use in combination with a dual chain biosensor eliminates possible artifacts from uneven expression levels of donor and acceptor proteins.

With this method, I have confirmed known models of Cdc42 activity. I detected the presence of active Cdc42 at the Golgi. This finding is consistent with results by Nalbant et al. with the MeroCBD probe, which detected endogenous Cdc42, (Nalbant *et al.*, 2004). My studies provide more detail about the Golgi-associated Cdc42 pool because I demonstrate the presence of active Cdc42 throughout the Golgi, which fits with cryo-EM data of CA-Cdc42 (Luna *et al.*, 2002). I observed an increase in activity at the leading edge of the cell after stimulation with PDGF. My results are in agreement with observations using the MeroCBD probe as well as with an improved single chain biosensor with an uninterrupted C-terminal domain (Machacek *et al.*, 2009; Hanna *et al.*, 2014). Furthermore, as seen by Hanna et al. with their single chain biosensor, areas with the highest FRET signal did not always correlate with areas of the highest biosensor concentration (Hanna *et al.*, 2014). These results demonstrate the validity of my method and its ability to measure intracellular Cdc42 activity.

A concern with most biosensors is that overexpression of the probe could alter Cdc42 activity, which affects cell morphology and behavior. Overexpression of Cdc42, the donor component of the biosensor, could affect actin and microtubule organization, microspike formation, and block retrograde transport (Olson *et al.*, 1996; Allen *et al.*, 1997; Luna *et al.*, 2002; Hehnly *et al.*, 2009). In contrast, overexpression of the CBD,

the acceptor component of the biosensor, could lower intracellular Cdc42 activity, which may result in disrupted centrosome organization or a block in forward transport (Meller *et al.*, 2002; Egorov *et al.*, 2009; Kodani *et al.*, 2009; Mo *et al.*, 2013). I verified expression of the Cdc42-FLARE biosensor did not produce any phenotypes linked to an increase or decrease in Cdc42 activity. First, I established stable cell lines that express the biosensor from an inducible plasmid. Even with induction, the expression level of Cdc42 was fairly low. Second, I monitored cellular structures that can be affected by changes in Cdc42 levels, and that include Golgi morphology, the ER, microtubules, the centrosome and Actin (phalloidin). I also observed Cdc42-dependent processes, such as microspike formation, forward transport and retrograde transport.

**Cdc42 activity at the Golgi was specific from the surrounding region**

I detected Cdc42 in the region immediately next to the Golgi, which likely corresponds to endosomes and vesicles. My Cdc42 activity measurements detected highest activity at the Golgi and the PM, but there was also significant Cdc42 activity in areas devoid of Golgi membranes or the PM. This signal was specific because there was little Cdc42 activity in areas further away from the Golgi, which contain fewer of these central membrane structures, suggesting that my method detected specific signals for Cdc42 activity. 3D tomography reconstruction of the Golgi showed that it is surrounded by organelles, including endosomes, endoplasmic reticulum, the ER-Golgi intermediate compartment and numerous vesicles (Mogelsvang *et al.*, 2004). Cdc42 is absent from the ER, but has been detected on endosomes and vesicles, which explains the FRET signal that I observed in areas immediately next to the Golgi, but without any

Golgi membranes (Michaelson *et al.*, 2003; Osmani *et al.*, 2010). Interestingly, Cdc42 in these regions appears to regulated differently than the Golgi pool because manipulations of Cdc42 regulators affected Cdc42 activity at the Golgi or the PM, but not in these regions. In future experiments, it would be interesting to examine Cdc42 regulation in these regions by manipulating other Cdc42 GEFs. For example Arf6 is known to recruit Cdc42 and β-PIX to the endosome (Osmani *et al.*, 2010). Thus, it would be feasible to mark the endosome by ARF6 expression and then measure effects of β-PIX depletion on Cdc42 activity in these areas. I would also predict that Cdc42 activity at the Golgi may not be affected with manipulation of such regulators.

**Visualization of Cdc42 activity in cells had lead to a new model of GM130 regulation of Cdc42 activity**

My findings support a modified model for the control of centrosome organization by structural Golgi proteins (Figure 5.1). Previous work by the Suetterlin lab proposed a model for GM130-mediated centrosome regulation in which GM130 associates with a protein at the Golgi, possibly the GEF Tuba, to activate the Golgi-associated pool of Cdc42. Cdc42 activity at the Golgi then controls centrosome organization, possibly through close physical proximity between these two organelles or by transiently moving from the Golgi to the centrosome. This model was based on several important findings in GM130 depleted cells. 1) GM130 depletion caused defects in centrosome organization and function, a phenotype that was also observed by with the depletion of Tuba or expression of dominant negative Cdc42 (Kodani and Sütterlin, 2008; Kodani *et al.*, 2009). 2) GM130 depletion resulted in a drop in total cellular Cdc42 activity by about

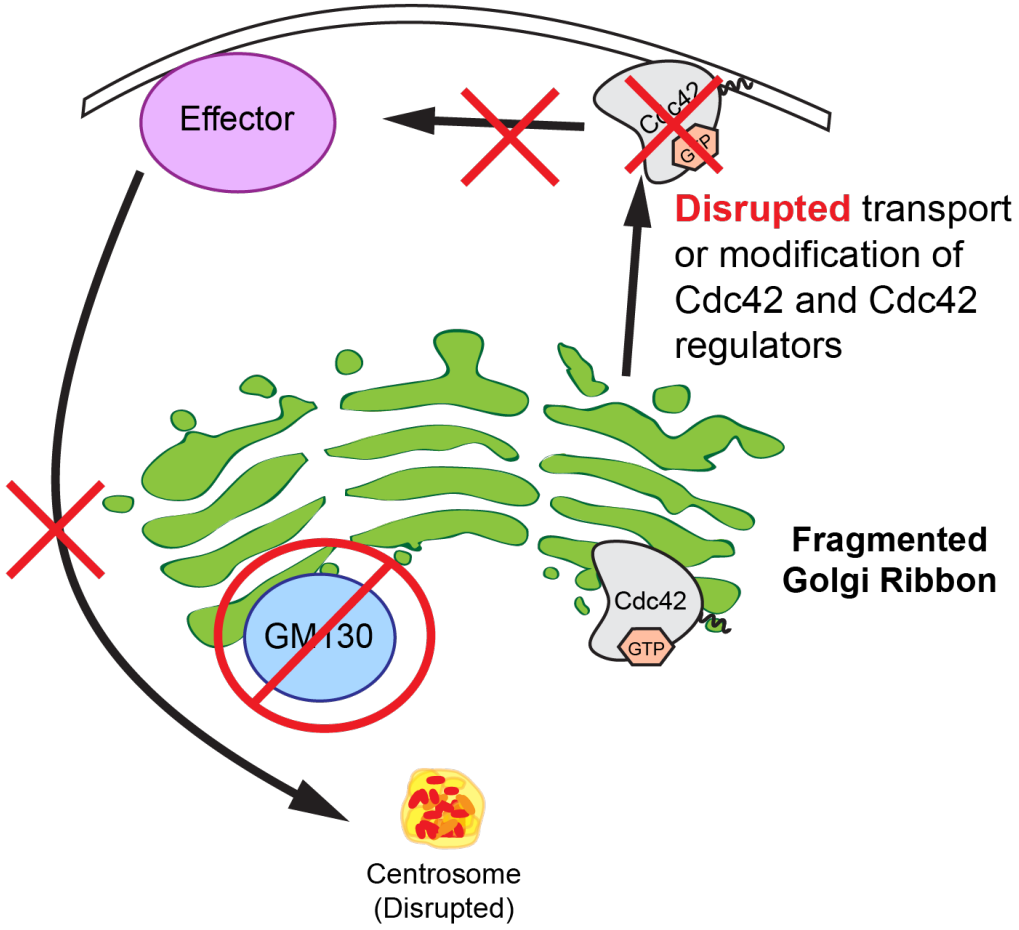


**Figure 5.1 Revised model of GM130 regulation of Cdc42 activity**
The revised model of GM130 regulation of the centrosome. I now propose that loss of GM130 leads to a disruption of the Golgi structure which will wither prevent transport of Cdc42 and/or its regulators or it may lead to improper modification of Cdc42 regulators. In turn this prevents activation of Cdc42 at the PM. Cdc42 will no longer be able to act on down stream effectors that may control centrosome organization through microtubules.

50%. 3) Expression of constitutive active Cdc42 restored centrosome organization and function in the absence of GM130 (Kodani *et al.*, 2009). My results did not support this model, therefore I now propose a modified version to explain GM130-dependant centrosome regulation from the PM.

**How does GM130 regulate Cdc42 activity at the PM?**

Loss of GM130 did not decrease Cdc42 activity at the Golgi, although there was a significant reduction at the PM. While this loss in activity was not at the Golgi, this finding is consistent with previous biochemical data that indicated a reduction in Cdc42 activity in total cell lysates. My new model suggests that GM130 controls Cdc42 activity at the PM, which is necessary for the control the centrosome, through one of its many diverse functions. For example, GM130 controls protein transport (Puthenveedu *et al.*, 2006), so that its loss could affect the transport of Cdc42 or one of its regulators. GM130 could also affect Cdc42 activity at the PM by controlling the modification of Cdc42 or its regulators. Other functions include autophagy, microtubule nucleation, polarization and migration, or protein sorting (Valsdottir *et al.*, 2001; Roti *et al.*, 2002; Hidaka *et al.*, 2004; Preisinger *et al.*, 2004; Puthenveedu *et al.*, 2006; Chiu *et al.*, 2008; Sun *et al.*, 2008; Rivero *et al.*, 2009; Bachert and Linstedt, 2010; Zhou *et al.*, 2010; Hurtado *et al.*, 2011; Joachim *et al.*, 2015). I tested this idea by observing Cdc42 activity in cells depleted of Golgin-84, which is known to fragment and disperse Golgi mini stacks, and to block protein transport (Diao *et al.*, 2003). There was loss of Cdc42 activity the PM, but not at the Golgi, suggesting that both an intact Golgi and Golgi to PM transport are necessary for Cdc42 activity at the PM. Future experiments can

directly address this point by blocking transport through expressing DN-Sar1a, which prevents forward transport by interfering with COPII coat formation (Kuge *et al.*, 1994; Aridor and Balch, 2000). These experiments could be done with a *ts*045-VSVG to monitor transport as a control.

**How does Cdc42 activity at the PM controlling the centrosome?**

Cdc42 activity at the PM could control the organization and function of the centrosome through microtubules. Interestingly, it has been shown that a similar centrosome phenotype to GM130 with centrin2 and kendrin staining is induced by with long-term low dose nocodazole treatment to disrupt microtubules (Dammermann and Merdes, 2002). Therefore Cdc42 may control centrosome organization through effects on microtubules. This could occur at the PM though Cdc42 interaction with Par6/aPKC which inhibits the protein GSK-3 to polarize microtubules (Etienne-Manneville and Hall, 2001; 2003; Cau and Hall, 2005). However, Cdc42 can also affect microtubules through other effectors such as the Microtubule Affinity Regulating Kinase-4 (MARK4; Naz, *et al.,* 2013). MARK4 phosphorylates microtubule binding proteins that stabilize the microtubules and causes their detachment, which leads to stabilized microtubules that resemble the GM130 phenotype (Naz, *et al.,* 2013). Therefore, it will be important to look at other effectors to determine if Cdc42 could affect microtubules though more than one pathway or effector. In the event that microtubules are not involved in forming the centrosome phenotype, isoforms of Par6 that have been shown to regulate the centrosome through a microtubule independent manner (Kodani, *et al.,* 2010; Dormoy et al., 2013).

**Can Cdc42 activity at the Golgi and PM be separated?**

While a reduction of Cdc42 activity could be detected at the PM without a loss of Cdc42 activity at the Golgi, I was unable to detect a reduction of Cdc42 activity only at the Golgi. My manipulations either affected Cdc42 only at the PM or at the Golgi and the PM. I attempted to dysregulate the activity of this small GTPase only at the Golgi by targeting the GAP ARHGAP10 to the Golgi. This was achieved by expressing a truncated form, which contains the GAP domain and the PH domain, which was shown to be sufficient to mediate Golgi localization (Dubois *et al.*, 2005). However, I detected effects of this truncation also on Cdc42 activity at the PM. It is possible that the Golgi targeting is not specific enough so that the truncation is at both, the Golgi and the PM. Future experiments may avoid this problem by fusing the GAP domain to a different Golgi targeting domain, e.g. the transmembrane domain of ManII.

It is questionable if it is possible to deplete Cdc42 activity at the Golgi without affecting Cdc42 activity at the PM. It has been shown both that Cdc42 activity relies on membrane traffic and that membrane traffic relies on Cdc42 activity because a loss of Cdc42 activity leads to a loss of forward transport from the Golgi-to-PM (Egorov, *et al.,* 2009; Osmani, *et al.* 2010). This produces a conundrum, in which the pool of Cdc42 activity at one location of the cell, such as the PM, may be dependent on Cdc42 activity at another location, such as the PM. This could be addressed through using different targeting motifs on the GAP as stated above or an alternative would be to overexpress Coronin7, which binds to Cdc42 in its inactive state as well as N-WASP to prevent Cdc42 activity and activation of N-WASP. To evaluate if these methods affected transport of Cdc42, a pair correlation analysis of a line scan could be done to monitor

the flow of Cdc42 from the Golgi to the plasma membrane. When done in parallel with FLIM-FRET that can be used to determine both the flow an distribution of activity (Hinde, *et al.,* 2013). Experiments such as these would aid in determining if Cdc42 activity at the Golgi is required for Cdc42 activity at the PM.

**How does FGD1 control Cdc42 activity?**

My findings suggest that Tuba, and not FGD1, is responsible for regulating Cdc42 activity at the Golgi. In agreement with previous reports on the association of Tuba with the Golgi, I have found that Cdc42 at the Golgi is regulated by Tuba (Salazar *et al.*, 2003). This is not the case with FGD1, which was proposed to mediate the recruitment of Cdc42 to the Golgi, followed by its activation at this organelle (Egorov *et al.*, 2009). However, these experiments relied heavily on over expression of FGD1 mutants and did not directly assess the effects of disrupting FGD1 on Cdc42 activity levels. Instead, they measured protein transport from the Golgi to the PM, which is disrupted by expression of dominant negative Cdc42 (Egorov *et al.*, 2009). It may be that expression of exogenous FGD1, particularly constitutive active or dominant negative forms overrides endogenous regulation of FGD1.

It has been suggested that FGD1 recruited to the PM and activated through a TGF-β mediated pathway by phosphorylation, which was found to be necessary for the formation of podosomes associated with TGF-β signaling (Daubon *et al.*, 2011). Interestingly, this same study showed that a constitutive active FGD1, which is well known for inducing microspikes and stress fibers (Olsen, *et al*., 1996), did not have the same drastic effects on the actin cytoskeleton and could not for podosomes if the site of

cortactin on FGD1 was mutated. These mechanisms for regulation of FGD1 activity and functions reenforce the idea that GEFs are regulated as well and to fully understand how Cdc42 is regulated we need to understand how the GEFs are regulated. While establishing the assay for FLIM-FRET with Cdc42-FLARE I addressed manipulation of the GEF proteins through depletion and observed Cdc42 activity. However, the use of Cdc42-FLARE could benefit future studies of GEF regulation. For example, this technique could be used to show how Cdc42 activity changes in response to mutants of FGD1 or depletion of potential regulators upstream of FGD1, such as TGF-β. Experiments such as these would provide information on how the GEFs are regulated, which is what ultimately controls Cdc42 activity, and experiments such as these could bridge the gaps in knowledge as to why my results differed from previous findings with FGD1.

**Could RasGRF interact with GM130 to control Cdc42 activity?**

My results with GM130 differ from a report that RasGRF interacts with GM130 at the Golgi to control Cdc42 activity (Baschieri, *et al.*, 2014). In their study, which was published in 2014, Baschieri, *et al*. detected an interaction of GM130 with RasGRF, which they detected at the Golgi and that binds inactive Cdc42. This finding led the authors to propose a model in which GM130 depletion lead to the release of RasGRF, which is then free to bind inactive Cdc42 and prevent the activation of the Golgi associated Cdc42 population (Baschieri *et al.*, 2014). The differences in our results likely stem from the methods that we have chosen to use. Baschieri, *et al.* used the Raichu-Cdc42 biosensor, measuring FRET with the acceptor photobleaching method.

The use of the Raichu biosensor is problematic. In this single chain biosensor, which is composed of YFP-CBD-Cdc42-CFP, Cdc42 is flanked by two different proteins. As a result, the C-terminal end of Cdc42, which mediates membrane localization and RhoGDI interaction, is blocked (Itoh *et al.*, 2002; Yoshizaki *et al.*, 2003). Baschieri, *et al.* stated that their probe uses the native CAAX box of Cdc42 attached to the CFP fluorophore to target this small GTPase to the correct membranes. However, in spite of this improvement, the RhoGDI interaction problem is not fixed. The inability to bind RhoGDIs leads to the constitutive targeting of the small GTPase to membranes and can alter Cdc42 location and activity (Hoffman *et al.*, 2000; Arozarena *et al.*, 2001; Michaelson *et al.*, 2001; Del Pozo *et al.*, 2002; Johnson *et al.*, 2009; Cherfils and Zeghouf, 2013). The single chain biosensor also displays a constant low level of FRET because the YFP and CFP are in the same peptide chain, which lowers the dynamic range of detection and prevents the observation of low levels of protein interaction (Hinde *et al.*, 2012). Additionally, the use of acceptor photobleaching requires fixation, which can lead to altered FRET signals and mislocalization of Cdc42 (Michaelson *et al.*, 2001; Valentin *et al.*, 2005; Malkani and Schmid, 2011).

Beyond the method of FRET measurement, much of the data reported by Baschieri, *et al*. is inconsistent with other reports. The GM130/RasGRF sequestering model directly conflicts with reports on RasGRF, which was shown not to localize to the Golgi (Arozarena *et al.*, 2004; Calvo and Crespo, 2009). Specifically, RasGRF is normally cytosolic but binding of RasGRF to Cdc42-GDP recruits RasGRF to the membrane (Arozarena *et al.*, 2001). This Cdc42-GDP-mediated recruitment of RasGRF to membranes could easily explain the findings by Baschieri *et al.* to provide support for

the GM130 - RasGRF interaction model. For example, they show that there is increase in the interaction between Cdc42-GDP and RasGRF binding in GM130-depleted cells. This is insufficient to implicate GM130 as a regulatory factor in this pathway because any increase in Cdc42-GDP will lead to an in increase in the binding between Cdc42-GDP and RasGRF (Arozarena *et al.*, 2004; Calvo and Crespo, 2009). Furthermore, the argument that depletion of RasGRF restored Cdc42 activity in GM130-depleted cells also does not support a GM130 involvement because the depletion of RasGRF by itself has been shown to increase Cdc42 activity (Arozarena *et al.*, 2004; Calvo and Crespo, 2009).

The study by Baschieri, *et al*. also contradicts numerous publications on GM130 by notable Golgi researchers such as Drs. Adam Linstedt, Martin Lowe, Gustavo Egea, Rosa Rios, and Maria Antonietta De Matteis. For example, in contrast to Baschieri, *et al*., the Linstedt lab reported that loss of GM130 promoted the disconnection of the Golgi ribbon so that the integrity of this organelle is affected (Puthenveedu *et al.*, 2006). Similarly, the Rios lab identified GM130 as a key regulator of Golgi-nucleated microtubules, with the loss of this protein leading to the absence of this population of microtubules (Rivero *et al.*, 2009; Hurtado *et al.*, 2011). To understand the link between GM130 and RasGRF, I tried to verify these RasGRF results with my Cdc42 activity measurement. However, I failed to  detect this protein with three different commercial antibodies in both U2OS or HeLa cells. In addition, I was unable to deplete this protein, using a published siRNA sequence. Baschieri, *et al*., also failed to confirm any protein depletion in the HEK293T cell line that they measured FRET in, even by biochemical methods. In conclusion, because of these differences in techniques, cell lines and an

obvious discrepancy with past literature, it is not surprising that my data differs from theirs.

**The future of Cdc42-FLARE**

We have begun to understand how Cdc42 is regulated in cells, however many questions still remain. The study I have shown here establishes a method for observing Cdc42 activity at specific locations in the cell. Determining locations of Cdc42 activity in cells has provided me with the spatial information to revise our lab's current model of Cdc42 that was based on bio chemical data. The use of Cdc42-FLARE with FLIM-FRET has also brought forth several questions about how Cdc42 activity is regulated at the Golgi and at the plasma membrane, such as how are Golgi proteins affecting Cdc42 activity at the plasma membrane? is it transport or post modification of Cdc42 proteins? Do other golgin proteins have the same effect on Cdc42 activity? How are GEFs, such as FGD1, controlled at the Golgi and PM? and finally how does Cdc42 activity at the PM control the centrosome? The use of this biosensor will be helpful in answering these questions in addition to providing a model to address other questions about how Cdc42 activity is functioning in cells.

**MacE analogs to determine sites of protein binding**

In my second project, which is described in Chapter 4, I examined the mechanism of MacE-mediated Golgi fragmentation. I used click chemistry to assess binding of MacE analogs to possible targets with the ultimate goal to identify the target of this small molecule and to understand how MacE disrupts the Golgi. I found in

microscopy-based and biochemical assays that MacE binds a wide number of proteins within the cell. To my surprise, I also found that non-specific lysine modifying molecules produce a similar results in respect to protein binding and Golgi organization. Thus, while I have not succeeded in identifying the MacE target, my studies have shown a use for this technique in visualizing targets of small molecules, which could be useful for addressing drug specificity.

My results demonstrated that clickable MacE analogs are a new tool to study the mechanism of MacE-induced Golgi fragmentation. I made three novel findings with a new generation of MacE analogs. First, I showed that these compounds induce a similar Golgi fragmentation phenotype as the natural compound MacE. Incubation with these compounds for 30 minutes, followed by 2 hour incubation in the absence of the compound, was sufficient to induce Golgi fragmentation. Second, I demonstrated that they can be used with click chemistry. Using cu-click or the Staudinger reaction, I was able to “add” various tags, including biotin for biochemical studies or rhodamine for microscopy studies. Third, I found that these compounds show specific binding to a wide number of proteins throughout the cell. Microscopy allowed for the detection of the “clicked” compounds in the cells, where they appeared enriched in the perinuclear region and also formed filamentous structures. Biochemical experiments revealed labeling of many proteins ranging in size from 45 to 30 KDa, these proteins were modified in a time and dose dependent reaction either in intact cells or in total cell lysates. The ability of the molecules to target specific binding sites was established through competition experiments with non-clickable analogs. The finding that binding of MacE analogs to cellular proteins precedes the development of the Golgi fragmentation

phenotype led me to re-evaluate the previously characterized molecule, *t*-Bu-DenA, which had been categorized as "non-active". Using higher concentrations and longer time points from this I found that this molecule could also affect the Golgi.

MacE may produce the Golgi fragmentation phenotype through covalently binding lysines (Schnermann *et al.*, 2011). Our previous studies identified a first correlation between the MacE-induced Golgi fragmentation and lysine modification. Incubation of *t*-Bu-MacE with lysozyme *in vitro* resulted in abundant modification of lysines present in lysozyme (Schnermann *et al.*, 2011). Analogs that bound lysines quickly, such as Ace-*t*-Bu-DenA, produced the Golgi fragmentation promptly, while *t*-Bu-DenA, which only bind one lysine induced the phenotype with some delay. I therefore investigated the random lysine binders NHS-ester with an azide attached and one that was designed after the MacE molecules  These molecules reproduced the MacE phenotype, while compounds that could not bind lysines did not. It is important to note that the NHS-azide was able to modify the Golgi, but was unable to have a tag added tough click chemistry. This may be due to the close proximity of the azide adjacent to the the run structure and it would most likely be able to be clicked if a PEG chain was added between the azide and ring structure. This suggest that these molecules function through bindings lysines. As lysines are present in most proteins, it is unclear how analogs produce such a unique phenotype. The finding that lysine modifying compounds produce a MacE-like Golgi fragmentation phenotype suggests that MacE may indeed modify a lysine in its target protein. Lysines are known to undergo a large number of modifications, including acetylation, glycosylation, methylation and

ubiqitination. I do not yet know if the MacE analogs prevent any of these modifications but such studies would be difficult, given that I do not know the target protein of MacE.

**How is the Golgi fragmented by MacE analogs without dispersal for the perinuclear space?**

An extensively fragmented Golgi in the perinuclear space has been seen with other drugs, such as H89, which block forward transport from the *trans*-Golgi (Lee and Linstedt, 2000). However, H89 is reversible and can lead to morphological changes in the cytoskeleton (Leemhuis *et al.*, 2002). Given the similarity in phenotype, H89 may actually provide some insights into the mechanism. H89 has been reported to function through a number of cellular kinases (Leemhuis *et al.*, 2002), For example, it is known to act on Rho Kinase, which is how it may control cell morphology. However, it also controls PKA to inhibit transport from the TGN to PM (Lee and Linstedt, 2000). Therefore for the in the future with MacE it will be important to investigate kinases like PKA that may have been inactivated by MacE-analogs.

**Future considerations for MacE analogs**

I was a surprising to find that MacE may bind to a large number of targets in cells and that this phenotype could be repeated by random lysine binders. While this result indicated that I was unlikely to find a specific proteins that produces the extensively fragmented Golgi phenotype, I have made a novel finding about MacE analogs and random lysine binders. Furthermore, I have demonstrated that click chemistry is a valuable tool for assessing how small molecules behave in cells.

## Summary

In summary, I have addressed different aspects of Golgi biology through two very different methods I have developed an assay to investigate Cdc42 activity at the Golgi, My assay is improved over those used in the past because it uses a dual chain biosensor with a high dynamic range of detection and can interact with its normal regulators. I used a superior FRET detection method and proteins that are manipulated can be confirmed by fixing the cells and preforming imunnofluorescence analysis. Also it is performed in living cells. Using this method I have shown that the Golgi regulates the centrosome during interphase in non-polarized cells through Cdc42 activity at the plasma membrane. My approach and the cell lines that I have established will be useful for the scientific community with interest in the spatial distribution of Cdc42 activity. I have also used click chemistry to investigate MacE analogs in cells. I found that these analogs bound specifically to a large number of proteins. However, while the Golgi fragmentation phenotype appears highly specific, it is not known how it is generated, in particular in light of the finding that general lysine modifiers also induce Golgi fragmentation. While different in nature, both of these methods have provided new insights from the spatial data they provide on activation or binding of proteins in cells and will provide to be a valuable resource in the future.

# References


Acharya, U., Mallabiabarrena, A., Acharya, J. K., and Malhotra, V. (1998). Signaling via mitogen-activated protein kinase kinase (MEK1) is required for Golgi fragmentation during mitosis. Cell *92*, 183–192.

Allen, W. E., Jones, G. E., Pollard, J. W., and Ridley, A. J. (1997). Rho, Rac and Cdc42 regulate actin organization and cell adhesion in macrophages. Journal of Cell Science *110*, 707–720.

Alvarez, C., Garcia-Mata, R., Hauri, H. P., and Sztul, E. (2001). The p115-interactive proteins GM130 and giantin participate in endoplasmic reticulum-Golgi traffic. J Biol Chem *276*, 2693–2700.

Anderhub, S. J., Krämer, A., and Maier, B. (2012). Centrosome amplification in tumorigenesis. Cancer Lett *322*, 8–17.

Añel, A. M. D., and Malhotra, V. (2005). PKCη is required for β1γ2/β3γ2- and PKD-mediated transport to the cell surface and the organization of the Golgi apparatus. J Cell Biol *169*, 83–91.

Arasaki, K., Takagi, D., Furuno, A., Sohda, M., Misumi, Y., Wakana, Y., Inoue, H., and Tagaya, M. (2013). A new role for RINT-1 in SNARE complex assembly at the trans-Golgi network in coordination with the COG complex. Molecular Biology of the Cell *24*, 2907–2917.

Arozarena, I., Matallanas, D., and Crespo, P. (2001). Maintenance of CDC42 GDP-bound state by Rho-GDI inhibits MAP kinase activation by the exchange factor Ras-GRF. Evidence for Ras-GRF function being inhibited by Cdc42-GDP but unaffected by Cdc42-GTP. J Biol Chem *276*, 21878–21884.

Arozarena, I., Matallanas, D., Berciano, M. T., Sanz-Moreno, V., Calvo, F., Munoz, M. T., Egea, G., Lafarga, M., and Crespo, P. (2004). Activation of H-Ras in the endoplasmic reticulum by the RasGRF family guanine nucleotide exchange factors. Mol Cell Biol *24*, 1516–1530.

Aureli, M., Samarani, M., Loberto, N., Bassi, R., Murdica, V., Prioni, S., Prinetti, A., and Sonnino, S. (2013). The Glycosphingolipid Hydrolases in the Central Nervous System. Mol Neurobiol *50*, 76–87.

Bannai, H., Inoue, T., Nakayama, T., Hattori, M., and Mikoshiba, K. (2004). Kinesin dependent, rapid, bi-directional transport of ER sub-compartment in dendrites of hippocampal neurons. Journal of Cell Science *117*, 163–175.

Barr, F. A. (1999). A novel Rab6-interacting domain defines a family of Golgi-targeted coiled-coil proteins. Curr Biol *9*, 381–384.

Barr, F. A. (2013). Review series: Rab GTPases and membrane identity: causal or inconsequential? The Journal of Cell Biology *202*, 191–199.

Barr, F. A., and Short, B. (2003). Golgins in the structure and dynamics of the Golgi apparatus. Curr Opin Cell Biol *15*, 405–413.

Barr, F. A., Nakamura, N., and Warren, G. (1998). Mapping the interaction between GRASP65 and GM130, components of a protein complex involved in the stacking of Golgi cisternae. The EMBO Journal *17*, 3258–3268.

Barr, F. A., Puype, M., Vandekerckhove, J., and Warren, G. (1997). GRASP65, a Protein Involved in the Stacking of Golgi Cisternae. Cell *91*, 253–262.

Baschieri, F., Confalonieri, S., Bertalot, G., Di Fiore, P. P., Dietmaier, W., Leist, M., Crespo, P., Macara, I. G., and Farhan, H. (2014). Spatial control of Cdc42 signalling by a GM130-RasGRF complex regulates polarity and tumorigenesis. Nat Commun *5*, 4839.

Bayer, M., Fischer, J., Kremerskothen, J., Ossendorf, E., Matanis, T., Konczal, M., Weide, T., and Barnekow, A. (2005). Identification and characterization of Iporin as a novel interaction partner for rab1. BMC Cell Biol *6*, 15.

Bettencourt-Dias, M., and Glover, D. M. (2007). Centrosome biogenesis and function: centrosomics brings new understanding. Nature Reviews Molecular Cell Biology *8*, 451–463.

Bhattacharya, K., Swaminathan, K., Peche, V. S., Clemen, C. S., Knyphausen, P., Lammers, M., Noegel, A. A., and Rastetter, R. H. (2016). Novel Coronin7 interactions with Cdc42 and N-WASP regulate actin organization and Golgi morphology. Sci. Rep., 1–17.

Bonfanti, L., Mironov, A. A., Martínez-Menárguez, J. A., Martella, O., Fusella, A., Baldassarre, M., Buccione, R., Geuze, H. J., and Luini, A. (1998). Procollagen traverses the Golgi stack without leaving the lumen of cisternae: evidence for cisternal maturation. Cell *95*, 993–1003.

Bretz, R., Bretz, H., and Palade, G. E. (1980). Distribution of terminal glycosyltransferases in hepatic Golgi fractions. J Cell Biol *84*, 87–101.

Brown, F. D., Rozelle, A. L., Yin, H. L., Balla, T., and Donaldson, J. G. (2001). Phosphatidylinositol 4,5-bisphosphate and Arf6-regulated membrane traffic. J Cell Biol *154*, 1007–1017.

Brown, R., Gray, R. H., and Bernstein, I. A. (1985). Retinoids alter the direction of differentiation in primary cultures of cutaneous keratinocytes. Differentiation *28*, 268–278.

Burakov, A., Nadezhdina, E., Slepchenko, B., and Rodionov, V. (2003). Centrosome positioning in interphase cells. J Cell Biol *162*, 963–969.

Burbelo, P. D., Drechsel, D., and Hall, A. (1995). A Conserved Binding Motif Defines Numerous Candidate Target Proteins for Both Cdc42 and Rac GTPases. J Biol Chem *270*, 29071–29074.

Burd, C. G., Strochlic, T. I., and Setty, S. R. G. (2004). Arf-like GTPases: not so Arf-like after all. Trends Cell Biol *14*, 687–694.

Burns, S., Avena, J. S., Unruh, J. R., Yu, Z., and Smith, S. E. (2015). Structured illumination with particle averaging reveals novel roles for yeast centrosome components during duplication. Elife.

Calvo, F., and Crespo, P. (2009). Structural and Spatial Determinants Regulating TC21 Activation by RasGRF Family Nucleotide Exchange Factors. Molecular Biology of the Cell *20*, 4289–4302.

Calvo, F., Sanz-Moreno, V., Agudo-Ibanez, L., Wallberg, F., Sahai, E., Marshall, C. J., and Crespo, P. (2011). RasGRF suppresses Cdc42-mediated tumour cell movement, cytoskeletal dynamics and transformation. Nat Cell Biol *13*, 819–826.

Campellone, K. G., Webb, N. J., Znameroski, E. A., and Welch, M. D. (2008). WHAMM is an Arp2/3 complex activator that binds microtubules and functions in ER to Golgi transport. *134*, 148–161.

Cau, J., and Hall, A. (2005). Cdc42 controls the polarity of the actin and microtubule cytoskeletons through two distinct signal transduction pathways. J Cell Sci *118*, 2579–2587.

Chan, E. K., and Fritzler, M. J. (1998). Golgins: coiled-coil-rich proteins associated with the Golgi Complex. Electronic Journal of Biotechnology *1*, 01–20.

Chen, T.-C., Lin, K.-T., Chen, C.-H., Lee, S.-A., Lee, P.-Y., Liu, Y.-W., Kuo, Y.-L., Wang, F.-S., Lai, J.-M., and Huang, C.-Y. F. (2014). Using an in Situ Proximity Ligation Assay to Systematically Profile Endogenous Protein–Protein Interactions in a Pathway Network. Journal of Proteome Research *13*, 5339–5346.

Chen, Y., Mills, J. D., and Periasamy, A. (2003). Protein localization in living cells and tissues using FRET and FLIM - Chen - 2003 - Differentiation - Wiley Online Library. Differentiation.

Cherfils, J., and Zeghouf, M. (2013). Regulation of Small GTPases by GEFs, GAPs, and GDIs. Physiological Reviews *93*, 269–309.

Chiu, C.-F., Ghanekar, Y., Frost, L., Diao, A., Morrison, D., McKenzie, E., and Lowe, M. (2008). ZFPL1, a novel ring finger protein required for cis-Golgi integrity and efficient ER-to-Golgi transport. The EMBO Journal *27*, 934–947.

Clegg, R. M. (1995). Fluorescence resonance energy transfer. Curr. Opin. Biotechnol. *6*, 103–110.

Climer, L. K., Dobretsov, M., and Lupashin, V. (2015). Defects in the COG complex and COG-related trafficking regulators affect neuronal Golgi function. Front. Neurosci. *9*, 1457–1459.

Cole, N. B., Ellenberg, J., Song, J., DiEuliis, D., and Lippincott-Schwartz, J. (1998). Retrograde transport of Golgi-localized proteins to the ER. J. Cell Biol. *140*, 1–15.

Cole, N. B., Sciaky, N., Marotta, A., Song, J., and Lippincott-Schwartz, J. (1996). Golgi dispersal during microtubule disruption: regeneration of Golgi stacks at peripheral endoplasmic reticulum exit sites. Molecular Biology of the Cell *7*, 631–650.

Colyer, R. A., Lee, C., and Gratton, E. (2008). A novel fluorescence lifetime imaging system that optimizes photon efficiency. Microsc. Res. Tech. *71*, 201–213.

Coso, O. A., Chiariello, M., Yu, J. C., Teramoto, H., Crespo, P., Xu, N., Miki, T., and Gutkind, J. S. (1995). The small GTP-binding proteins Rac1 and Cdc42 regulate the activity of the JNK/SAPK signaling pathway. Cell *81*, 1137–1146.

Csépányi-Kömi, R., Lévay, M., and Ligeti, E. (2012). Small G proteins and their regulators in cellular signalling. Mol. Cell. Endocrinol. *353*, 10–20.

Dalton, A. J., and Felix, M. D. (1954). Cytologic and cytochemical characteristics of the Golgi substance of epithelial cells of the epididymis–in situ, in homogenates and after isolation. American Journal of Anatomy *94*, 171–207.

Dammermann, A., and Merdes, A. (2002). Assembly of centrosomal proteins and microtubule organization depends on PCM-1. J Cell Biol *159*, 255–266.

Daubon, T., Buccione, R., and Genot, E. (2011). The Aarskog-Scott syndrome protein Fgd1 regulates podosome formation and extracellular matrix remodeling in transforming growth factor β-stimulated aortic endothelial cells. Mol Cell Biol *31*, 4430–4441.

de Figueiredo, P., Polizotto, R. S., Drecktrah, D., and Brown, W. J. (1999). Membrane tubule-mediated reassembly and maintenance of the Golgi complex is disrupted by phospholipase A2 antagonists. Molecular Biology of the Cell *10*, 1763–1782.

Del Pozo, M. A., Kiosses, W. B., Alderson, N. B., Meller, N., Hahn, K. M., and Schwartz, M. A. (2002). Integrins regulate GTP-Rac localized effector interactions through dissociation of Rho-GDI. Nat Cell Biol *4*, 232–239.

DerMardirossian, C., Rocklin, G., Seo, J.-Y., and Bokoch, G. M. (2006). Phosphorylation of RhoGDI by Src regulates Rho GTPase binding and cytosol-membrane cycling. Molecular Biology of the Cell *17*, 4760–4768.

Deutscher, S. L., Creek, K. E., Merion, M., and Hirschberg, C. B. (1983). Subfractionation of rat liver Golgi apparatus: separation of enzyme activities involved in the biosynthesis of the phosphomannosyl recognition marker in lysosomal enzymes. Proceedings of the National Academy of Sciences of the United States of America *80*, 3938–3942.

Diao, A., Frost, L., Morohashi, Y., and Lowe, M. (2008). Coordination of golgin tethering and SNARE assembly: GM130 binds syntaxin 5 in a p115-regulated manner. J Biol Chem *283*, 6957–6967.

Diao, A., Rahman, D., Pappin, D. J. C., Lucocq, J., and Lowe, M. (2003). The coiled-coil membrane protein golgin-84 is a novel rab effector required for Golgi ribbon formation. J. Cell Biol. *160*, 201–212.

Digman, M. A., Caiolfa, V. R., Zamai, M., and Gratton, E. (2008). The phasor approach to fluorescence lifetime imaging analysis. Biophys J *94*, L14–L16.

Dippold, H. C. *et al.* (2009). GOLPH3 Bridges Phosphatidylinositol-4-Phosphate and Actomyosin to Stretch and Shape the Golgi to Promote Budding. Cell *139*, 337–351.

Do, M. T. *et al.* (2014). Ilimaquinone induces death receptor expression and sensitizes human colon cancer cells to TRAIL-induced apoptosis through activation of ROS-ERK/p38 MAPKâ€“CHOP signaling pathways. Food and Chemical Toxicology *71*, 51–59.

Donaldson, J. G., Finazzi, D., and Klausner, R. D. (1992a). Brefeldin A inhibits Golgi membrane-catalysed exchange of guanine nucleotide onto ARF protein.

Donaldson, J., Finazzi, D., and Klausner, R. (1992b). Brefeldin-a Inhibits Golgi Membrane-Catalyzed Exchange of Guanine-Nucleotide onto Arf Protein. Nature *360*, 350–352.

Dormoy, V., Tormanen, K., and Suetterlin, C. (2013). Par6 gamma is at the mother centriole and controls centrosomal protein composition through a Par6 alpha-dependent pathway. Journal of Cell Science *126*, 860–870.

Droscher, A. (1998). The history of the Golgi apparatus in neurones from its discovery in 1898 to electron microscopy. Brain Res. Bull. *47*, 199–203.

Dubois, T., and Chavrier, P. (2005). Une nouvelle protéine RhoGAP impliquée dans la régulation du complexe Arp2/3 au niveau de l'appareil de Golgi : Un relais entre les protéines G ARF1 et Cdc42. Med Sci (Paris) *21*, 692–694.

Dubois, T., Paléotti, O., Mironov, A. A., Fraisier, V., Stradal, T. E. B., de Matteis, M. A., Franco, M., and Chavrier, P. (2005). Golgi-localized GAP for Cdc42 functions downstream of ARF1 to control Arp2/3 complex and F-actin dynamics. Nat Cell Biol *7*, 353–364.

Dukhovny, A., Yaffe, Y., Shepshelovitch, J., and Hirschberg, K. (2009). The length of cargo-protein transmembrane segments drives secretory transport by facilitating cargo concentration in export domains. Journal of Cell Science *122*, 1759–1767.

Dunphy, W. G., Brands, R., and Rothman, J. E. (1985). Attachment of terminal N-acetylglucosamine to asparagine-linked oligosaccharides occurs in central cisternae of the Golgi stack. Cell *40*, 463–472.

Efimov, A., Kharitonov, A., Efimova, N., Loncarek, J., Miller, P. M., Andreyeva, N., Gleeson, P., Galjart, N., Maia, A. R. R., and McLeod, I. X. (2007). Asymmetric CLASP-Dependent Nucleation of Noncentrosomal Microtubules at the trans-Golgi Network. Developmental Cell *12*, 917–930.

Egea, G., Serra-Peinado, C., Salcedo-Sicilia, L., and Gutiérrez-Martínez, E. (2013). Actin acting at the Golgi. Histochem Cell Biol *140*, 347–360.

Egorov, M. V. *et al.* (2009). Faciogenital Dysplasia Protein (FGD1) Regulates Export of Cargo Proteins from the Golgi Complex via Cdc42 Activation. Molecular Biology of the Cell *20*, 2413–2427.

Ehrenreich, J. H., Bergeron, J. J., Siekevitz, P., and Palade, G. E. (1973). Golgi fractions prepared from rat liver homogenates. I. Isolation procedure and morphological characterization. J Cell Biol *59*, 45–72.

Elangovan, M., Day, R. N., and Periasamy, A. (2002). Nanosecond fluorescence resonance energy transfer−fluorescence lifetime imaging microscopy to localize the protein interactions in a single living cell. J Microsc *205*, 3–14.

Erickson, J. W., Zhang, C. J., Kahn, R. A., Evans, T., and Cerione, R. A. (1996). Mammalian Cdc42 is a brefeldin A-sensitive component of the Golgi apparatus. J Biol Chem *271*, 26850–26854.

Estrada, L., Caron, E., and Gorski, J. L. (2001). Fgd1, the Cdc42 guanine nucleotide exchange factor responsible for faciogenital dysplasia, is localized to the subcortical actin cytoskeleton and Golgi membrane. Human Molecular Genetics *10*, 485–495.

Etienne-Manneville, S., and Hall, A. (2001). Integrin-mediated activation of Cdc42 controls cell polarity in migrating astrocytes through PKCzeta. Cell *106*, 489–498.

Etienne-Manneville, S., and Hall, A. (2003). Cdc42 regulates GSK-3|[beta]| and adenomatous polyposis coli to control cell polarity. *421*, 753–756.

Farquhar, M. G., and Palade, G. E. (1981). The Golgi apparatus (complex)-(1954-1981)-from artifact to center stage. The Journal of Cell Biology.

Farquhar, M. G., and Palade, G. E. (1998). The Golgi apparatus: 100 years of progress and controversy. Trends Cell Biol.

Feng, Q., Baird, D., Peng, X., Wang, J., Ly, T., Guan, J.-L., and Cerione, R. A. (2006). Cool-1 functions as an essential regulatory node for EGF receptor- and Src-mediated cell growth. Nat Cell Biol *8*, 945–U955.

Fleischer, B., Fleischer, S., and Ozawa, H. (1969). Isolation and characterization of Golgi membranes from bovine liver. J Cell Biol *43*, 59–79.

Förster, T. (2012). Energy migration and fluorescence. 1946. J Biomed Opt *17*, 011002–01100210.

Freeze, H. H., and Ng, B. G. (2011). Golgi Glycosylation and Human Inherited Diseases. Cold Spring Harbor Perspectives in Biology *3*, a005371–a005371.

Friend, D. S., and Murray, M. J. (1965). Osmium impregnation of the Golgi apparatus. American Journal of Anatomy *117*, 135–149.

Gao, Y., Niu, Y., Wang, X., Wei, L., Zhang, R., Lv, S., Yu, Q., and Yang, X. (2011). Chromosome aberrations associated with centrosome defects: a study of comparative genomic hybridization in breast cancer. Hum. Pathol. *42*, 1693–1701.

Garcia-Mata, R., and Burridge, K. (2007). Catching a GEF by its tail. Trends Cell Biol *17*, 36–43.

Gillingham, A. K., and Munro, S. (2016). Finding the Golgi: Golgin Coiled-Coil Proteins Show the Way. Trends in Cell Biology *26*, 399–408.

Gillingham, A. K., Tong, A. H. Y., Boone, C., and Munro, S. (2004). The GTPase Arf1p and the ER to Golgi cargo receptor Erv14p cooperate to recruit the golgin Rud3p to the cis-Golgi. J Cell Biol *167*, 281–292.

Glick, B. S., and Malhotra, V. (1998). The Curious Status of the Golgi Apparatus. Cell *95*, 883–889.

Glick, B. S., and Nakano, A. (2009). Membrane traffic within the Golgi apparatus. Annu. Rev. Cell Dev. Biol. *25*, 113–132.

Goicoechea, S. M., Awadia, S., and Garcia-Mata, R. (2014). I'm coming to GEF you: Regulation of RhoGEFs during cell migration. Cell Adh Migr *8*, 535–549.

Golgi, C. (1898). Sulla struttura delle cellule nervose dei gangli spinali. Bollettino Della Societa Medico-Chirurgica Di Pavia. *13*, 53–63.

Gomes, E. R., and Gundersen, G. G. (2006). Real-time centrosome reorientation during fibroblast migration. Meth Enzymol *406*, 579–592.

Gonçalves, J., Nolasco, S., Nascimento, R., Lopez Fanarraga, M., Zabala, J. C., and Soares, H. (2010). TBCCD1, a new centrosomal protein, is required for centrosome and Golgi apparatus positioning. EMBO Rep. *11*, 194–200.

Griffith, K. J., Chan, E. K., Lung, C. C., Hamel, J. C., Guo, X., Miyachi, K., and Fritzler, M. J. (1997). Molecular cloning of a novel 97-kd Golgi complex autoantigen associated with Sjögren's syndrome. Arthritis Rheum. *40*, 1693–1702.

Griffiths, G., Brands, R., Burke, B., Louvard, D., and Warren, G. (1982). Viral membrane proteins acquire galactose in trans Golgi cisternae during intracellular transport. J Cell Biol *95*, 781–792.

Griffiths, G., Quinn, P., and Warren, G. (1983). Dissection of the Golgi complex. I. Monensin inhibits the transport of viral membrane proteins from medial to trans Golgi cisternae in baby hamster kidney cells infected with Semliki Forest virus. J Cell Biol *96*, 835–850.

Gu, Y., Di, W. L., Kelsell, D. P., and Zicha, D. (2004). Quantitative fluorescence resonance energy transfer (FRET) measurement with acceptor photobleaching and spectral unmixing - GU - 2004 - Journal of Microscopy - Wiley Online Library. J Microsc.

Guizzunti, G., Brady, T. P., Malhotra, V., and Theodorakis, E. A. (2006). Chemical analysis of norrisolide-induced Golgi vesiculation. Journal of the American Chemical Society *128*, 4190–4191.

Guo, Y., Sirkis, D. W., and Schekman, R. (2014). Protein Sorting at the trans-Golgi Network. Annu. Rev. Cell Dev. Biol. *30*, 169–206.

Gurel, P. S., Hatch, A. L., and Higgs, H. N. (2014). Connecting the cytoskeleton to the endoplasmic reticulum and Golgi. Curr Biol *24*, R660–R672.

Hanna, S., Miskolci, V., Cox, D., and Hodgson, L. (2014). A new genetically encoded single-chain biosensor for Cdc42 based on FRET, useful for live-cell imaging. *9*, e96469.

Hayles, J., Wood, V., Jeffery, L., Hoe, K. L., Kim, D. U., Park, H. O., Salas-Pino, S., Heichinger, C., and Nurse, P. (2013). A genome-wide resource of cell cycle and cell shape genes of fission yeast. Open Biology *3*, 130053–130053.

Head, J., Lee, L. L., Field, D. J., and Lee, J. C. (1985). Equilibrium and rapid kinetic studies on nocodazole-tubulin interaction. J. Biol. Chem. *260*, 11060–11066.

Hehnly, H., Longhini, K. M., Chen, J.-L., and Stamnes, M. (2009). Retrograde Shiga toxin trafficking is regulated by ARHGAP21 and Cdc42. Molecular Biology of the Cell *20*, 4303–4312.

Hidaka, S., Könecke, V., Osten, L., and Witzgall, R. (2004). PIGEA-14, a novel coiled-coil protein affecting the intracellular distribution of polycystin-2. J Biol Chem *279*, 35009–35016.

Hinde, E., Digman, M. A., Welch, C., Hahn, K. M., and Gratton, E. (2012). Biosensor Förster resonance energy transfer detection by the phasor approach to fluorescence lifetime imaging microscopy. Microsc. Res. Tech. *75*, 271–281.

Hodgson, L., Pertz, O., and Hahn, K. M. (2008). Design and optimization of genetically encoded fluorescent blosensors: GTPase blosensors. Methods Cell Biol *85*, 63–.

Hodgson, L., Shen, F., and Hahn, K. (2010). Biosensors for characterizing the dynamics of rho family GTPases in living cells. Curr Protoc Cell Biol *Chapter 14*, Unit14.11.1–Unit14.11.26.

Hoffman, G. R., Nassar, N., and Cerione, R. A. (2000). Structure of the Rho family GTP-binding protein Cdc42 in complex with the multifunctional regulator RhoGDI. *100*, 345–356.

Hurtado, L., Caballero, C., Gavilan, M. P., Cardenas, J., Bornens, M., and Rios, R. M. (2011). Disconnecting the Golgi ribbon from the centrosome prevents directional cell migration and ciliogenesis. The Journal of Cell Biology *193*, 917–933.

Infante, C., Ramos-Morales, F., Fedriani, C., Bornens, M., and Rios, R. M. (1999). GMAP-210, A cis-Golgi network-associated protein, is a minus end microtubule-binding protein. J Cell Biol *145*, 83–98.

Ishida, R., Yamamoto, A., Nakayama, K., Sohda, M., Misumi, Y., Yasunaga, T., and Nakamura, N. (2015). GM130 is a parallel tetramer with a flexible rod-like structure and N-terminally open (Y-shaped) and closed (I-shaped) conformations. Febs Journal *282*, 2232–2244.

Ishikawa-Ankerhold, H. C., Ankerhold, R., and Drummen, G. P. C. (2012). Advanced Fluorescence Microscopy Techniques—FRAP, FLIP, FLAP, FRET and FLIM. Molecules *17*, 4047–4132.

Itin, C., Schindler, R., and Hauri, H. P. (1995). Targeting of protein ERGIC-53 to the ER/ERGIC/cis-Golgi recycling pathway. J Cell Biol *131*, 57–67.

Itoh, R. E., Kurokawa, K., Ohba, Y., Yoshizaki, H., Mochizuki, N., and Matsuda, M. (2002). Activation of Rac and Cdc42 Video Imaged by Fluorescent Resonance Energy Transfer-Based Single-Molecule Probes in the Membrane of Living Cells. Molecular and Cellular Biology *22*, 6582–6591.

Itoh, T., Fujita, N., Kanno, E., Yamamoto, A., Yoshimori, T., and Fukuda, M. (2008). Golgi-resident Small GTPase Rab33B Interacts with Atg16L and Modulates Autophagosome Formation. Molecular Biology of the Cell *19*, 2916–2925.

Jamora, C., Takizawa, P. A., Zaarour, R. F., Denesvre, C., Faulkner, D. J., and Malhotra, V. (1997). Regulation of Golgi structure through heterotrimeric G proteins. Cell *91*, 617–626.

Jaspersen, S. L., and Winey, M. (2004). The budding yeast spindle pole body: Structure, duplication, and function. Annu. Rev. Cell Dev. Biol. *20*, 1–28.

Jin, L., Pahuja, K. B., Wickliffe, K. E., Gorur, A., Baumgärtel, C., Schekman, R., and Rape, M. (2012). Ubiquitin-dependent regulation of COPII coat size and function. Nature *482*, 495–500.

Joachim, J., Jefferies, H. B. J., Razi, M., Frith, D., Snijders, A. P., Chakravarty, P., Judith, D., and Tooze, S. A. (2015). Activation of ULK Kinase and Autophagy by GABARAP Trafficking from the Centrosome Is Regulated by WAC and GM130. Molecular Cell *60*, 899–913.

Johnson, J. L., Erickson, J. W., and Cerione, R. A. (2012). C-terminal di-arginine motif of Cdc42 protein is essential for binding to phosphatidylinositol 4, 5-bisphosphate-containing membranes and inducing cellular transformation. J. Biol. Chem. *287*, 5764–5774.

Kakinuma, T., Ichikawa, H., Tsukada, Y., Nakamura, T., and Toh, B.-H. (2004). Interaction between p230 and MACF1 is associated with transport of a glycosyl phosphatidyl inositol-anchored protein from the Golgi to the cell periphery. Exp Cell Res *298*, 388–398.

Karrenbauer, A., Jeckel, D., Just, W., Birk, R., Schmidt, R. R., Rothman, J. E., and Wieland, F. T. (1990). The Rate of Bulk Flow From the Golgi to the Plasma-Membrane. Cell *63*, 259–267.

Kellokumpu, S., Hassinen, A., and Glumoff, T. (2015). Glycosyltransferase complexes in eukaryotes: long-known, prevalent but still unrecognized. Cell. Mol. Life Sci. *73*, 305–325.

Keyzers, R. A., Northcote, P. T., and Davies-Coleman, M. T. (2006). Spongian diterpenoids from marine sponges. Natural Product Reports *23*, 321–334.

Khodjakov, A., and Rieder, C. L. (1999). The Sudden Recruitment of γ-Tubulin to the Centrosome at the Onset of Mitosis and Its Dynamic Exchange Throughout the Cell Cycle, Do Not Require Microtubules. J Cell Biol *146*, 585–596.

Kim, J. H., Lee, S.-R., Li, L.-H., Park, H.-J., Park, J.-H., Lee, K. Y., Kim, M.-K., Shin, B. A., and Choi, S.-Y. (2011). High Cleavage Efficiency of a 2A Peptide Derived from Porcine Teschovirus-1 in Human Cell Lines, Zebrafish and Mice. PLoS ONE *6*, e18556.

Kim, S. H., Li, Z., and Sacks, D. B. (2000). E-cadherin-mediated cell-cell attachment activates Cdc42. J Biol Chem *275*, 36999–37005.

Klausner, R. D., Donaldson, J. G., and Lippincott-Schwartz, J. (1992). Brefeldin A: insights into the control of membrane traffic and organelle structure. J. Cell Biol. *116*, 1071–1080.

Kodani, A., and Sütterlin, C. (2008). The Golgi protein GM130 regulates centrosome morphology and function. Molecular Biology of the Cell *19*, 745–753.

Kodani, A., and Sütterlin, C. (2009). A new function for an old organelle: microtubule nucleation at the Golgi apparatus. Embo J *28*, 995–996.

Kodani, A., Kristensen, I., Huang, L., and Sütterlin, C. (2009). GM130-dependent control of Cdc42 activity at the Golgi regulates centrosome organization. Molecular Biology of the Cell *20*, 1192–1200.

Kodani, A., Tonthat, V., Wu, B., and Sütterlin, C. (2010). Par6 alpha interacts with the dynactin subunit p150 Glued and is a critical regulator of centrosomal protein recruitment. Molecular Biology of the Cell *21*, 3376–3385.

Kremers, G.-J., Hazelwood, K. L., Murphy, C. S., Davidson, M. W., and Piston, D. W. (2009). Photoconversion in orange and red fluorescent proteins. Nat. Methods *6*, 355–358.

Ku, G. M., Yablonski, D., Manser, E., Lim, L., and Weiss, A. (2001). A PAK1-PIX-PKL complex is activated by the T-cell receptor independent of Nck, Slp-76 and LAT. Embo J *20*, 457–465.

Kuge, O., Dascher, C., Orci, L., Rowe, T., Amherdt, M., Plutner, H., Ravazzola, M., Tanigawa, G., Rothman, J. E., and Balch, W. E. (1994). Sar1 promotes vesicle budding from the endoplasmic reticulum but not Golgi compartments. J Cell Biol *125*, 51–65.

Kunida, K., Matsuda, M., and Aoki, K. (2012). FRET imaging and statistical signal processing reveal positive and negative feedback loops regulating the morphology of randomly migrating HT-1080 cells. Journal of Cell Science *125*, 2381–2392.

Kupfer, A., Louvard, D., and Singer, S. J. (1982). Polarization of the Golgi apparatus and the microtubule-organizing center in cultured fibroblasts at the edge of an experimental wound. Proceedings of the National Academy of Sciences of the United States of America *79*, 2603–2607.

Lee, T. H., and Linstedt, A. D. (2000). Potential role for protein kinases in regulation of bidirectional endoplasmic reticulum-to-Golgi transport revealed by protein kinase inhibitor H89. Molecular Biology of the Cell *11*, 2577–2590.

Leemhuis, J., Boutillier, S., Schmidt, G., and Meyer, D. K. (2002). The Protein Kinase A Inhibitor H89 Acts on Cell Morphology by Inhibiting Rho Kinase. J Pharmacol Exp Ther *300*, 1000–1007.

Ligeti, E., and Settleman, J. (2006). Regulation of RhoGAP specificity by phospholipids and prenylation. Meth Enzymol *406*, 104–117.

Liljedahl, M., Maeda, Y., Colanzi, A., Ayala, I., van Lint, J., and Malhotra, V. (2001). Protein kinase D regulates the fission of cell surface destined transport carriers from the trans-Golgi network. *104*, 409–420.

Lippincott-Schwartz, J., Donaldson, J. G., Schweizer, A., Berger, E. G., Hauri, H. P., Yuan, L. C., and Klausner, R. D. (1990). Microtubule-dependent retrograde transport of proteins into the ER in the presence of brefeldin A suggests an ER recycling pathway. Cell *60*, 821–836.

Lisauskas, T. *et al.* (2012). Live-Cell Assays to Identify Regulators of ER-to-Golgi Trafficking. Traffic *13*, 416–432.

Liu, W., Duden, R., Phair, R., and Lippincott-Schwartz, J. (2005). ArfGAP1 dynamics and its role in COPI coat assembly on Golgi membranes of living cells. J Cell Biol *168*, 1053–1063.

Lu, L., and Hong, W. (2003). Interaction of Arl1-GTP with GRIP domains recruits autoantigens Golgin-97 and Golgin-245/p230 onto the Golgi. Molecular Biology of the Cell *14*, 3767–3781.

Lucocq, J., Warren, G., and Pryde, J. (1991). Okadaic acid induces Golgi apparatus fragmentation and arrest of intracellular transport. Journal of Cell Science *100 ( Pt 4)*, 753–759.

Luna, A., Matas, O. B., Martínez-Menárguez, J. Á., Mato, E., Durán, J. M., Ballesta, J., Way, M., and Egea, G. (2002). Regulation of protein transport from the Golgi complex to the endoplasmic reticulum by CDC42 and N-WASP. Molecular Biology of the Cell *13*, 866–879.

Machacek, M., Hodgson, L., Welch, C., Elliott, H., Pertz, O., Nalbant, P., Abell, A., Johnson, G. L., Hahn, K. M., and Danuser, G. (2009). Coordination of Rho GTPase activities during cell protrusion. Nature *461*, 99–103.

Malkani, N., and Schmid, J. A. (2011). Some secrets of fluorescent proteins: distinct bleaching in various mounting fluids and photoactivation of cyan fluorescent proteins at YFP-excitation. *6*, e18586.

Manneville, J. B., Etienne-Manneville, S., Skehel, P., Carter, T., Ogden, D., and Ferenczi, M. (2003). Interaction of the actin cytoskeleton with microtubules regulates secretory organelle movement near the plasma membrane in human endothelial cells. J Cell Sci *116*, 3927–3938.

Manser, E., Loo, T. H., Koh, C. G., Zhao, Z. S., Chen, X. Q., Tan, L., Tan, I., Leung, T., and Lim, L. (1998). PAK kinases are directly coupled to the PIX family of nucleotide exchange factors. Molecular Cell *1*, 183–192.

Marra, P., Maffucci, T., Daniele, T., Tullio, G. D., Ikehara, Y., Chan, E. K., Luini, A., Beznoussenko, G., Mironov, A., and De Matteis, M. A. (2001). The GM130 and GRASP65 Golgi proteins cycle through and define a subdomain of the intermediate compartment. Nat Cell Biol *3*, 1101–1113.

Marra, P., Salvatore, L., Mironov, A., Di Campli, A., Di Tullio, G., Trucco, A., Beznoussenko, G., and de Matteis, M. A. (2007). The biogenesis of the Golgi ribbon: the roles of membrane input from the ER and of GM130. Molecular Biology of the Cell *18*, 1595–1608.

Martin, T. F. (2001). PI(4,5)P(2) regulation of surface membrane traffic. Curr Opin Cell Biol *13*, 493–499.

Matas, O. B., Martínez-Menárguez, J. Á., and Egea, G. (2004). Association of Cdc42/N-WASP/Arp2/3 Signaling Pathway with Golgi Membranes. Traffic *5*, 838–846.

McIntyre, J. C. *et al.* (2012). Gene therapy rescues cilia defects and restores olfactory function in a mammalian ciliopathy model. Nat. Med.

Meller, N., Irani-Tehrani, M., Kiosses, W. B., del Pozo, M. A., and Schwartz, M. A. (2002). Zizimin1, a novel Cdc42 activator, reveals a new GEF domain for Rho proteins. Nat Cell Biol *4*, 639–647.

Ménétrey, J., Perderiset, M., Cicolari, J., Dubois, T., Elkhatib, N., Khadali, El, F., Franco, M., Chavrier, P., and Houdusse, A. (2007). Structural basis for ARF1-mediated recruitment of ARHGAP21 to Golgi membranes. Embo J *26*, 1953–1962.

Michaelson, D., Rush, M., and Philips, M. R. (2003). Intracellular Targeting of Rho Family GTPases. Rho GTPases.

Michaelson, D., Silletti, J., Murphy, G., D'Eustachio, P., Rush, M., and Philips, M. R. (2001). Differential localization of Rho GTPases in live cells: regulation by hypervariable regions and RhoGDI binding. J Cell Biol *152*, 111–126.

Millarte, V., and Farhan, H. (2012). The Golgi in Cell Migration: Regulation by Signal Transduction and Its Implications for Cancer Cell Metastasis. The Scientific World Journal *2012*, 1–11.

Miller, P. M., Folkmann, A. W., Maia, A. R. R., Efimova, N., Efimov, A., and Kaverina, I. (2009). Golgi-derived CLASP-dependent microtubules control Golgi organization and polarized trafficking in motile cells. Nat Cell Biol *11*, 1069–1080.

Minin, A. A. (1997). Dispersal of Golgi apparatus in nocodazole-treated fibroblasts is a kinesin-driven process. J Cell Sci *110 ( Pt 19)*, 2495–2505.

Misago, M., Liao, Y. F., Kudo, S., Eto, S., Mattei, M. G., Moremen, K. W., and Fukuda, M. N. (1995). Molecular-Cloning and Expression of Cdnas Encoding Human Alpha-Mannosidase-Ii and a Previously Unrecognized

Alpha-Mannosidase-Iix Isozyme. Proceedings of the National Academy of Sciences of the United States of America *92*, 11766–11770.

Mo, X.-Y., Li, T., and Hu, Z.-P. (2013). Decreased levels of cell-division cycle 42 (Cdc42) protein in peripheral lymphocytes from ischaemic stroke patients are associated with Golgi apparatus function. Journal of International Medical Research *41*, 642–653.

Mogelsvang, S., Marsh, B. J., Ladinsky, M. S., and Howell, K. E. (2004). Predicting function from structure: 3D structure studies of the mammalian Golgi complex. Traffic *5*, 338–345.

Molinski, T. F., and Faulkner, D. J. (1986). Aromatic norditerpenes from the nudibranch Chromodoris macfarlandi. J. Org. Chem. *51*, 2601–2603.

Mollenhauer, H. H., Morré, D. J., and Rowe, L. D. (1990). Alteration of intracellular traffic by monensin; mechanism, specificity and relationship to toxicity. Biochim Biophys Acta *1031*, 225–246.

Monypenny, J., Zicha, D., Higashida, C., Oceguera-Yanez, F., Narumiya, S., and Watanabe, N. (2009). Cdc42 and Rac family GTPases regulate mode and speed but not direction of primary fibroblast migration during platelet-derived growth factor-dependent chemotaxis. Mol Cell Biol *29*, 2730–2747.

Moreno-Mateos, M. A., Espina, Á. G., Torres, B., Gámez del Estal, M. M., Romero-Franco, A., Rios, R. M., and Pintor-Toro, J. A. (2011). PTTG1/securin modulates microtubule nucleation and cell migration. Molecular Biology of the Cell *22*, 4302–4311.

Moyer, B. D., Allan, B. B., and Balch, W. E. (2001). Rab1 interaction with a GM130 effector complex regulates COPII vesicle cis--Golgi tethering. Traffic *2*, 268–276.

Nagase, T., Kikuno, R., Ishikawa, K. I., Hirosawa, M., and Ohara, O. (2000). Prediction of the coding sequences of unidentified human genes. XVI. The complete sequences of 150 new cDNA clones from brain which code for large proteins in vitro. DNA Res. *7*, 65–73.

Nakamura, N., Lowe, M., Levine, T. P., Rabouille, C., and Warren, G. (1997). The vesicle docking protein p115 binds GM130, a cis-Golgi matrix protein, in a mitotically regulated manner. Cell *89*, 445–455.

Nakamura, N., Rabouille, C., Watson, R., Nilsson, T., Hui, N., Slusarewicz, P., Kreis, T. E., and Warren, G. (1995). Characterization of a cis-Golgi matrix protein, GM130. J Cell Biol *131*, 1715–1726.

Nalbant, P., Hodgson, L., Kraynov, V., Toutchkine, A., and Hahn, K. M. (2004). Activation of endogenous Cdc42 visualized in living cells. Science *305*, 1615–1619.

Naz, F., Anjum, F., Islam, A., Ahmad, F., and Hassan, M. I. (2013). Microtubule Affinity-Regulating Kinase 4: Structure, Function, and Regulation. Cell Biochem. Biophys. *67*, 485–499.

Neutra, M., and Leblond, C. P. (1966a). RaDioautographic COmparison Of The Uptake Of Galactose-H3 And Glucose-H3 In The Golgi Region Of Various Cells Secreting Glycoproteins Or Mucopolysaccharides. J Cell Biol *30*, 137–150.

Neutra, M., and Leblond, C. P. (1966b). Synthesis of the carbohydrate of mucus in the golgi complex as shown by electron microscope radioautography of goblet cells from rats injected with glucose-H3. J Cell Biol *30*, 119–136.

Ng, M. M., Dippold, H. C., Buschman, M. D., Noakes, C. J., and Field, S. J. (2013). GOLPH3L antagonizes GOLPH3 to determine Golgi morphology. Molecular Biology of the Cell *24*, 796–808.

Nguyen, A. W., and Daugherty, P. S. (2005). Evolutionary optimization of fluorescent proteins for intracellular FRET. Nat. Biotechnol. *23*, 355–360.

Nigg, E. A. (2002). Centrosome aberrations: cause or consequence of cancer progression? Nature Reviews Cancer *2*, 815–825.

Nigg, E. A., and Raff, J. W. (2009). Centrioles, Centrosomes, and Cilia in Health and Disease. Cell *139*, 663–678.

Nigg, E. A., and Stearns, T. (2011). The centrosome cycle: Centriole biogenesis, duplication and inherent asymmetries. Nature Publishing Group *13*, 1154–1160.

Nobes, C. D., and Hall, A. (1995). Rho, rac, and cdc42 GTPases regulate the assembly of multimolecular focal complexes associated with actin stress fibers, lamellipodia, and filopodia. *81*, 53–62.

Novikoff, A. B., and Goldfischer, S. (1961). Nucleosidediphosphatase activity in the Golgi apparatus and its usefulness for cytological studies.

Olson, M. F., Pasteris, N. G., Gorski, J. L., and Hall, A. (1996). Faciogenital dysplasia protein (FGD1) and Vav, two related proteins required for normal embryonic development, are upstream regulators of Rho GTPases. Curr. Biol. *6*, 1628–1633.

Orci, L., Ravazzola, M., Volchuk, A., Engel, T., Gmachl, M., Amherdt, M., Perrelet, A., Söllner, T. H., and Rothman, J. E. (2000). Anterograde flow of cargo

across the Golgi stack potentially mediated via bidirectional “percolating” COPI vesicles. Proceedings of the National Academy of Sciences of the United States of America *97*, 10400–10405.

Orcl, L., Tagaya, M., Amherdt, M., Perrelet, A., Donaldson, J. G., Lippincott-Schwartz, J., Klausner, R. D., and Rothman, J. E. (1991). Brefeldin A, a drug that blocks secretion, prevents the assembly of non-clathrin-coated buds on Golgi cisternae. Cell *64*, 1183–1195.

Osmani, N., Peglion, F., Chavrier, P., and Etienne-Manneville, S. (2010). Cdc42 localization and cell polarity depend on membrane traffic. The Journal of Cell Biology *191*, 1261–1269.

Palade, G. (1975). Intracellular aspects of the process of protein synthesis. Science *189*, 867–358.

Patterson, G. H., Hirschberg, K., Polishchuk, R. S., Gerlich, D., Phair, R. D., and Lippincott-Schwartz, J. (2008). Transport through the Golgi apparatus by rapid partitioning within a two-phase membrane system. Cell *133*, 1055–1067.

Pelham, H. R. B., and Rothman, J. E. (2000). The Debate about Transport in the Golgi—Two Sides of the Same Coin? Cell *102*, 713–719.

Pineau, L., Bonifait, L., Berjeaud, J.-M., Alimardani-Theuil, P., Berges, T., and Ferreira, T. (2008). A Lipid-mediated Quality Control Process in the Golgi Apparatus in Yeast. Molecular Biology of the Cell *19*, 807–821.

Polishchuk, E. V., Di Pentima, A., Luini, A., and Polishchuk, R. S. (2003). Mechanism of constitutive export from the golgi: bulk flow via the formation, protrusion, and en bloc cleavage of large trans-golgi network tubular domains. Molecular Biology of the Cell *14*, 4470–4485.

Popoff, V., Adolf, F., Brügger, B., and Wieland, F. (2011). COPI budding within the Golgi stack. Cold Spring Harb Perspect Biol *3*, a005231–a005231.

Preisinger, C., Korner, R., Wind, M., Lehmann, W. D., Kopajtich, R., and Barr, F. A. (2005). Plk1 docking to GRASP65 phosphorylated by Cdk1 suggests a mechanism for Golgi checkpoint signalling. The EMBO Journal *24*, 753–765.

Preisinger, C., Short, B., De Corte, V., Bruyneel, E., Haas, A., Kopajtich, R., Gettemans, J., and Barr, F. A. (2004). YSK1 Is Activated by the Golgi Matrix Protein GM130 and Plays a Role in Cell Migration through Its Substrate 14-3-3ζ. The Journal of Cell Biology *164*, 1009–1020.

Preuss, D., Mulholland, J., Franzusoff, A., Segev, N., and Botstein, D. (1992). Characterization of the Saccharomyces Golgi complex through the cell cycle by immunoelectron microscopy. Molecular Biology of the Cell *3*, 789–803.

Puri, S., and Linstedt, A. D. (2003). Capacity of the golgi apparatus for biogenesis from the endoplasmic reticulum. Molecular Biology of the Cell *14*, 5011–5018.

Puthenveedu, M. A., and Linstedt, A. D. (2001). Evidence that Golgi structure depends on a p115 activity that is independent of the vesicle tether components giantin and GM130. J Cell Biol *155*, 227–238.

Puthenveedu, M. A., and Linstedt, A. D. (2004). Gene replacement reveals that p115/SNARE interactions are essential for Golgi biogenesis. Proceedings of the National Academy of Sciences of the United States of America *101*, 1253–1256.

Puthenveedu, M. A., Bachert, C., Puri, S., Lanni, F., and Linstedt, A. D. (2006). GM130 and GRASP65-dependent lateral cisternal fusion allows uniform Golgi-enzyme distribution. Nat Cell Biol *8*, 238–248.

Rabouille, C. (2009). The Golgi apparatus: lessons from Drosophila. FEBS Lett *583*, 3827–3838.

Radeke, H., Digits, C., Casaubon, R., and Snapper, M. (1999). Interactions of (-)-ilimaquinone with methylation enzymes: implications for vesicular-mediated secretion. Chemistry & Biology *6*, 639–647.

Reitz, C. (2014). The role of the retromer complex in aging-related neurodegeneration: a molecular and genomic review. Mol Genet Genomics *290*, 413–427.

Rios, R. M. (2014). The centrosome-Golgi apparatus nexus. Philos. Trans. R. Soc. Lond., B, Biol. Sci. *369*, 20130462–20130462.

Rios, R. M., Sanchís, A., Tassin, A. M., Fedriani, C., and Bornens, M. (2004). GMAP-210 recruits gamma-tubulin complexes to cis-Golgi membranes and is required for Golgi ribbon formation. *118*, 323–335.

Rivero, S., Cardenas, J., Bornens, M., and Rios, R. M. (2009). Microtubule nucleation at the cis-side of the Golgi apparatus requires AKAP450 and GM130. Embo J *28*, 1016–1028.

Rivinoja, A., Pujol, F. M., Hassinen, A., and Kellokumpu, S. (2012). Golgi pH, its regulation and roles in human disease. Annals of Medicine *44*, 542–554.

Rizzo, M. A., Springer, G. H., Granada, B., and Piston, D. W. (2004). An improved cyan fluorescent protein variant useful for FRET. Nat. Biotechnol. *22*, 445–449.

Rossanese, O. W., Soderholm, J., Bevis, B. J., Sears, I. B., O'Connor, J., Williamson, E. K., and Glick, B. S. (1999). Golgi structure correlates with transitional endoplasmic reticulum organization in Pichia pastoris and Saccharomyces cerevisiae. J Cell Biol *145*, 69–81.

Rossman, K. L., Der, C. J., and Sondek, J. (2005). GEF means go: turning on RHO GTPases with guanine nucleotide-exchange factors. Nature Reviews Molecular Cell Biology *6*, 167–180.

Rothman, J. E., and Wieland, F. T. (1996). Protein sorting by transport vesicles. Science *272*, 227–234.

Roti, E., Myers, C. D., Ayers, R. A., Boatman, D. E., Delfosse, S. A., Chan, E., Ackerman, M. J., January, C. T., and Robertson, G. A. (2002). Interaction with GM130 during HERG ion channel trafficking - Disruption by type 2 congenital long QT syndrome mutations. J Biol Chem *277*, 47779–47785.

Sadigh-Eteghad, S., Askari-Nejad, M. S., Mahmoudi, J., and Majdi, A. (2016). Cargo trafficking in Alzheimer's disease: the possible role of retromer. Neurological Sciences *37*, 17–22.

Salazar, M. A., Kwiatkowski, A. V., Pellegrini, L., Cestra, G., Butler, M. H., Rossman, K. L., Serna, D. M., Sondek, J., Gertler, F. B., and de Camilli, P. (2003). Tuba, a novel protein containing bin/amphiphysin/Rvs and Dbl homology domains, links dynamin to regulation of the actin cytoskeleton. J Biol Chem *278*, 49031–49043.

Schaub, B. E., Berger, B., Berger, E. G., and Rohrer, J. (2006). Transition of galactosyltransferase 1 from trans-Golgi cisternae to the trans-Golgi network is signal mediated. Molecular Biology of the Cell *17*, 5153–5162.

Scheffler, K. (2014). Microtubule-dependent nuclear congression in fission yeast and a novel factor in cellular morphogenesis of fission yeast. Http:// Www.Theses.Fr.

Schmidt, A., and Hall, A. (2002). Guanine nucleotide exchange factors for Rho GTPases: turning on the switch. Gene Dev *16*, 1587–1609.

Schnermann, M. J., Beaudry, C. M., Egorova, A. V., Polishchuk, R. S., Sütterlin, C., and Overman, L. E. (2010). Golgi-modifying properties of macfarlandin E and the synthesis and evaluation of its 2,7-dioxabicyclo[3.2.1]octan-3-one core. Proc Natl Acad Sci U S A *107*, 6158–6163.

Schnermann, M. J., Beaudry, C. M., Genung, N. E., Canham, S. M., Untiedt, N. L., Karanikolas, B. D. W., Sütterlin, C., and Overman, L. E. (2011). Divergent synthesis and chemical reactivity of bicyclic lactone fragments of complex rearranged spongian diterpenes. Journal of the American Chemical Society *133*, 17494–17503.

Schreij, A. M. A., Fon, E. A., and McPherson, P. S. (2015). Endocytic membrane trafficking and neurodegenerative disease. Cell. Mol. Life Sci. *73*, 1529–1545.

Schweizer, A., Ericsson, M., Bächi, T., Griffiths, G., and Hauri, H. P. (1993). Characterization of a novel 63 kDa membrane protein. Implications for the organization of the ER-to-Golgi pathway. Journal of Cell Science *104 ( Pt 3)*, 671–683.

Sciaky, N., Presley, J., Smith, C., Zaal, K., Cole, N., Moreira, J., Terasaki, M., Siggia, E., and Lippincott-Schwartz, J. (1997). Golgi tubule traffic and the effects of brefeldin A visualized in living cells. J Cell Biol *139*, 1137.

Sengupta, D., and Linstedt, A. D. (2010). Mitotic Inhibition of GRASP65 Organelle Tethering Involves Polo-like Kinase 1 (PLK1) Phosphorylation Proximate to an Internal PDZ Ligand. J Biol Chem *285*, 39994–40003.

Sengupta, D., Truschel, S., Bachert, C., and Linstedt, A. D. (2009). Organelle tethering by a homotypic PDZ interaction underlies formation of the Golgi membrane network. The Journal of Cell Biology *186*, 41–55.

Seth, A., Otomo, T., Yin, H. L., and Rosen, M. K. (2003). Rational design of genetically encoded fluorescence resonance energy transfer-based sensors of cellular Cdc42 signaling. Biochemistry *42*, 3997–4008.

Shaner, N. C., Patterson, G. H., and Davidson, M. W. (2007). Advances in fluorescent protein technology. Journal of Cell Science *120*, 4247–4260.

Shima, D. T., Haldar, K., Pepperkok, R., Watson, R., and Warren, G. (1997). Partitioning of the Golgi Apparatus during Mitosis in Living HeLa Cells. J Cell Biol *137*, 1211–1228.

Short, B., Haas, A., and Barr, F. A. (2005). Golgins and GTPases, giving identity and structure to the Golgi apparatus. Biochim. Biophys. Acta *1744*, 383–395.

Short, B., Preisinger, C., Korner, R., Kopajtich, R., Byron, O., and Barr, F. A. (2001). A GRASP55-rab2 effector complex linking Golgi structure to membrane traffic. J Cell Biol *155*, 877–883.

Shorter, J., Beard, M. B., Seemann, J., Dirac-Svejstrup, A. B., and Warren, G. (2002). Sequential tethering of Golgins and catalysis of SNAREpin assembly by the vesicle-tethering protein p115. J Cell Biol *157*, 45–62.

Siddhanta, A., Backer, J. M., and Shields, D. (2000). Inhibition of Phosphatidic Acid Synthesis Alters the Structure of the Golgi Apparatus and Inhibits Secretion in Endocrine Cells. Journal of Biological Chemistry *275*, 12023–12031.

Sircar, K. *et al.* (2012). Mitosis phase enrichment with identification of mitotic centromere-associated kinesin as a therapeutic target in castration-resistant prostate cancer. *7*, e31259.

Sjöstrand, F. S., and Hanzon, V. (1954). Ultrastructure of golgi apparatus of exocrinecells of mouse pancreas. Experimental Cell Research *7*, 415–429.

Sonoda, H., Okada, T., Jahangeer, S., and Nakamura, S.-I. (2007). Requirement of phospholipase D for ilimaquinone-induced Golgi membrane fragmentation. J. Biol. Chem. *282*, 34085–34092.

Spiering, D., Bravo-Cordero, J. J., Moshfegh, Y., Miskolci, V., and Hodgson, L. (2013). Chapter 25 Quantitative Ratiometric Imaging of FRET-Biosensors in Living Cells, Elsevier.

Stanley, H., Botas, J., and Malhotra, V. (1997). The mechanism of Golgi segregation during mitosis is cell type-specific. Proceedings of the National Academy of Sciences of the United States of America *94*, 14467–14470.

Stauber, T., Simpson, J. C., Pepperkok, R., and Vernos, I. (2006). A Role for Kinesin-2 in COPI-Dependent Recycling between the ER and the Golgi Complex. Current Biology *16*, 2245–2251.

Sulistio, Y. A., and Heese, K. (2015). The Ubiquitin-Proteasome System and Molecular Chaperone Deregulation in Alzheimer's Disease. Mol Neurobiol *53*, 905–931.

Sun, K. H., de Pablo, Y., Vincent, F., Johnson, E. O., Chavers, A. K., and Shah, K. (2008). Novel Genetic Tools Reveal Cdk5"s Major Role in Golgi Fragmentation in Alzheimer"s Disease. *19*, 3052–3069.

Sundaramoorthy, V., Sultana, J. M., and Atkin, J. D. (2015). Golgi fragmentation in amyotrophic lateral sclerosis, an overview of possible triggers and consequences. Front. Neurosci. *9*, 536–11.

Sutterlin, C., Polishchuk, R., Pecot, M., and Malhotra, V. (2005). The Golgi-associated protein GRASP65 regulates spindle dynamics and is essential for cell division. Molecular Biology of the Cell *16*, 3211–3222.

Sütterlin, C., Hsu, P., Mallabiabarrena, A., and Malhotra, V. (2002). Fragmentation and Dispersal of the Pericentriolar Golgi Complex Is Required for Entry into Mitosis in Mammalian Cells. Cell *109*, 359–369.

Sweeney, D. A., Siddhanta, A., and Shields, D. (2002). Fragmentation and Re-assembly of the Golgi Apparatus in Vitro. A Requirement For Phosphatidic Acid And Phosphatidylinositol 4,5-Bisphosphate Synthesis. Journal of Biological Chemistry *277*, 3030–3039.

Takizawa, P. A., Yucel, J. K., Veit, B., Faulkner, D. J., Deerinck, T., Soto, G., Ellisman, M., and Malhotra, V. (1993). Complete vesiculation of Golgi membranes and inhibition of protein transport by a novel sea sponge metabolite, ilimaquinone. Cell *73*, 1079–1090.

Thyberg, J., and Moskalewski, S. (1999). Role of Microtubules in the Organization of the Golgi Complex. Experimental Cell Research *246*, 263–279.

Turner, J. R., and Tartakoff, A. M. (1989). The response of the Golgi complex to microtubule alterations: the roles of metabolic energy and membrane traffic in Golgi complex organization. J Cell Biol *109*, 2081–2088.

Valderrama, F., Babia, T., Ayala, I., Kok, J. W., Renau-Piqueras, J., and Egea, G. (1998). Actin microfilaments are essential for the cytological positioning and morphology of the Golgi complex. Eur J Cell Biol *76*, 9–17.

Valentin, G., Verheggen, C., Piolot, T., Neel, H., Coppey-Moisan, M., and Bertrand, E. (2005). Photoconversion of YFP into a CFP-like species during acceptor photobleaching FRET experiments. Nat. Methods *2*, 801.

Valsdottir, R., Hashimoto, H., Ashman, K., Koda, T., Storrie, B., and Nilsson, T. (2001). Identification of rabaptin-5, rabex-5, and GM130 as putative effectors of rab33b, a regulator of retrograde traffic between the Golgi apparatus and ER. FEBS Letters *508*, 201–209.

Van Valkenburgh, H., Shern, J. F., Sharer, J. D., Zhu, X., and Kahn, R. A. (2001). ADP-ribosylation factors (ARFs) and ARF-like 1 (ARL1) Have Both Specific and Shared Effectors CHARACTERIZING ARL1-BINDING PROTEINS. J Biol Chem *276*, 22826–22837.

Vasile, E., Perez, T., Nakamura, N., and Krieger, M. (2003). Structural Integrity of the Golgi is Temperature Sensitive in Conditional-Lethal Mutants with No Detectable GM130 - Vasile - 2003 - Traffic - Wiley Online Library. Traffic.

Vilela, M., Halidi, N., Besson, S., Elliott, H., Hahn, K., Tytell, J., and Danuser, G. (2013). Chapter Nine Fluctuation Analysis of Activity Biosensor Images for the Study of Information Flow in Signaling Pathways, Elsevier.

Vinogradova, T., Paul, R., Grimaldi, A. D., Loncarek, J., Miller, P. M., Yampolsky, D., Magidson, V., Khodjakov, A., Mogilner, A., and Kaverina, I. (2012). Concerted effort of centrosomal and Golgi-derived microtubules is required for proper Golgi complex assembly but not for maintenance. Molecular Biology of the Cell *23*, 820–833.

Wallrabe, H., and Periasamy, A. (2005). Imaging protein molecules using FRET and FLIM microscopy. Curr. Opin. Biotechnol. *16*, 19–27.

Wallrabe, H., Chen, Y., Periasamy, A., and Barroso, M. (2006). Issues in confocal microscopy for quantitative FRET analysis. Microsc. Res. Tech. *69*, 196–206.

Wang, S., Li, H., Chen, Y., Wei, H., Gao, G. F., Liu, H., Huang, S., and Chen, J.-L. (2012). Transport of influenza virus neuraminidase (NA) to host cell surface is regulated by ARHGAP21 and Cdc42 proteins. J Biol Chem *287*, 9804–9816.

Wei, J.-H., Zhang, Z. C., Wynn, R. M., and Seemann, J. (2015). GM130 Regulates Golgi-Derived Spindle Assembly by Activating TPX2 and Capturing Microtubules. Cell *162*, 287–299.

Weide, T., Bayer, M., Köster, M., Siebrasse, J. P., Peters, R., and Barnekow, A. (2001). The Golgi matrix protein GM130: a specific interacting partner of the small GTPase rab1b. EMBO Rep. *2*, 336–341.

Witkos, T. M., and Lowe, M. (2016). The Golgin Family of Coiled-Coil Tethering Proteins. Front. Cell Dev. Biol. *3*, 253–259.

Woods, C. G., Bond, J., and Enard, W. (2005). Autosomal Recessive Primary Microcephaly (MCPH): A Review of Clinical, Molecular, and Evolutionary Findings. The American Journal of Human Genetics *76*, 717–728.

Wouters, F. S., and Bastiaens, P. I. H. (2006). Imaging Protein−Protein Interactions by Fluorescence Resonance Energy Transfer (FRET) Microscopy, John Wiley & Sons, Inc.

Wu, W. J., Erickson, J. W., Lin, R., and Cerione, R. A. (2000). The gamma-subunit of the coatomer complex binds Cdc42 to mediate transformation. Nature *405*, 800–804.

Wu, Y., Gadina, M., Tao-Cheng, J., and Youle, R. (1994). Retinoic acid disrupts the Golgi apparatus and increases the cytosolic routing of specific protein toxins. The Journal of Cell Biology *125*, 743–753.

Xiang, Y., and Wang, Y. (2010). GRASP55 and GRASP65 play complementary and essential roles in Golgi cisternal stacking. *188*, 237–251.

Xu, K., Schwarz, P., and Luduena, R. (2002). Interaction of nocodazole with tubulin isotypes. Drug Develop Res *55*, 91–96.

Yadav, S., Puri, S., and Linstedt, A. D. (2009). A primary role for Golgi positioning in directed secretion, cell polarity, and wound healing. Molecular Biology of the Cell *20*, 1728–1736.

Yadav, S., Puthenveedu, M. A., and Linstedt, A. D. (2012). Golgin160 recruits the dynein motor to position the Golgi apparatus. Developmental Cell *23*, 153–165.

Yilmaz Dejgaard, S., Murshid, A., Dee, K. M., and Presley, J. F. (2007). Confocal Microscopy-based Linescan Methodologies for Intra-Golgi Localization of Proteins. Journal of Histochemistry and Cytochemistry *55*, 709–719.

Yoshimura, S. I., Nakamura, N., Barr, F. A., Misumi, Y., Ikehara, Y., Ohno, H., Sakaguchi, M., and Mihara, K. (2001). Direct targeting of cis-Golgi matrix proteins to the Golgi apparatus. Journal of Cell Science *114*, 4105–4115.

Yoshizaki, H., Ohba, Y., Kurokawa, K., Itoh, R. E., Nakamura, T., Mochizuki, N., Nagashima, K., and Matsuda, M. (2003). Activity of Rho-family GTPases during cell division as visualized with FRET-based probes. J Cell Biol *162*, 223–232.

Young, A., Dictenberg, J. B., Purohit, A., Tuft, R., and Doxsey, S. J. (2000). Cytoplasmic dynein-mediated assembly of pericentrin and gamma tubulin onto centrosomes. Molecular Biology of the Cell *11*, 2047–2056.

Zaal, K. J. *et al.* (1999). Golgi membranes are absorbed into and reemerge from the ER during mitosis. *99*, 589–601.

Zhang, C.-H. *et al.* (2011). GM130, a cis-Golgi protein, regulates meiotic spindle assembly and asymmetric division in mouse oocyte. Cc *10*, 1861–1870.

Zhou, W., Chang, J., Wang, X., Savelieff, M. G., Zhao, Y., Ke, S., and Ye, B. (2014). GM130 is required for compartmental organization of dendritic golgi outposts. Curr Biol *24*, 1227–1233.